UNITED NATIONS UNIVERSITY

UNU-GTP

ORKUSTOFNUN

Meyjarauga hot spring, Hveravellir, Kjölur, Central Iceland

Irma Khoirunissa

AERMOD MODELLING OF HYDROGEN SULFIDE (H_2S) CONCENTRATION FROM GEOTHERMAL POWER PLANTS IN ULUBELU, INDONESIA AND HELLISHEIDI-NESJAVELLIR, ICELAND

Report 6
November 2018

UNITED NATIONS UNIVERSITY
UNU-GTP
Geothermal Training Programme

Orkustofnun, Grensasvegur 9,
IS-108 Reykjavik, Iceland

Reports 2018
Number 6

AERMOD MODELLING OF HYDROGEN SULFIDE (H_2S) CONCENTRATION FROM GEOTHERMAL POWER PLANTS IN ULUBELU, INDONESIA, AND HELLISHEIDI-NESJAVELLIR, ICELAND

MSc thesis
School of Engineering and Natural Sciences
Faculty of Earth Sciences
University of Iceland

by

Irma Khoirunissa
PT. Pertamina Geothermal Energy (PGE)
M.H. Thamrin, No. 9, Central Jakarta 10340
INDONESIA
irmak@pertamina.com

United Nations University
Geothermal Training Programme
Reykjavík, Iceland
Published in November 2018

ISBN 978-9979-68-487-9 (PRINT)
ISBN 978-9979-68-488-6 (PDF)
ISSN 1670-7427

This MSc thesis has also been published in November 2018 by the
School of Engineering and Natural Sciences, Faculty of Earth Sciences
University of Iceland

INTRODUCTION

The Geothermal Training Programme of the United Nations University (UNU) has operated in Iceland since 1979 with six-month annual courses for professionals from developing countries. The aim is to assist developing countries with significant geothermal potential to build up groups of specialists that cover most aspects of geothermal exploration and development. During 1979-2018, 694 scientists and engineers from 61 developing countries have completed the six month courses, or similar. They have come from Africa (39%), Asia (35%), Latin America (14%), Europe (11%), and Oceania (1%). There is a steady flow of requests from all over the world for the six-month training and we can only meet a portion of the requests. Most of the trainees are awarded UNU Fellowships financed by the Government of Iceland.

Candidates for the six-month specialized training must have at least a BSc degree and a minimum of one-year practical experience in geothermal work in their home countries prior to the training. Many of our trainees have already completed their MSc or PhD degrees when they come to Iceland, but many excellent students with only BSc degrees have made requests to come again to Iceland for a higher academic degree. From 1999, UNU Fellows have also been given the chance to continue their studies and study for MSc degrees in geothermal science or engineering in co-operation with the University of Iceland. An agreement to this effect was signed with the University of Iceland. A similar agreement was also signed with Reykjavik University in 2013. The six-month studies at the UNU Geothermal Training Programme form a part of the graduate programme.

It is a pleasure to introduce the 62nd UNU Fellow to complete the MSc studies under a UNU-GTP Fellowship. Irma Khoirunissa, an Environmental Engineer from PT Pertamina Geothermal Energy - PGE in Indonesia, completed the six-month specialized training in *Environmental Sciences* at UNU Geothermal Training Programme in October 2011. Her research report was entitled: *Hydrogen sulphide dispersion for Hellisheidi and Nesjavellir geothermal power plants, SW-Iceland, using AERMOD.* After five years of geothermal work for PGE in Indonesia, she came back to Iceland for MSc studies at the School of Engineering and Natural Sciences, Faculty of Earth Sciences, University of Iceland in August 2016. In October 2018, she defended her *MSc thesis* in *Environmental Sciences* presented here, entitled: *AERMOD modelling of hydrogen sulphide (H_2S) concentration from geothermal power plants in Ulubelu, Indonesia, and Hellisheidi-Nesjavellir, Iceland.* Her studies in Iceland were financed by the Government of Iceland through a UNU-GTP Fellowship from the UNU Geothermal Training Programme. We congratulate Irma on the achievements and wish her all the best for the future. We thank the School of Engineering and Natural Sciences, Faculty of Earth Sciences, University of Iceland for the co-operation, and her supervisors for the dedication.

Finally, I would like to mention that Irma's MSc thesis with the figures in colour is available for downloading on our website *www.unugtp.is*, under publications.

With warmest greetings from Iceland,

Lúdvík S. Georgsson, Director
United Nations University
Geothermal Training Programme

ACKNOWLEDGEMENTS

I would first like to express my most profound gratitude to Lúdvík S. Georgsson, Director, and, Ingimar G. Haraldsson, Deputy Director of the *UNU-GTP*, for giving me the opportunity for studying Environment and Natural Resources at the Institute of Earth Sciences, University of Iceland. Furthermore, thanks to Málfríður Ómarsdóttir, Thórhildur Ísberg, Markús A.G Wilde, Jóhann F. Kristjánsson, and Rósa S. Jónsdóttir for their help during my study. My sincere thanks to my supervisors, Professor Thröstur Thorsteinsson and Elín Björk Jónasdóttir for guidance, many useful discussions, and advice throughout the study as well as examiner, Einar Sveinbjörnsson.

My sincere appreciation goes to Erdi Suroso S.T.P., M.T.A - University Lampung, Fahrizal - Meteorological Office, Lampung Province and Icelandic Meteorological Office for helping me in providing Indonesian and Iceland weather data collections. Special thanks to my colleagues from the PGE Ulubelu, and PGE headquarter for their assistance in data gathering as well useful technical discussion; Eko Nugroho Budiyanto, Asep Rahmat, Dadang Rahmat, Bhaskara Aji Pawita, Fajar Adi Prasetyo, Anjani Puspadianti, Yanuardi Herdiyono, Febriardy, Asep Rahmat, Eko Nugroho, Israyudi, and Indra Mantik Oentara. My gratitude also goes to PGE's Health, Safety, Environment and Security Headquarter division, Human Capital division, Kamojang teams, for their support to handling off work responsibilities at Kamojang geothermal site while I was away for study.

I am also grateful thank Irfan Zainuddin, former President Director of PT. Pertamina Geothermal Energy (PGE), Ali Mudakir, President Director of PGE, Board of Directors PGE, Wawan Darmawan, GM Geothermal Kamojang Site, and Wilmar Napitupulu, Head of HSSE division for permission, to attend this programme.

Special thanks goes to my mates and colleagues, Marmelia Puja Dewi, Saraswati, Mpomwenda Veronica, Eugenio Luciano, Patricia Edmunds, Samual Nganga, Kennedy Mativo who helped checking my report and had great discussions to improve the report. Thanks to the UNU-GTP Fellows, we were having a great time together during this study; Tingting, Melissa, Samuel, Hamoud, Moneer, Linh, Daniel, Getenesh, Kennedy, Charles, Geoffrey, Winnie, Chagaka, and Diego.

Last but not least, my family, most of all, Ibu, Baba, sisters, brothers, nephews, for all the prayers, endless support, motivations, as well as encourage me 'when you believe something, it will exist, along prayer with action'.

DEDICATION

Dedicated to my family who always give me endless support.

ABSTRACT

The AERMOD model was evaluated with the aim to assess the applicability of the software to give reasonable results, in estimating H_2S concentration from two geothermal fields affected by different weather conditions. The study cases were geothermal emissions from the Ulubelu power plants in Indonesia, and the emissions from the Hellisheidi and Nesjavellir power plants in Iceland. The modelled H_2S distribution was also compared to observation H_2S values with periods of up to one-year data. AERMOD was used to calculate the maximum concentration of 1-hour (odour standard), 8-hour (occupational health standard), 24-hour and annual time averages (public health standard). The test cases included different model setup of elevated and flat terrain options, as well as various meteorological data (e.g. onsite and offsite). Overall, the model performed better for a long-term period (annual) than a short-term period (1-hour and 24-hour), except for the Ulubelu case, where the model at 24-hour period agreed well with the measurement data sample points taken from up to 3 km from the source. In contrast, for the Hellisheidi and Nesjavellir case, the models had difficulty in predicting the concentration at receptors within 25 km from the sources. When evaluating the level of H_2S concentration based on seasons, the results of the model showed higher concentrations during the winter season than summer season for the Hellisheidi and Nesjavellir case. For the Ulubelu case, the predicted H_2S concentration during the dry season was estimated to be higher than during the wet season. The study highlighted the influence of weather conditions (i.e., wind stability in a tropical climate compared to cold weather) on the dispersion of geothermal emissions, as well as the effect distance of meteorological stations, receptor´s and source's location, and terrain height have on the results of model simulations. The study shows that the model simulation does not work well when the source is far away, the weather changes rapidly and the terrain is complex. However, for stable weather conditions, it provides valuable information and can assist in mitigations measures decisions, for instance, to define H_2S monitoring station points at receptors, which indicates high concentration of H_2S.

TABLE OF CONTENTS

LIST OF FIGURES

LIST OF TABLES

ABBREVIATIONS

AERMAP	American Meteorological Society/Environmental Protection Agency Regulatory Model terrain pre-processor
AERMOD	American Meteorological Society/Environmental Protection Agency Regulatory Model
AERMET	American Meteorological Society/Environmental Protection Agency Regulatory Model Meteorological Processor
AERSURFACE	American Meteorological Society/Environmental Protection Agency Regulatory Model Land Cover Processor
AMS	American Meteorological Society
APHA	American Public Health Association
EIA	Environmental Impact Assessment
CBL	Convective boundary layer
GRE	Grensasvegur H_2S station
GHG	Green house gas
GEA	Geothermal Energy Association
HELS	Hellisheidi Meteorological Station
HEL	Hellisheidi power plants
HEH	Hvaleyrarholt H_2S station
KOP	Kópavogur H_2S station
MOEF	Indonesian Ministry of Environment and Forestry
MOL	Indonesian Ministry of Labour
MOE	Ministry of Environment
m a.s.l	Metres above sea level
NCG	Non-condensable gases
NES	Nesjavellir power plants
NLH	Nordlingaholt H_2S station
OECD	Organization for Economic Co-operation and Development
OLKE	Ölkelduháls meteorological station
OR	Orkuveita Reykjavíkur (Reykjavik Energy)
OSHA	Occupational Safety and Health Administration
RMSE	Root mean square error
REYK	Reykjavik meteorological station
SBL	Stable boundary layer
SD	Standard deviation
SRTM	Shuttle Radar Topography Mission
STRM	Straumsvík meteorological station
US EPA	U.S. Environmental Protection Agency
UBL	Ulubelu power plants
PGE	Pertamina Geothermal Energy
PLN	Perusahaan Listrik Negara (Indonesian Electricity State Owned Company)
PBL	Planetary boundary layer
WHO	World Health Organization
WKP	Wilayah Kerja Panas Bumi (Geothermal Working Area)

1. INTRODUCTION

Geothermal energy is the heat that comes from the earth's interior, and it is associated with the decay of radioactive elements (Dickson and Fanelli, 2004). The common usage of high-temperature steam is to transform it into electricity, while for low-temperature resources it is used directly for space heating. Geothermal power is considered clean energy when, compared to fossil fuel, because no combustion of fuel takes place during its production; thus, it is considered a sustainable source of renewable energy and vital in combating climate change.

However, the sulphur gas associated with geothermal exploration and utilization causes air pollution (Kristmannsdóttir et al., 2000; Thorsteinsson et al., 2013). The sulphur gas emitted from the geothermal power plants is in the form of hydrogen sulphide (H_2S). H_2S is toxic at high concentrations, with an unpleasant rotten-egg odour at concentration ranges 0.69-417 $\mu g/m^3$ (ATSDR, 2014). The health effects of the pollutant at low concentrations (less than 70 mg/m^3) include eyes irritation (5 mg/m^3), and respiratory problems (14 mg/m^3). When immediately exposed to concentrations greater than 140 mg/m^3, a person can experience loss of consciousness, coma, respiratory paralysis, seizures, and death (ATSDR, 2014; Chou, 2003). Inhalation is the most common route of exposure (Chou, 2003). Thus, its presence is often of great concern both to occupational and public health especially in villages or towns within the vicinity of, as well as those located further away from a power plant (Thorsteinsson, et al., 2013). The impacts of H_2S on the environment around geothermal fields have been found to cause increasing sulphur depositions in terrestrial ecosystems, which has been linked to the emissions of geothermal power plants. The effect has included damage to moss (e.g., *Racomitrium lanuginosum* in Iceland) (Mutia, 2016).

Air quality modelling is required by policy makers to determine the consequences of geothermal development and to gauge the need to manage geothermal emissions in current and future conditions. AERMOD was used for the model simulations. This software is recommended by the US Environmental Protection Agency for a regulatory purpose (US EPA, 2005). Understanding the performance of model prediction is necessary for establishing and reviewing regulation policy, as well as potential mitigation action.

Two case studies were done to evaluate different parameters within the model predictions. The case studies were differentiated according to weather conditions, distances from the sources, and model setup with different terrain options (flat and elevated). Ulubelu geothermal site, Indonesia is located in a tropical climate; the model was set a short impact distance of less than 3 km from the emission sources. Hellisheidi and Nesjavellir geothermal sites, Iceland are located in cold weather conditions. In the Hellisheidi and Nesjavellir case, the model simulation focused on the impact of H_2S concentration at up to a 25 km distance.

This study, therefore, assessed the H_2S pollution from geothermal power plants at Ulubelu in Indonesia, and Nesjavellir and Hellisheidi in Iceland. The aim was to evaluate the applicability of the AERMOD model in predicting H_2S concentration based on observation data from the Ulubelu, and the H_2S measurements in Reykjavík city. Subsequently, the predicted H_2S levels at residential areas and the geothermal workplaces were compared to the Icelandic H_2S legislation, Indonesia H_2S legislation, and the WHO air quality guidelines.

1.1 The significance of the study

Global energy policy aims for renewable energy to account for two-thirds of all energy production by 2040 to tackle GHG emissions (IEA, 2018). The geothermal production in the world is expected to reach 32 GW_e by 2030 (GEA, 2016). Geothermal energy is widely used for electricity production, currently, the installed capacity of geothermal power generation is 14 GW_e as of January 2018 (Richter, 2018). In Indonesia, the government is planning to boost the geothermal power portion from 1,924.5 MW to 7,242 MW by 2025 (MEMR, 2015). In Iceland, the current (2016) installed capacity of the geothermal power plants is about 755 MW (Orkustofnun, 2018). The electricity consumption in Iceland is projected to

increase by 2.8% per year until 2020, and at a steady rate of 2% by 2030 (MIT Energy, 2017a; 2017b). The GEA (2016) reported that Iceland planned to develop about 575 MW from geothermal resources.

There are many tools for estimating air pollution, AERMOD was used for the research to address concerns on evaluating model applicability. The performance of the model prediction is necessary for making informed decisions about the setting up and reviewing of regulation policy and mitigation action. For instance, making a decision based on an underestimation of the model threatens to lead to unhealthy air pollution within society around the geothermal field or as well as an inhabited area that is located even further away from the emission sources. On the other hand, if the model prediction is overestimated, it results in excessively high costs for H_2S abatement at the power plant facility (Langner and Klemm, 2011). In this respect, Indonesia has not developed an H_2S public health policy, though the government does set odour and emission standards. Meanwhile, in Iceland, the government's regulation of H_2S in ambient air is three times more stringent than the WHO air guidelines (150 $\mu g/m^3$ for 24-hour average).

If we look at these countries' energy policies as mentioned above, the utilization of geothermal power will continue to increase in the next decades. Indonesia utilizes geothermal power to achieve the goals of their climate change commitment to replace fossil fuel sources with renewable energy sources. Iceland continues to utilize renewable energy as well to pursue their climate change goals. However, the geothermal energy utilization is expected to increase H_2S air pollution in the future. Residential areas, a sensitive ecosystem, geothermal workplaces, and public facilities are of particular concern. The policy on H_2S air pollution requires a collaborative effort among relevant institutions and stakeholders, such as local communities and geothermal producers, so as to anticipate the effect of emissions from geothermal power generation and to raise public awareness on the topic.

This research studies model simulations which require proper meteorological database records (meteorological institution), a terrain map with high resolution (survey institution), continued H_2S observation data (environmental institution), and H_2S background information. This data cannot be archived without collaborative work of numerous institutions.

For further study, replication research in other geothermal fields is also expected, which combines the multi-disciplinary approach of *engineering* (i.e. environmental aspects of geothermal power plant operation), *geoscience*, (i.e. subsurface of geothermal reservoirs), *social aspects* (i.e. public health studies), *meteorology*, and *environmental science* (i.e. evaluating weather condition and model simulations).

1.2 Objectives

The study aimed to evaluate the performance of the AERMOD model in determining concentration from the Ulubelu power plants (UBL case) and Hellisheidi and Nesjavellir power plants (HELS-NES case) at residential areas and geothermal workplaces. The following are three specific objectives stipulated to achieve that goal:

- Compare the model applicability for predicting concentration at different time scales (1-hour, 24-hour, 8-hour, annual, seasonal periods) with the model's terrain setup (flat and elevated options) and using onsite and offsite meteorological data as the input data.
- Analyse the model applicability between the UBL and HELS-NES cases by comparing the model results with the H_2S measurements at residential areas in Reykjavík city (HELS-NES case) and Ulubelu village (UBL case) as well as evaluate the predicted H_2S concentration to the WHO air quality guidelines for H_2S, the Indonesian occupational health standard, and the Icelandic H_2S legislations.
- To recommend how to enhance air pollution policy based on the model applicability and the model results.

2. BACKGROUND

2.1 Hydrogen sulphide (H_2S)

2.1.1 Impact of H_2S

Gas emission is the main environmental impact resulting from geothermal utilization (Ármannsson and Kristmannsdóttir, 1992). The emissions from a geothermal field are varied and contain carbon dioxide (CO_2), hydrogen sulphide (H_2S), ammonia (NH_3), methane (CH_4), and trace amounts of other gasses (Dickson and Fanelli, 2004). In this study, the focus is on H_2S emission.

H_2S is a flammable, hazardous, colorless gas, with a characteristic odour of rotten eggs at a low concentration ranging from 0.69 to 417 $\mu g/m^3$ (ATSDR, 2014). H_2S is slightly heavier than air, and at high levels of concentration (> 560 mg/m^3), the gas is toxic, predominantly affecting the respiratory system. As such, H_2S has been classified among asphyxiate gasses (Chou, 2003).

Bates et al. (2002) suggested that low levels of H_2S concentration lead to chronic health hazards on the nervous system, cardio circulatory–diseases, and respiratory diseases. Also, Bates et al. (2015) studied the effect of hydrogen sulfide on the human body with focused on lung function, asthma and chronic obstructive pulmonary disease (COPD) at the geothermal area in Rotorua, New Zealand. The result confirmed that there was no evidence that exposure to chronic hydrogen to cause COPD. However, the researchers acknowledge only one sample area was taken and comparison cohort might have had problems to interpret. Those findings show human exposure even to low levels of H_2S concentration is still rare and more research is required to evaluate risk on health.

Some findings have indicated that human health impacts are more likely to occur given a high H_2S concentration. A good example is Lin et al. (2010) who investigated the combination of automobile emission and H_2S pollution in metropolitan Taipei. The authors highlighted that the mean concentration of H_2S at the geothermal area was 440.06 ppb or 612 $\mu g/m^3$ above the recommend the WHO air guidelines for H_2S (105 ppb or 150 $\mu g/m^3$) which might cause eye irritation. The pollutant leads the formation of secondary acid aerosol due to photochemical reactions. As a result, the concentration of acid aerosol in the city is the highest of any city. The study highlights that the combination of an H_2S pollutant from geothermal emissions and automobile emission might affect health issues in the city.

The geothermal impacts on human health have also been studied and could be influenced due to seasonality and age of the population. Finnbjörnsdóttir et al. (2015) identified the percentage increases in risk of death (IR %) due to natural and cardiovascular disease in a relationship with hydrogen sulfide emission from the geothermal power plant and traffic in Reykjavík, Iceland. Based on the study´s observed values of H_2S for a 24-hour averaging period, the mean concentration of H_2S is greater during the winter season (4 ± 8) $\mu g/m^3$ than the summer season (1.6 ± 2) $\mu g/m^3$, thus posing a greater risk of possible effects on human health during winter season than in summer. Based on age, Finnbjörnsdóttir et al. (2015) studied a sample population during 2003 – 2009 in Reykjavík. That indicated that elderly participants were more likely to die from a cardiovascular event (IR=1.99, 95% CL 0.1 to 1 for lag 0 and IR=1.99, 95% CL 0.2 to 1 for lag 1). However, the study highlighted a small population; it raises the question as to whether the effect of hydrogen sulfide was genuinely dependent on ages.

Also, OECD (2014) published the OECD Environmental performance for Iceland and indicated that there was still H_2S concentration exceeding the limit of the H_2S guideline in the Reykjavík area. It reported that the H_2S has increased since 2000 with increased geothermal activity. This might affect human health (i.e., increased asthma medicines) and the ecosystem (i.e. harmful to the moss vegetation).

Mutia (2016) studied the effects on the ecosystem of pollutant emissions from the Hellisheidi and Nesjavellir geothermal power plant (Iceland case) and Olkaria geothermal power plant (Kenya case). The results showed the pollutant of H_2S, indicated sulfur decomposition and accumulation affected on the growth of moss, e.g. *Racomitrium lanuginosum* around the geothermal area (for the Iceland case) and it showed weak indication of the effect on the shrub growth, e.g. *Tarchnonanthus camphoratus* in

Kenya. The study also highlighted tolerable limit of aqueous H_2S concentration (10.96 ppm or 15 mg/m^3 in air) for plants and soil around geothermal power plants for both cases.

2.1.2 H_2S standards and policies

Several geothermal producing countries have set up the hydrogen standards for odour, occupational health, and public health limit to reduce the environmental and human impact of H_2S. For example, in Iceland, the Icelandic Ministry of the Environment and Natural Resources (MOE) implements the Regulation No. 514/2010 regarding the concentration of hydrogen sulfide in the atmosphere. The standard public health limit for the 24-averaging period is 50 μg/m^3 (Icelandic Ministry for Environmental and Natural Resources, 2010). It is interesting, however, that the Government of Iceland regulates the level of H_2S more stringent than the WHO air quality guidelines, which is a minimum recommendation. It is because the standard limit considers avoiding long-term exposure to the human health (Björnsson and Thorsteinsson, 2013). This limit is three times lower than the WHO air quality guideline for the 24-hour averaging period (Chou, 2003). The occupational standard was also set by the Iceland government through the Ministry of Social Affairs. The limit for the 8-hour time-weighted average (TWA) for a day of work is about 7,000 μg/m^3 in order to protect worker`s health in the workplace (Icelandic Ministry of Welfare, 2012).

Ministry for Environment in Indonesia (MfE) legislates the odour standard No. 50 of 1996 for general industry. The odour standard sets about 0.02 ppm (28 μg/m^3), but it does not define averaging period (Ministry for Environment, 1996). In terms of protecting labour, the Government regulates the limit of 6970 μg/m^3 for 15 minutes occupational exposure or 1400 μg/m^3 for 8-hour exposure (Ministry of Manpower and Transmigration, 2011).

When a country does not have legislation on the odour and human impact of H_2S, the WHO air quality guidelines can be a reference indicator that serves as a standard limit of H_2S in the atmosphere. For instance, Nicaragua and Iran use the international legislation for 24 hours averaging period of H_2S exposure or standard public health limit at residential locations (Aráuz Torres; 2014; Hosseinzadeh, 2014). The WHO air quality guidelines have given a guidance value of 150 μg/m^3 average value for 24 hours (public health guideline) and 7-μg/m^3 for the 30-minute averaging period (odour standard) (WHO, 2000). Currently, Indonesia and Iceland do not have specific regulation or guideline for odour standard at geothermal fields.

The current international guidelines, the Indonesian legislation, and Iceland regulations of H_2S standards are presented in Table 1.

2.1.3 Modelling of hydrogen sulphide (H_2S)

Various studies on H_2S dispersion have been conducted to assess the environmental impact of the gas in the geothermal field, residential area, and terrestrial ecosystem. AERMOD results have been used in predicting the H_2S concentration in geothermal areas. The air pollutant simulation is useful for public health and environment management, especially when geothermal areas are near residential areas and sensitive ecosystems. Based on H_2S modelling, there are several factors that affect the predicted H_2S concentration, such as H_2S emission rate and terrain and meteorological conditions.

Several studies for predicting emissions of geothermal power plants have been conducted, such as Hosseinzadeh (2014), who studied H_2S modelling of a 55 MW geothermal power plant in Sabalan, Iran. The H_2S flow rate of the power plant was about 21.6 g/s and the predicted concentration range of H_2S for a 24-hour averaging period was 10 to 141 μg/m^3, 100 m northwest of the power plant. The H_2S concentration was below the limit of the WHO air quality guidelines. However, in some countries, for example, in Iceland, the standard of H_2S for a 24-hour averaging period is more stringent (50 μg/m^3) than the WHO air quality guidelines. Thus, the predicted H_2S would be considered harmful to the community nearby geothermal area in Sabalan, Iran.

TABLE 1: H_2S standard and guideline

Country /Institution	Averaging time	Value ($\mu g/m^3$)	Value* (ppm)	Standard	References
WHO air quality guidelines	24 hours 30 minute	150 7	0.11 0.005	Public health Odour	WHO (2000)
European Union	8 hours** 15 minute*** (STEL)	7000 14000	5 10	Occupational health	European Agency for Safety and Health at Work, 2009
Iceland	Annual	5	0.0036	Public health	Ministry for Environmental and Natural Resources, Iceland (2010)
	24 Hours	50	0.036		
	8 hours**	7000	5	Occupational health	Ministry of Welfare, Iceland (2012)
	15 minutes***	14000	10	Occupational health	Ministry of Welfare, Iceland (2012)
Indonesia	****	28	0.02	Odour	Ministry for Environment, Indonesia (1996)
	8 hours**	1400	1	Occupational health	Ministry of Manpower and Transmigration, Indonesia (2011)
	15 minutes***	7000	5	Occupational health	Ministry of Manpower and Transmigration, Indonesia (2011)

* Conversion concentrations of ppm based on the molar value at 25°C and 1 atm, 1 ppm = 1400 $\mu g/m^3$
** Time weighted average (TWA); workers are allowed to be exposed to the average H_2S concentration in air for an 8-hour work shift of a 40-hour work week.
***Short-term exposure limit (STEL); the H_2S concentration at working place exposes a maximum of 15-minute duration for workers
**** The standard does not state information of averaging period

Comparably, Aráuz Torres (2014) performed a study in the San-Jacinto Tizate geothermal system in Nicaragua that has a 72 MW installed capacity with an H_2S flow rate of about 45.5 g/s, or 1436.2 tons / year. The result of the H_2S modelling showed that some of the areas exceeded the 24-hour average value of the WHO air quality guidelines within 1 km from the source on the west side of the power plant. However, those locations affected by the exceeding the 24-hour averaging period were not in populated locations.

Ólafsdóttir (2014) studied the impact of H_2S distribution from the power plant of Hellisheidi (HEL) and Nesjavellir (NES). The power plants are about 28 km and 35 km east of Reykjavík, and the median flow rates of H_2S are 399 g/s and 279 g/s, for HEL and NES, respectively. The study highlighted that meteorological conditions at the HEL power plants affect the distribution of H_2S concentration. Furthermore, meteorological conditions such as wind speed, air stability, and the absence of precipitation also contributed to a higher concentration of H_2S in these areas.

As mentioned above, AERMOD has been used by the researchers to simulate the areas affected by the H_2S emitted from geothermal power plants whether in residential areas or workplaces for both, short-term and long-term exposure. However, it is also essential to evaluate the performance of the model simulation by comparing the model prediction with observation data (Zannetti, 1990). The performance of the dispersion model can be estimated by comparing the model result against field observation data.

Rzeszutek et al. (2017) demonstrated assessment of the AERMOD model in complex terrain using various prognosis meteorological data for a 1-hour averages period. The study evaluated the impact of SF6 emitted from the Tracy power plant experiment, Nevada, and the receptors located in the valley surrounded by the mountains. The study concluded the model results underestimated the observed pollutant concentration. The authors highlighted that the terrain height of the receptors are below the emission height as well as complex topography conditions might be affected by the model results.

Langner and Klemm (2011) studied the performance of the AERMOD model, which indicated a better performance than the software AUTSAL2000. It is because AERMOD uses meteorological data, complex topography, and vertical structure of the boundary layer, while AUTSAL2000 only use simple meteorological data and inaccuracy of rounding error. Based on this study, AERMOD was selected to assess the model performance and model distribution of hydrogen sulfide concentration from the emission sources of Ulubelu power plant (Indonesia), and Hellisheidi and Nesjavellir power plants (Iceland).

Zou et al. (2010) analysed the performance of AERMOD for various averaging periods. The exposure time of 1-hour, 3-hours, 24-hours, monthly, and annual averages were studied to simulate the impact of an SO_2 pollutant from mobile source (highway and major roads) and stationary emission sources located in Dallas and Ellis, USA. The authors summarized that the results of the model for short-term exposure (1-hour and 3-hour) did not perform as well as the model results for long-term exposure; AERMOD simulated better for a monthly averaging period or long-term periods.

Putranto (2016) modelled the H_2S and NH_3 distribution from the Kamojang geothermal power plant units 1-5 (235 MW total installed capacity). The results showed that the H_2S concentration was lower than the limits set by the WHO air quality guidelines of the 24-hour averaging period at receptors near the power plants. It was also highlighted that weather conditions such as wind direction temperature and air stability influenced the model simulations of H_2S concentration. The results showed that concentration during the wet season was 76 μg/m^3 while the H_2S concentration during the dry season predicted at 38 μg/m^3. The concentrations occurred mainly during the night until morning. The AERMOD performed better in determining the concentration of H_2S than the concentration of NH_3. The correlation of the predicted concentration between the observed values and the model values at the 24-hour average for H_2S and NH_3 were 0.89 and 0.5, respectively.

Various studies have been conducted to simulate the H_2S concentration from the emission of geothermal power plants using AERMOD. Therefore, the study to evaluate the performance of AERMOD in a geothermal area is vital to estimate the predicted concentration for short term and long term periods for mitigating the air pollution impact for the current and future development.

2.2 Dispersion model

AERMOD uses a Gaussian formula for simulating air pollutants. This section presents the basic concept of the Gaussian model adopted by the software and the modelling structure of AERMOD. Parameters for model simulations are also presented, such as plume rise, wind speed with height and air stability classification.

2.2.1 The basic concept of the Gaussian model

The Gaussian approach is often used to predict pollutant concentration. The model simulates the distribution of a plume from a point emission source (Q) released at elevation (H_e) to receptor points (x, y, z), which considers three-dimensional directions downwind (x), vertical (z) and crosswind (y). The expanding vertical plume (σ_z) and horizontal plume (σ_y) follow a normal distribution of concentration in vertical and lateral directions (Figure 1).

The formulae of the Gaussian plume (Figure 1) approach is presented by the equation (Harrison, 2014),

$$C\ (x,y,z) = \frac{Q}{2\pi\sigma_y\sigma_z u_h} exp\left[-\frac{y^2}{2\sigma_y^2}\right]\left(exp\left[-\frac{(z-He)^2}{2\sigma_z^2}\right] + exp\left[\frac{-(z+He)^2}{2\sigma_z^2}\right]\right) \quad (1)$$

where C = The air pollutant concentration (μg/m^3);
Q = The pollutant emission rate in mass per time unit (μg/s);
u_h = The wind speed at stack height (m/s);
σ_y = Standard deviation of concentration distribution in crosswind direction,

downwind C (m);

σ_z = Standard deviation of concentration distribution in vertical direction, downwind *C* (m);
y = Crosswind distance from the receptor to the plume centre;
z = Vertical distance from the receptor to the plume centre;
x = Downwind distance from the receptor to the plume centre;
H_s = Actual stack height (m);
Δh = Plume rise (m); and
H_e = Effective stack height or pollutant release height plus plume height ($H_s + \Delta h$);

In the case the plume drifts in a downwind direction (x) to a specified receptor at a ground level concentration; the parameters of y and z are assumed to be zero. The Gaussian equation from Equation 1 is computed as follows:

$$C\ (\mathrm{y} = 0, z = 0) = \frac{Q}{\pi \sigma_y \sigma_z u_h} exp\left(-\frac{He^2}{2\sigma_z^2}\right) \quad (2)$$

2.2.2 Plume rise (Δh)

The gasses are discharged through the emission stacks or pushed out by cooling fans through the cooling tower cooling tower. The exit flow rate mixes the gasses with the ambient air and the gases from a turbulent plume and travels in a downwind direction. The plume rise depends on the temperature of the gas, exit velocity, and atmospheric stability (Cooper and Alley, 1994).

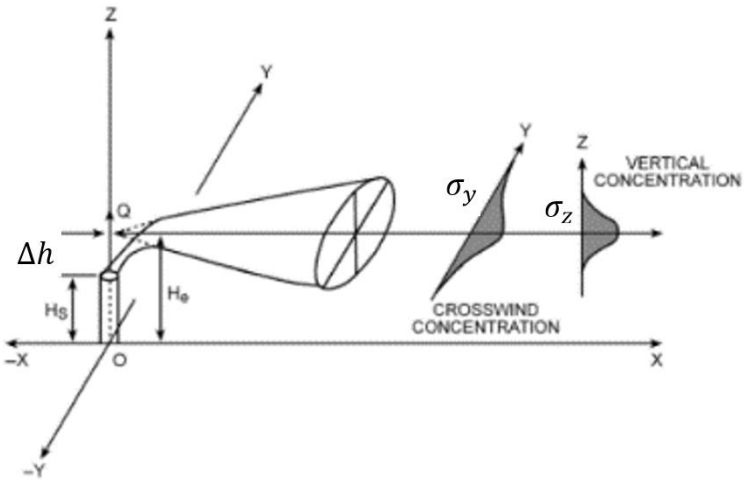

FIGURE 1: Gaussian air pollutant dispersion plume (Harrison, 2014, page 233)

A combination of the rising momentum and the buoyancy effect cause the gasses released to rise. The rising momentum contributes to the gases upward kinetic energy due to the exit velocity of the emission; this momentum weakens when the plumes start following the wind direction, whereas the buoyancy effect (thermal rise) still occurs after the plume is bending over. This effect changes due to the different temperature between the stack plume and ambient air (Cooper and Alley, 1994).

The Briggs method is widely used for calculating the plume rise, and this method is preferred for model simulation, including AERMOD, as it handles various surface wind speeds (US EPA, 2005; Lakes Environmental Software, 2018).

2.2.3 Wind speed with height (u_h)

In stable and unstable atmospheric conditions, wind speed profile changes due to air stability (Table 2). In the Gaussian equation (Equation 1), the wind speed at stack height is calculated from the equation as follows (US EPA, 2005):

$$u_h = \left(\frac{\boldsymbol{z_h}}{\boldsymbol{Z}}\right)^{\boldsymbol{P}} \quad (3)$$

where u_h = Wind speed at stack height (m/s);
z_h = Physical stack height; and
P = Wind shear exponent.

TABLE 2: Exponent values for determining the wind speed at height (retrieved from US EPA, 2005)

Stability	Exponent (*P*)
A	0.10
B	0.15
C	0.20
D	0.25
E	0.30
F	0.30

Table 2 provides exponent values for stability classes A to F. In AERMOD, these values are used for defining the wind profile based on air stability.

2.2.4 Air stability

Air stability is an essential factor that affects the concentration of air pollutants (Cooper and Alley, 1994). AERMOD uses the Pasquill approach as modified by Turner to classify stability based on parameters of solar insolation, wind speed, and cloud cover (US EPA, 2005). Based on Turner's method, the net radiation index (Table 3) and solar insolation class number (Table 4) for determining atmospheric class stability. The procedure of class stability is determined as described in Appendix A-1.

Atmospheric class stability is classified into six categories (A-F): 1/A, (extremely unstable), 2/B (moderately unstable), 3/C (slightly unstable), 4/D (neutral), 5/E (slightly stable), and 6/7/F (stable). In Turner´s method, air stability category-6, and category-7 are joined into category-F.

TABLE 3: Net radiation index (retrieved from Meteorological Resource Center, 2002, section 6.4.1)

Wind speed (m/s)	Net radiation index						
	4	**3**	**2**	**1**	**0**	**-1**	**-2**
0 – 0.7	1/A	1/A	2/B	3/C	4/D	6/F	7/F
0.8 – 1.8	1/A	2/B	2/B	3/C	4/D	6/F	7/F
1.9 – 2.8	1/A	2/B	3/C	4/D	4/D	5/E	6/F
2.9 – 3.3	2/B	2/B	3/C	4/D	4/D	5/E	6/F
3.4 – 3.8	2/B	2/B	3/C	4/D	4/D	4/D	5/E
3.9 – 4.8	2/B	3/C	3/C	4/D	4/D	4/D	5/E
4.9 – 5.4	3/C	3/C	4/D	4/D	4/D	4/D	5/E
5.5 – 5.9	3/C	3/C	4/D	4/D	4/D	4/D	4/D
≥ 6.0	3/C	4/D	4/D	4/D	4/D	4/D	4/D

TABLE 4: Solar insolation class number (retrieved from Meteorological Resource Center, 2002, section 6.4.1)

Solar altitude Φ (degrees)	Insolation	Solar insolation class number
$60 < \Phi$	Strong	4
$35 < \Phi \leq 60$	Moderate	3
$15 < \Phi \leq 35$	Slight	2
$\Phi \leq 15$	Weak	1

2.2.5 AERMOD modelling system

AMS and EPA collaborated and formed a working group, called AERMIC (AMS/EPA Regulatory Model Improvement Committee) in 1991 (Cimorelli et al., 2017). AERMIC developed the software AERMOD, which employed a regulatory application for assessing air pollution modelling.

AERMOD is a steady-state plume model that follows the Gaussian plume principals. The model is applied to elevated sources in simple and complex terrain, multiple sources, and urban and rural areas (US EPA, 2005; Cimorelli et al. 2017). The software introduces the concepts of the planetary boundary layer (PBL), turbulence structure, and vertical structure. Those concepts are an essential part of the application for air quality modelling (Cimorelli et al. 2017).

The PBL has an essential role in air pollution modelling, as the layer where pollutants are transported, diffused, deposited, advected, mixed, and chemically transformed (Moreira and Marco, 2009). This layer is formed by local conditions such as surface parameters; surface roughness, albedo, and topography. The layer consists of the Stable Boundary Layer (SBL) and Convective Boundary Layer (CBL).

In AERMOD, to calculate the concentration in the SBL the model assumes that the distribution in the vertical and horizontal direction follows a Gaussian probability function, but for the CBL, only a bi-Gaussian probability density function is used to measure vertical distribution (Cimorelli et al. 2017).

The technical calculation of those parameters is described in the AERMOD Model Formulation and Evaluation (Cimorelli et al. 2017). AERMOD calculates parameter assumptions and predicted concentration based on the conditions of the SBL and CBL layers. These parameters included wind profile, potential temperature, temperature gradient, lateral and vertical turbulence and predicted concentration both stable and convective layers.

The software requires wind speed and wind direction profiling for calculating model dispersion for PBL parameters. The potential temperature gradient is used to define buoyant plume penetration into and above the surface layer while the potential temperature profile parameter is applied for estimating the vertical temperature gradient. Those parameters are obtained for calculating the plume rise and estimating the distribution. AERMOD estimates the potential vertical temperature profile, which is a function of the potential temperature gradient profile (Cimorelli et al., 2017, page 30)

Cimorelli et al. (2017) describe the AERMOD two pre-processors AERMET and AERMAP. AERMET is the meteorological pre-processor, providing information for characterizing the PBL. The input data includes surface roughness length (z_0), albedo and Bowen ratio, and standard meteorological observations including wind speed, wind direction, temperature, relative humidity, precipitation, surface pressure, and cloud cover. AERMET calculates the PBL parameters which contain surface friction velocity (u^*), Monin-Obukhov length (L), convective scaling velocity (w^*), vertical potential temperature gradient above PBL (θ^*), convective and mechanical mixed layer heights (i_c and i_m), and surface heat flux (H). These scaling parameters are used to construct vertical profiles of wind speed (u), lateral and vertical turbulent fluctuations (σ), potential temperature gradient ($d\theta/dz$), and potential temperature (θ). Classification of surface heat flux defines the stability of the PBL, whereby $H < 0$, and $H > 0$ are stable and convective, respectively.

AERMAP is the terrain pre-processor designed to simplify and standardize the input of terrain data for AERMOD. AERMAP uses gridded terrain data for the modelling area to calculate a representative terrain-influence height or hill height scale (h_c) associated with each receptor's location (x_r, y_r). The terrain pre-processor computes elevations for both discrete receptors and receptor grids.

AERMOD handles the computation of pollutant impacts in both flat and complex terrain within the same modelling framework (Cimorelli et al., 2004). The modelling system structure of AERMOD is presented in Figure 2.

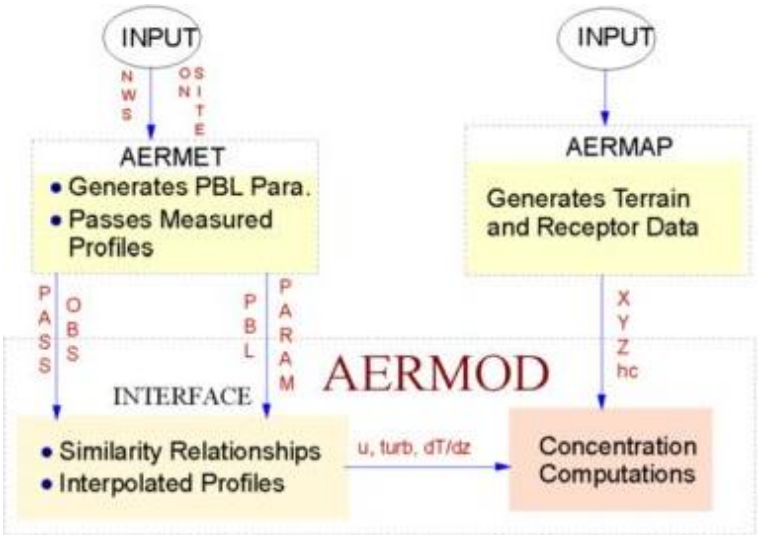

FIGURE 2: The modelling system structure of AERMOD consists of two inputs AERMET and AERMAP for simulating impact of pollutant concentrations (from Cimorelli et al. 2017, page 9)

2.3 Model performance

There are several methods to compare the model and the observation data. The Taylor Diagram was used to summarize the performance of the models. This method was chosen because it is suitable for comparing the performance of different models (Taylor, 2005). The diagram function from RStudio Team (2016) was applied to compute statistics for the modeled and measurement values. In RStudio, the packages of plotrix, datasets, ncdf4, and open-air were downloaded to draw and calculate the Taylor diagram formula.

In this study, the results of the model using AERMOD were validated using three statistical values to describe the performance of the model, these are coefficient of correlation (*r*), standard deviations (*SD*), and the root mean square error (*RMSE*). Results of the model are significant when the values of correlation are high, and the values of RMSE indicate a low error (Harrison, 2014). These results are visualized using the Taylor diagram in summarizing how close the modeled to the observed data. The following are the statistical formulas for determining the correlation coefficient, standard deviation, and RMSE are defined by (Taylor, 2001; 2005),

$$\boldsymbol{r} = \frac{\frac{\mathbf{1}}{\boldsymbol{N}}\sum_{\boldsymbol{n=1}}^{\boldsymbol{N}}\left(\boldsymbol{f_n} - \bar{\boldsymbol{f}}\right)\left(\boldsymbol{r_n} - \bar{\boldsymbol{r}}\right)}{\boldsymbol{\sigma_f \sigma_r}} \tag{4}$$

$$RMSE' = \frac{1}{N}\sum_{n=1}^{N}\left\{\left[\left(f_n - \bar{f}\right) - \left(r_n - \bar{r}\right)\right]^2\right\}^{1/2}$$

$$\sigma_f^2 = \frac{1}{N}\sum_{n=1}^{N}\left(f_n - \bar{f}\right)^2$$

$$\sigma_r^2 = \frac{1}{N}\sum_{n=1}^{N}\left(r_n - \bar{r}\right)^2$$

where f = Test field (predicted value);
r = Reference field (observed value);
$\bar{f}$ = Mean value for a test field;
$\bar{r}$ = Mean value for a reference field;
r = Correlation coefficient (range of correlation (r) are -1 to 1);
N = Sample;
σf = Standard deviation of an observed value;
σr = Standard deviation of a predicted value; and
$RMSE'$ = Root mean square difference error for test field and reference.

The Taylor Diagram is used to show a statistical comparison of the model performance (Figure 3). Six models are indicated by white, filled gray, and filled black circles. The correlation of the model is denoted along the arc from the x-axis to the

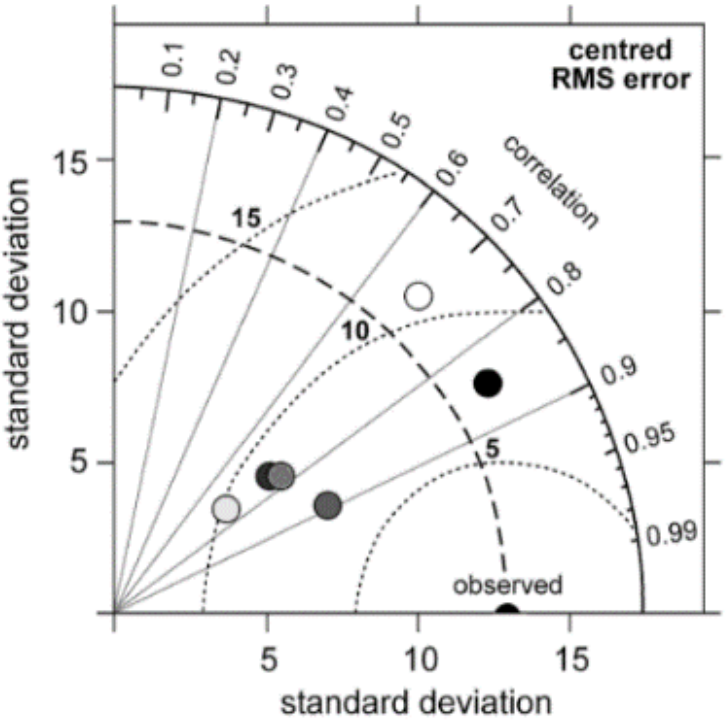

FIGURE 3: A sample Taylor diagram showing the performance of 6-models against observation data (Harrison, 2014, page 241)

y-axis. The RMSE value of the predicted value is determined by the dotted lines, and the dashed lines correspond to the SD of the predicted value at the observed value. Based on the diagram, the ranking of each model is examined by comparing the distance of the model to the observed data. A good model performance appears when the model point is closer to the observed data.

Positive values of correlation indicate a strong relationship between variables of the observed and the predicted values. On the contrary, the negative value of *r* indicates the relationship between the variables is strongly anti-correlated. Zero (null) value of correlation shows the two variables are not connected with each other (Harrison, 2014). Evans (1996) classifies the strength of correlation values by five levels such as very weak (0.00-0.19), weak (0.2-0.39), moderate (0.4-0.59), strong (0.6-0.79) and very strong (0.8-1.0).

RMSE indicates the difference between the observed and the predicted values. The lower values of the RMSE means the predicted value fits the observation data. Meanwhile, the standard deviation measures the spread out of mean values between the two variables (Figure 3).

3. DATA AND METHODS

This chapter describes the steps needed to perform the dispersion modelling. Firstly, the power plants that have been chosen as the study subject are described in a detailed manner regarding location, the running capacity, and profile of the surrounding area, including its population. Secondly, the data required to run the dispersion model comprised of the modelling software and site domain, input data, meteorological as well as the terrain data, which is needed not only for the model but also especially necessary for defining receptors and grids for the proposed study. Lastly, the analysis of the results of the model was carried out to compare the observed and the modeled values, and its result is further presented in the subsequent chapter.

3.1 Power plants

3.1.1 The power plant in Ulubelu

PT Pertamina Geothermal Energy (PGE) was established on 12 December 2006. The company is a subsidiary of PT Pertamina (Energy state-owned company), its geothermal division for upstream and downstream activities. PGE has a mandate from the Government of Indonesia (GOI) to develop 14 Wilayah Kerja Panas Bumi (WKP) or geothermal production areas in Indonesia. Among those WKP, five geothermal areas are already in operation; Kamojang (WKP Kamojang Darajat), Sibayak (WKP Sibayak-Sinabung), Lahendong (WKP Lahendong Tompaso), and Ulubelu (WKP Way Panas), Karaha (WKP Karaha Bodas). Other geothermal production areas are still being developed simultaneously and are divided into 3 projects, which are Hululais (WKP Hululais-Bukit Daun), Lumut Balai (WKP Lumut Balai-Margabayur), Sungai Penuh (WKP Sungai Penuh). Three production areas are in the exploration stage namely Gunung Lawu (WKP Argopuro), Seulawah (WKP Seulawah), Bukit Daun (WKP Hululais-Bukit Daun). Other production areas are under joint operation contract, which is located in Tabanan (WKP Tabanan Bedugul Bali), Salak (WKP Cibeureum Parabakti), Sarullla (WKP Sibual Buali), Patuha and Wayang Windu (WKP Pangalengan), and Darajat (WKP Kamojang Darajat). (PGE, 2015; Puja Dewi, 2018).

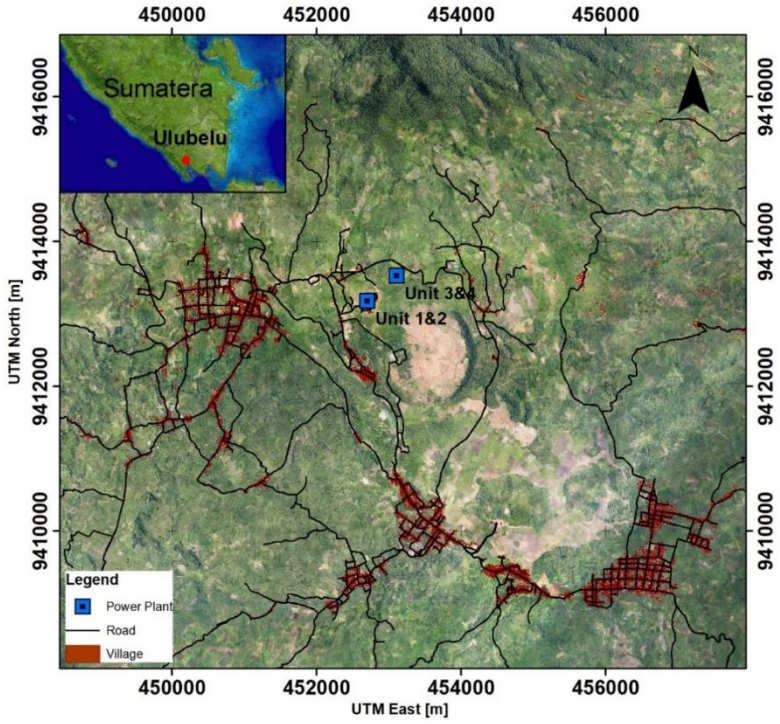

FIGURE 4: The study area in Indonesia, the map shows the Ulubelu geothermal area, residential area and coffee plantation

PGE supplies geothermal steam to Ulubelu power plant (Unit-1 is 55 MW_e), run by Indonesia Power (IP – a subsidiary electricity state-owned company in Indonesia), since September 2012, followed by a second unit (55 MW_e) on 24 October 2012 (PGE, 2015). The power plant for Unit-3 (55 MW_e), operated by PGE, began operation in 2016, while Unit-4 (55 MW) started commercial operation in March 2017. The Ulubelu geothermal area is located in Ulubelu Regency, Lampung Province, the size of the population nearby the power plant is 21,148 (Ulubelu District, 2017). Ulubelu villages, forest, and coffee farming surround the power plants at distances up to 7 km (Figure 4).

3.1.2 The power plants in Hellisheidi and Nesjavellir

The study area of the Hellisheidi and Nesjavellir power plants is located in the Hengill volcanic system (Figure 5). The inhabited areas of Hveragerdi town and City of Reykjavík are located 10 km southeast and 25-35 km northwest of the Hellisheidi power plants, respectively (Figure 6).

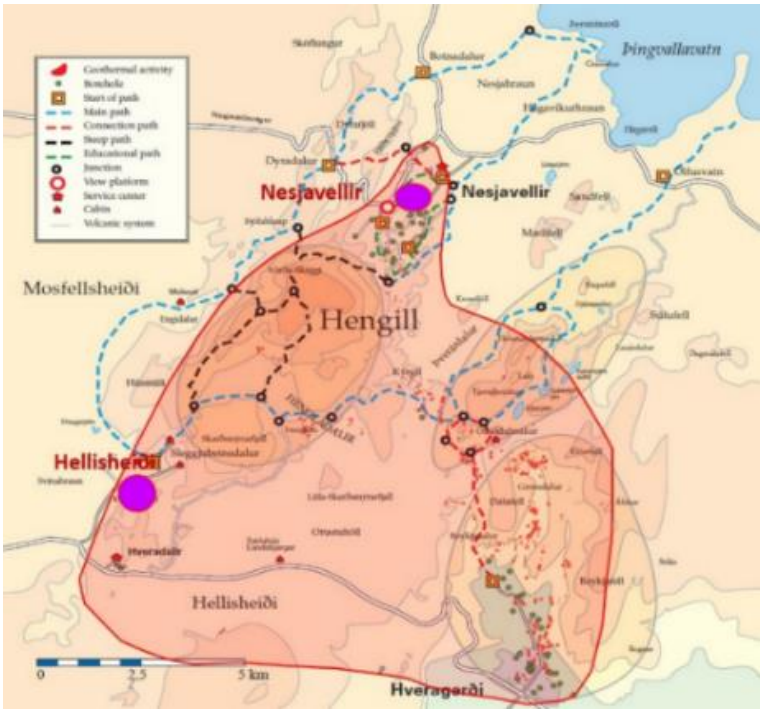

FIGURE 5: Map of Hellisheidi and Nesjavellir geothermal fields (Gunnlaugsson, 2016)

Reykjavík Energy operates the Hellisheidi and Nesjavellir power plants. The Nesjavellir power plant generates electricity with an installed capacity of 120 MW_e. It consists of two turbines operated from 1998, with 2x30 MW capacity, and third and fourth turbines (2x30 MW_e) installed in 2001 and 2005, respectively. Nesjavellir power plant has supplied 290 MW_{th} for district heating in Reykjavík since 2005.

Hellisheidi power plant produces 303 MW_e and 133 MW_{th}. It was commissioned in five stages during 2006-2011. The first and second turbines (2x45 MW_e) went into operation in 2006. The third, a low-temperature turbine (33 MW_e), went into production in 2007. Additional geothermal turbines were added in 2008 (2x45 MW_e) and in 2011 (also 2x45 MW_e). The hot water production started in 2010 with a 133 MW_{th} (Gunnarsson et al. 2013).

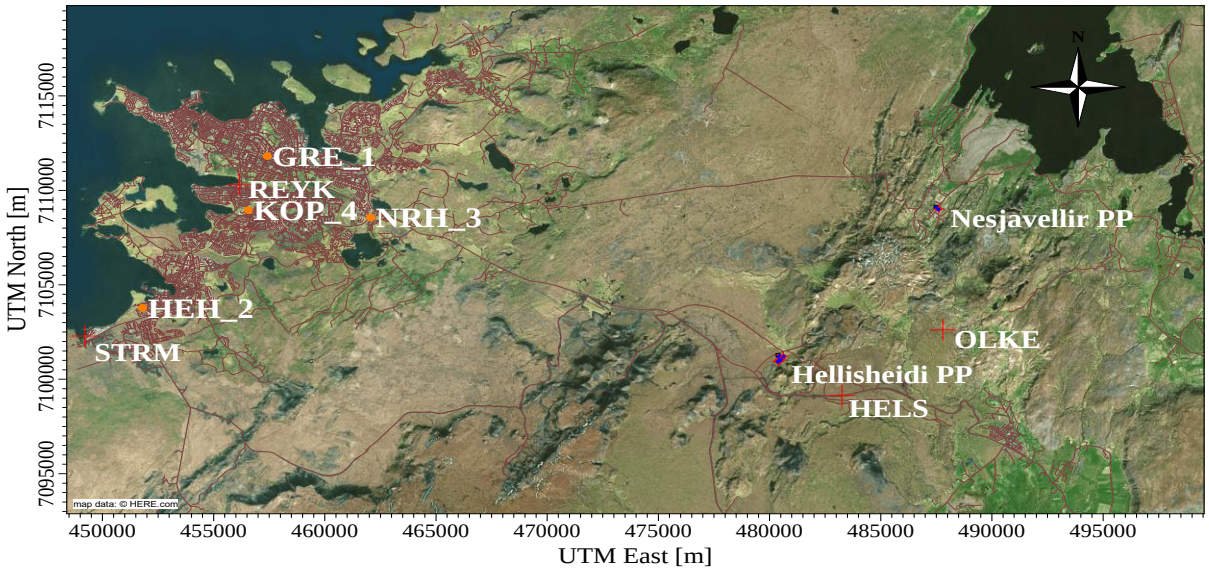

FIGURE 6: Map of Hellisheidi and Nesjavellir power plants and residential areas in Hveragerdi and Reykjavík city (Lakes Environmental Software, 2017)

3.2 Input data

3.2.1 Modelling software

In this research, the software application used for this assessment was AERMOD View^{tm} Version 9.4 supplied by Lake Environmental Software released on 11 May 2017 (Lakes Environmental Software, 2017). The setting used in the model using; default regulatory, non-default options, and concentration type was selected in the AERMOD.

3.2.2 Site domain

The projection of the study area for the Ulubelu (UBL case) and Hellisheidi and Nesjavellir (HELS-NES case) assigned the Universal Transverse Mercator (UTM) zone 27 North (Iceland), and zone 48 South (Indonesia). The site domain of the modelling area for the UBL case was set UTM coordinates of 434523 mE, 5292764 mS and 449523 mE, 5310625 mS, while for the HELS-NES case was plotted on UTM coordinates of 448078 mW, 9407804 mN and 457911 mW, 9419052 mN.

3.2.3 Source emission data

AERMOD requires information of H_2S emission data cooling tower structures for the model simulation, the data used for modelling is collected from the power plants to be operating at Ulubelu (UBL case) and Hellisheidi and Nesjavellir (HELS-NES case).

Ulubelu geothermal power plants release gas from the cooling towers into the atmosphere. The model considered the power plants to be operating at full load capacity. The H_2S emission from the power plants was calculated based on the data of Non-Condensable Gases (NCG) content and steam flowrate. The data of NCG and source input parameters are presented in Tables 5 and 6.

TABLE 5: NCG and H_2S content for Ulubelu geothermal plants

Source	Unit 1	Unit 2	Unit 3	Unit 4
NCG Content* (%)	0.6	0.6	0.5	0.6
H_2S Content of NCG (%)	3	3	3.5	3
Steam flowrate (ton/hour)	396	396	375.5	375.5

*NCG = Non-condensable gases

TABLE 6: Input parameters for the Ulubelu, Hellisheidi, and Nesjavellir geothermal power plants

Source	H_2S flow (g/s)	Gas exit temperature (°C)	Stack inside diameter (m)	Exit velocity (m/s)	Release height (m)
Ulubelu Unit 1	21	35	24.5	7	15
Ulubelu Unit 2	21	35	24.5	7	15
Ulubelu Unit 3	17	35	26	7	14.5
Ulubelu Unit 4	21	35	26	7	14.5
Hellisheidi	540	30	19.8	8.5	13.8
Nesjavellir	358	40	17.8	9.6	13

3.2.4 Building input data

AERMOD considers building impacts on H_2S concentration near the emission sources. In this study, the powerhouse and cooling tower structure were included in the AERMOD model to determine the effect H_2S concentration around the power plants.

In the AERMOD model, the rectangular building option was selected to define building dimensions in the graphical mode, and tiers of cooling tower structure and powerhouse were classified based on the

distance from the base elevation and height of the structures. The three-dimensional (3D) view of Ulubelu and Hellisheidi and Nesjavellir building structures are presented in Figures 7 and 8; model building properties are found in Appendix A-2.

FIGURE 7: Building structure of the Ulubelu power plants Units 1 and 2 and Units 3 and 4

3.2.5 Meteorological data

AERMET, the meteorological pre-processor required by AERMOD. The minimum weather data to generate meteorological files (i.e., surface file and profile) are wind speed, wind direction, cloud cover, and temperature (hourly surface observations) and upper air data (Weil et al., 2016). For the study, the meteorological data input in AERMET were wind speed (m/s) and wind direction (degree), temperature (°C), precipitation (mm), solar radiation (W/m^2), cloud cover (tenths), humidity (%), ceiling height (m), and station pressure (mbar).

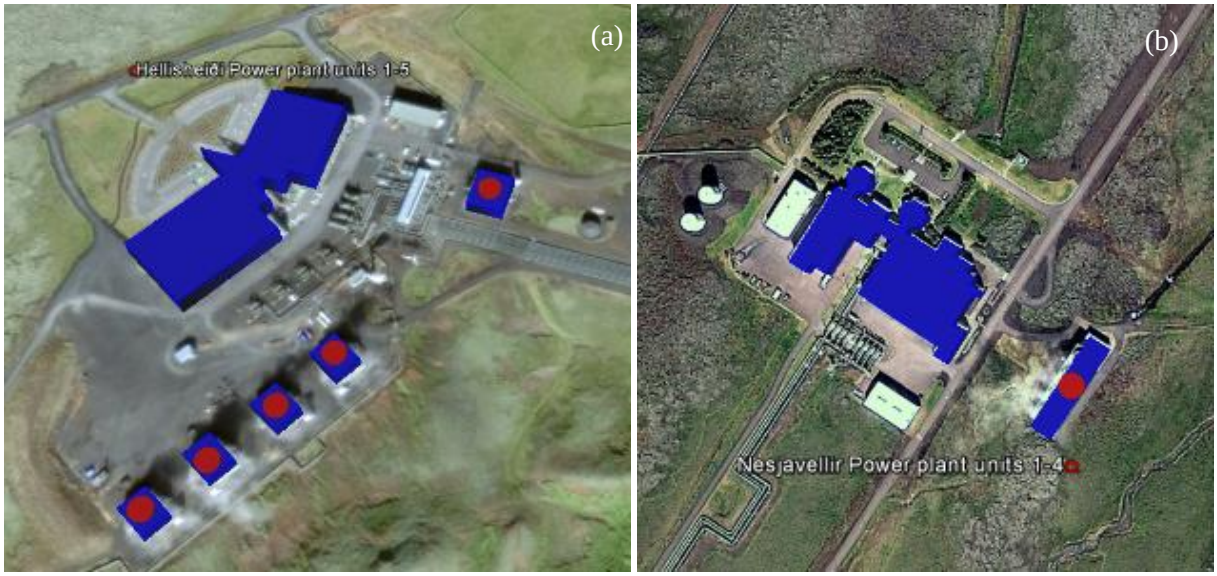

FIGURE 8: Building structures of (a) Hellisheidi power plants and (b) Nesjavellir power plants

AERMET runs meteorological from data based on hourly surface observation data and generates a surface file with planetary boundary layer parameters and profile file.

An upper air estimator mode was selected for the model to estimate the vertical profile. Five years of representative meteorological data and or at least 1-year site-specific weather data is recommended for model simulations (US EPA, 2005).

US EPA (2005) recommends calm hours and missing values of weather data should be less than 90% in model simulations for the regulatory purposes. The calm condition is defined as wind speed less than 1 m/s and this wind data is treated as missing values (US EPA, 2005). To review the missing values; "Procedures for substituting values for missing NWS meteorological data for use in regulatory air quality models" was applied for this study (Atkinson and Lee, 1992; Lakes Environmental Software, 2017).

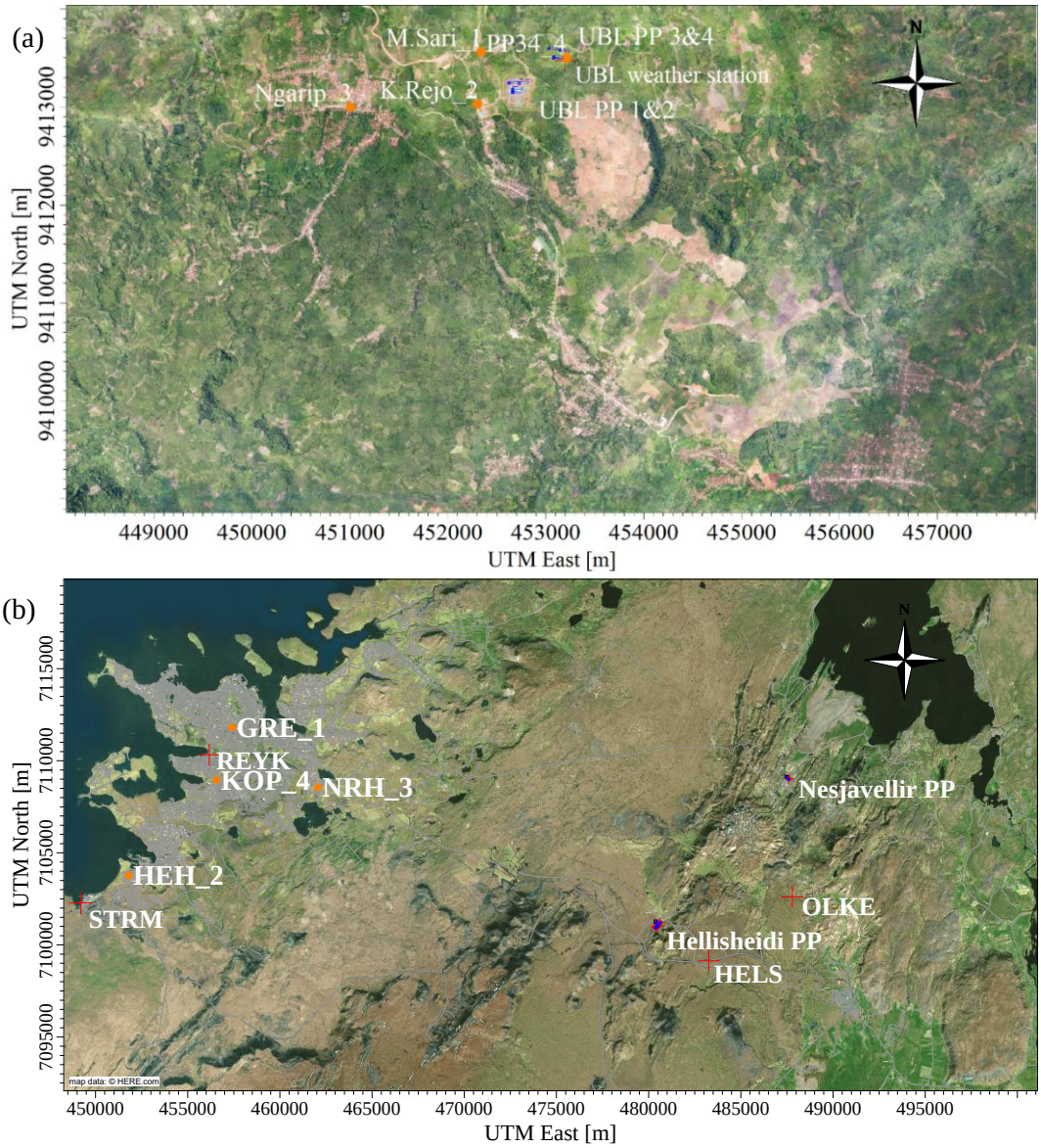

FIGURE 9: Location of H_2S measurement points (a) Ulubelu power plants and (b) Hellisheidi and Nesjavellir power plants. Circle and cross symbols present H_2S measurement points and location weather stations, respectively

The weather data were obtained for the model simulations at Ulubelu (UBL case) and Hellisheidi and Nesjavellir (HELS-NES case). The stations Ulubelu and Radin Inten II, Bandar Lampung, was used as input meteorological data, these stations were the most representative and provided relevant information necessary for the study, considering the availability and the quality of the data. Those meteorological data were obtained for a period from August 2016 to August 2017.

The direction of Radin Inten II and Ulubelu meteorological stations (see Figure 9a.) from the emission sources of PP units 1 and 2 are E83°N (67 km) and E60°S (up to 600 m), respectively. The Ulubelu weather station supplied meteorological data on wind speed, wind direction, temperature, station pressure, precipitation, and humidity. Cloud cover and ceiling height are required for running AERMET. Therefore, those were substituted using data from Meteorology Radin Inten II Bandar Lampung. For the HELS-NES case, the meteorological data (covering Hellisheidi and Nesjavellir power plant) was gathered from Hellisheidi (onsite weather station No. 31392) and Reykjavík (offsite weather station No. 1475) (see Figure 9b). The meteorological data were used for comparing various model scenarios as discussed in Section 3.2.8. The direction of Hellisheidi weather station from the Hellisheidi emission

sources is E72°N (7.5km) whereas Reykjavík meteorological station is located about 27 km (W68°N) from the emission sources.

All parameters of meteorological data for running AERMET were supplied from each of those stations, a parameter of solar radiation, cloud cover, ceiling height, and station pressure was substituted from the Reykjavík meteorological station. The meteorological data were collected from 1 January 2012 - 30 September 2017, except for the Reykjavík meteorological station was obtained from 1 January 2012 - 30 April 2017. Those meteorological data were provided for more than 5 years, as it is suggested by the U.S Air Quality Guideline (US EPA, 2005).

AERMET requires weather data as well as surface parameters of planetary boundary layers such as albedo, Bowen ratio, and surface roughness. For the Ulubelu study, these parameter values were obtained using the model land cover processor (AERSURFACE) (Weil et al. 2016; Lakes Environmental Software, 2017). This processor calculated surface values based on different types of land cover categories (i.e., forest, agriculture, residential area) with radius 5 km from the sources point. The surface values calculated by the AERSURFACE tool were albedo (0.17), Bowen ratio (0.58), and surface roughness (varies between 0.1 m and 0.7 m). For the HELS-NES case, the surface parameters used for the model were based on Wieringa (1992), Aradóttir et al. (1997); those parameters measured during summer. The surface roughness of east and west side was 0.25 m (rough) and 0.10 m (roughly open), respectively. Aradóttir et al. (1997) studied the range Bowen ratio at the south of Iceland was from 0.5 to 2 during the summer season, this study, the Bowen ratio (1) and albedo (0.2) were applied to all sectors for all seasons as reported by (Ólafsdóttir, 2014).

The weather data from both two cases mentioned above were identified in the study area for the Ulubelu, Hellisheidi and Nesjavellir power plants. The predominant wind direction at Ulubelu was southwesterly.

The average wind directions during the dry and wet seasons were 196$\pm$ 8° and 230 $\pm$ 4°, respectively. On an annual basis, the average wind direction was 212 $\pm$ 8° (Figures 10 a to c). For the HELS-NES case, the weather data was observed during winter and summer seasons as well as the annual period for the 5 years' data. Reykjavík (REYK) represents an off-site meteorological station, and Hellisheidi (HELS) weather station characterizes as an on-site meteorological station. The prevailing wind direction of REYK was easterly winds. The average wind direction or resultant vector of REYK for the winter and summer seasons were 118° and 169°, respectively, and 123° for the annual periods (Figure 10 d to f). For the HELS data, the prevailing wind direction for the winter and the annual period was northeasterly winds, while the predominant wind direction during summer was shifted and it flowed from the northwest (Figures 10 g to i).

The mean wind speeds of the UBL case reported 2$\pm$ 0.3 m/s (wet season), 2 $\pm$ 0.2 m/s (dry season), and 2 $\pm$ 0.3 m/s (annual). For the HELS-NES case, the average wind speeds of REYK data were 4.6 $\pm$ 0.1 m/s (winter season), 3 $\pm$ 0.6 m/s (summer season), and 3.7$\pm$ 0.3 m/s (annual). The mean wind speeds HELS reported 8 $\pm$ 0.1 m/s (winter season), 5 $\pm$ 0.7 m/s (summer season), and 6.7$\pm$0.3 m/s (annual) (Figure 11a).

Figure 11b shows that the average air temperature for the UBL case were 23 $\pm$ 1°C (wet season), 23 $\pm$ 1°C (dry season), 23 $\pm$ 1°C (annual). The mean temperature of REYK reported 1 $\pm$ 0.3°C (winter season), 11 $\pm$ 1°C (summer season), and 6 $\pm$ 0.8°C (annual). Meanwhile, the seasonal and annual air temperature of HELS were -1.7 $\pm$ 0.1°C (winter season), 8 $\pm$ 2°C (summer season), and 3 $\pm$ 0.9°C (annual).

The plots for the UBL case shows a stable condition of wind speed and temperature at 2 m/s and 23 ^{0}C, respectively. For the REYK and HELS data, it showed fluctuated values between the winter and summer season, the wind speeds fell off at 3 m/s –8 m/s, whereas temperature range was -1.7 – 11°C. The white circle indicates that the HELS data has outliers which the temperature values beyond the upper limit during the winter season, and some temperature values (HELS data) during the summer and annual periods were falling further outside the lower limit

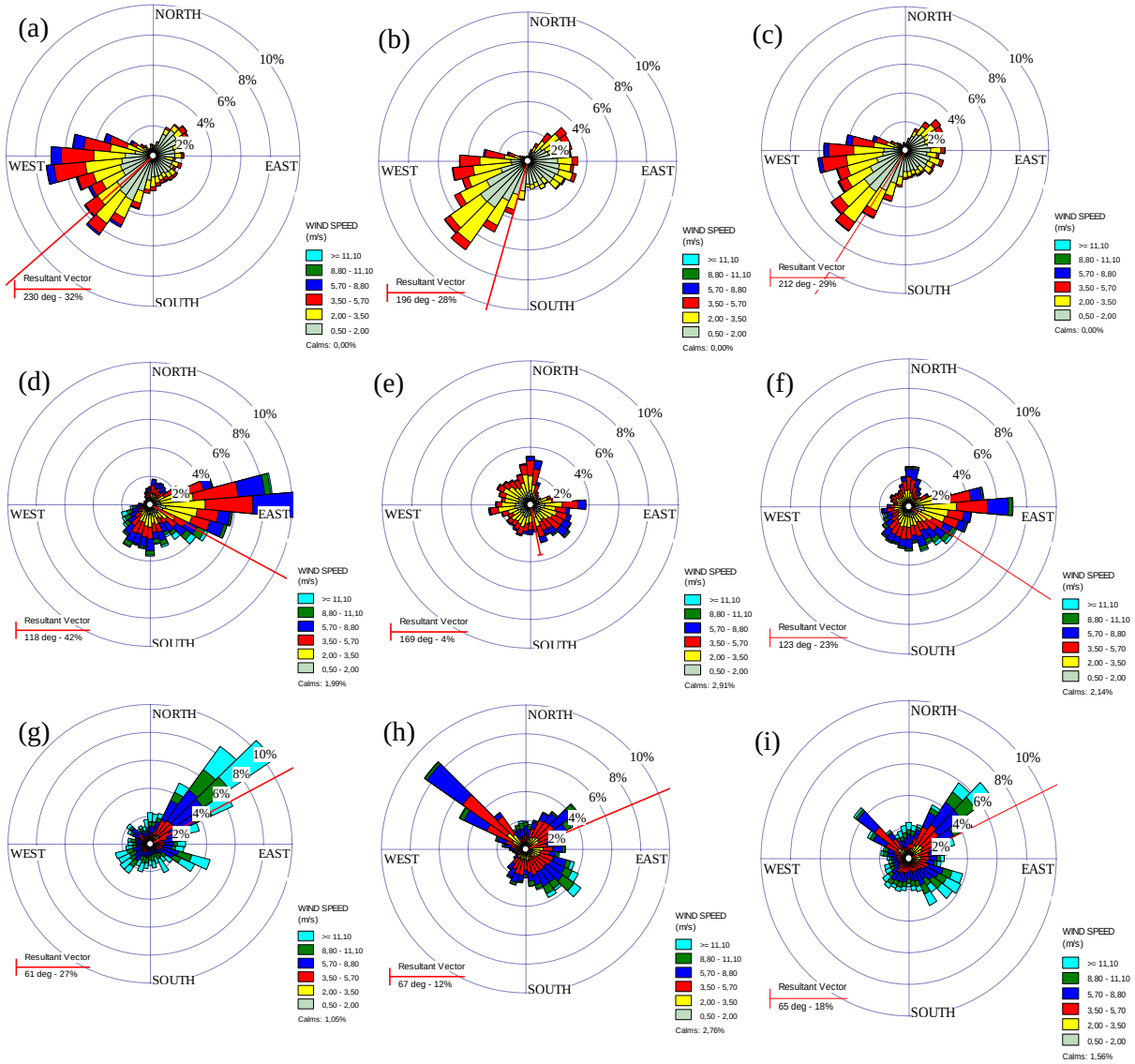

FIGURE 10: The wind rose plots illustrate wind patterns of the Ulubelu (UBL), Reykjavík (REYK) and Hellisheidi (HELS) meteorological data. The rose diagram for the UBL shows the patterns of wind direction during the wet season (October-March), dry season (April-September), and the annual period from August 2016 to August 2017. For the HELS-NES case, the diagrams present the weather data during the summer period starts from June to August, the winter season period begins December to February and the annual period January 2012 to December 2016. (a) UBL wet, (b) UBL dry, (c) UBL annual, (d) REYK winter, (e) REYK summer, (f) REYK annual, (g) HELS winter, (h) HELS summer, and (i) HELS annual

3.2.6 Terrain data

AERMAP, the terrain pre-processor, calculates elevation and height scale (*hc*) at each receptor based on terrain data provided as an input data. The output file produced by AERMAP is an input file in AERMOD (US EPA, 2004). In AERMOD, the terrain data is essential to check the accuracy of receptors elevations.

AERMAP pre-processor is designed for flat and complex terrain (i.e., elevated terrain option) conditions. AERMOD recommends flat terrain option where the base elevation of the receptor is lower than the base elevation of emission sources, whereas the model set up of elevated terrain option is recommended when the terrain height of receptor is higher than the elevation of the emission source

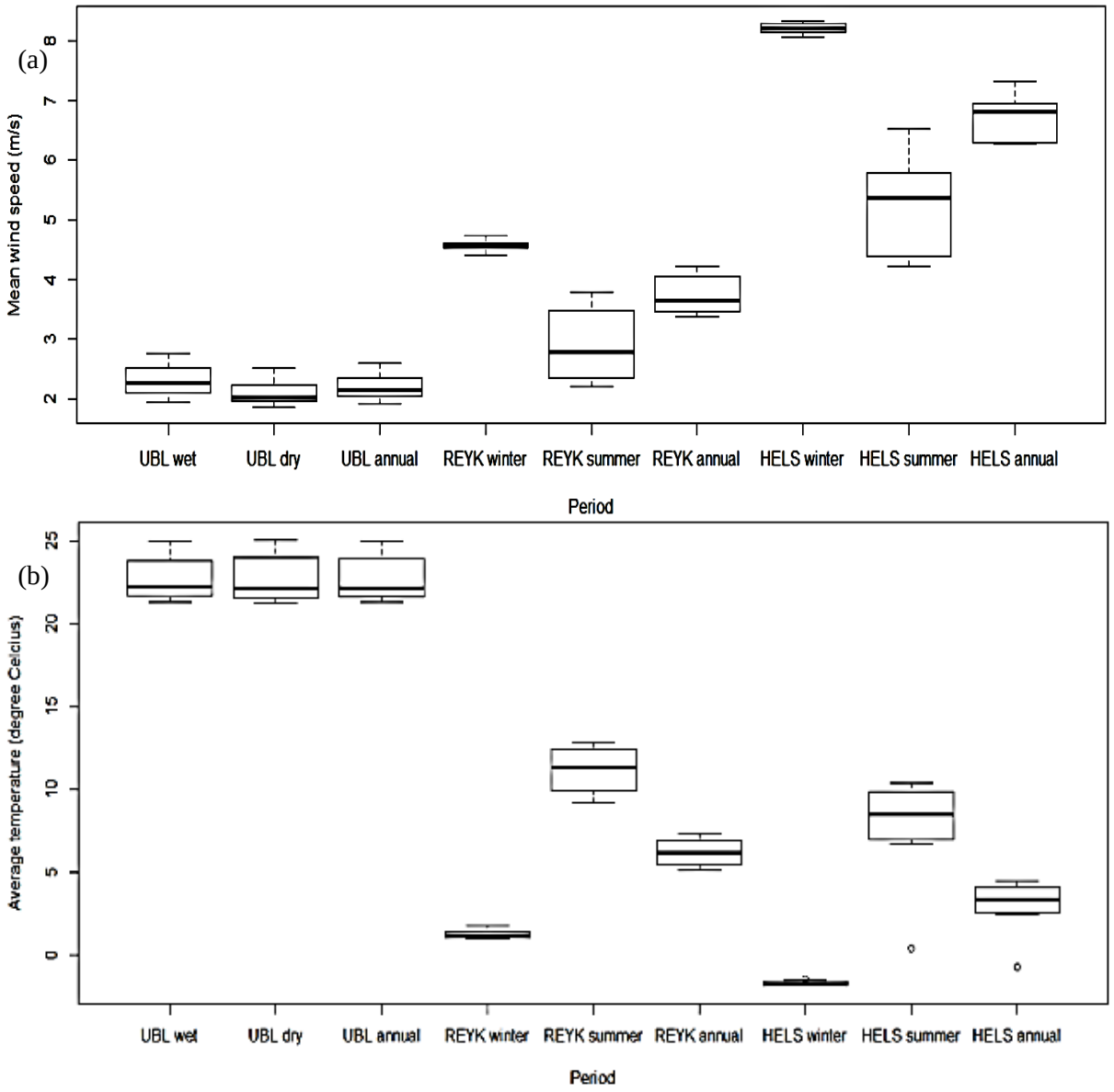

FIGURE 11: The box plots present (a) mean wind speed distribution, and (b) average hourly air temperature during the seasonal and annual period for the UBL, REYK and HELS meteorological station data

concentration (U.S. Environmental Protection Agency, 2016). In the software, this elevated terrain option is set as a default for the regulatory model.

AERMAP uses the Universal Transverse Mercator (UTM) coordinate system and accepts three types of terrain data; National Elevation Dataset (NED), Digital Elevation Model (DEM), and Spatial Data Transfer Standard (SDTS). However, only DEM data follows the standard format of USGS "blue book" that is suitable for AERMAP. Another type of terrain data need to change and follows the "blue book" format (US EPA, 2004, p. 1-2). US EPA (2016) recommends NED data being used for AERMOD, as this data is updated frequently.

For the study, in UBL case, a DEM (digital elevation model) terrain data was extracted from the U.S. Geological Survey (USGS). This data has a resolution of 30 m (1 arc-second). The terrain conditions of receptors and sources were considered in the model simulations. The terrain height of receptor location is identified, that some receptors are located lower and higher than the emission height. The input of terrain options (i.e., elevated and flat) was considered to predict concentration in the residential area (Ulubelu villages) and geothermal workplaces.

The HELS-NES case, A NAD GEOTIFF digital terrain data (The Shuttle Radar Topography Mission, SRTM version-3) with a resolution of 30 m (1 arc-second) downloaded from the USGS. The reference datum of SRTM elevation data is typically based on WGS-84 datum, whereas, AERMET was only accepted the NED terrain data with reference datum of NAD83. Therefore, this datum was converted to NAD-83 by using a Global Mapper software; this software has datum lists and transformation parameters, which configured the WGS-84 datum into NAD-83. A NAD terrain data then imported into AERMAP.

The domain boundary was set to cover modelling area within the study; included receptors, grids and emission sources locations. For the HELS-NES case, all the receptor are located below the emission height. AERMOD recommends that the model set up of flat terrain option considered the terrain height of receptors are below the terrain height of the stack (U.S. Environmental Protection Agency, 2016). In this case, the flat and elevated terrain options were considered to evaluate model performance to predict concentration in the residential area (Reykjavík area); in further details are explained in Chapter 4.

3.2.7 Grid point receptors

AERMAP uses gridded terrain data for the modelling area to calculate a representative terrain-influence height (*hc*) associated with each receptor's location (x_r, y_r). The terrain pre-processor computes elevations for both discrete receptors and receptor grids (US EPA, 2004). In the software, the receptor is defined within the boundary of the model that calculates the concentration of a pollutant in a specific location.

For the study, discrete Cartesian receptors and uniform Cartesian grids were defined in the model simulation; these receptors were located in the residential area and workplaces of geothermal power plants. In Ulubelu, the receptors were located at Ulubelu villages including Ngarip, Muara Dua, and Karang Rejo have a population of 9941 people (Ulubelu district, 2017). For the Iceland case, the receptors were located in Reykjavík City and at Nesjavellir and Hellisheidi. The city (capital area) is the the area with highest population density in Iceland and close to the power plants; the population 216,879 (Statistics Iceland, 2018).

The identification of particular discrete receptors also counted H_2S monitoring locations; the purpose of this was to compare the results of the modelled with the observed H_2S concentration.

The following are the gridded sizes, receptors, and emission sources were used for the models simulation:

Ulubelu power plants:

- Grid 1 – 9 km by 9 km at 20 m resolution;
- Grid 2 – 9 km by 9 km at 100 m resolution;
- Grid 3 – 9 km by 9 km at 500 m resolution;
- A total of 234,348 receptors and 15 particular receptors, and 4-emission sources were processed in AERMAP.

Hellisheidi and Nesjavellir power plants:

- Grid 1 – 50 km by 30 km at 100 m resolution; and
- Grid 2 – 50 km by 30 km at 1000 m resolution;
- A total of 157,848 receptors and 12 particular receptors, and 6-emission sources were processed in AERMAP.

3.2.8 Model scenarios

The models of Ulubelu power plants (4 x 55 MW_e) (UBL case), the Hellisheidi power plants (303 MW_e), and Nesjavellir power plants (120 MW_e) (HELS-NES case) were examined at different timescales, 1-hour, 8-hour, 24-hour, annual, and season average periods, using different terrain set up (i.e. flat and elevated options) and various meteorological data.

The scenario for the UBL case considered the dispersion modelling to evaluate the accordance with the observation data on 28-31 August 2017. The input meteorological data were obtained from the Ulubelu meteorological data representing site-specific meteorological data. The test case A evaluated the performance of the model simulation run at 8-hour period (i.e., occupational exposure) located at Power Plant Units 3 and 4, combined with the model results for the 24-hour averaging time option (i.e., public health exposure), focused on the concentration for the receptors located at residential areas of Mekar Sari, Ngarip, and Karang Rejo. Considering the terrain correction, the test cases A were simulated based on both possible model setups. Flat terrain option was selected where terrain height of the receptor was lower than terrain height of the emission sources, whereas the terrain set up elevated option was selected where terrain height of the receptor was higher than the elevation of the emission source (Appendix B, Table B-1). The test case A was also run and the case for the 8-hour averaging period option was excluded, the test case predicted using the 24-hour period where the H_2S concentration might have some impacts in the Ulubelu village residential area (Appendix B, Table B-1)

The Ulubelu power plants are located in a tropical climate and have two seasons; therefore, the models were evaluated three different periods; dry season (April-September), wet season (October-March), and annual period (meteorological data from August 2016 - August 2017. Each of season periods, the model simulations were run with different averaging time options (1-hour, 8-hour, and 24-hour period). The terrain correction of flat and elevated options was also examined in the model simulations.

The model evaluations for the HELS-NES were carried out and compared to the observed values on 9 November 2015, 1 March 2017, 23 June 2016, also seasonal as well as annual period using weather data from 2012 to 2016. Different time periods, terrain correction (flat and elevated options), and weather data was considered in the model simulations. Data from two weather stations were used with different distances from the source, Reykjavík Meteorological Station (REYK) as off-site meteorological data. This weather station was used to evaluate the model performance for long-distance dispersal. Meanwhile, the onsite meteorological data were obtained from the nearest weather station from the sources, which Hellisheidi (HELS). Subsequently, the results of the model were compared with the observed data at the receptors located at the Grensásvegur H_2S station (GRE), Hvaleyrarholt H_2S station (HEH), and Nordlingaholt H_2S station (NLH).

The model performances of the HELS-NES case were divided into two different cases; the first case B.1 was performed to evaluate the effect of using different meteorological data. The results of the model with different time scales for the 1-hour and 24-hour average were compared with the H_2S observation data at GRE, HEH, and NLH. The second test case B.2 examined the effect of terrain correction (i.e., flat vs. elevated options) and inputted meteorological data for the different averaging periods of 1-hour, 24-hour and annual periods. The results model were compared with the hourly H_2S observation station data at GRE, HEH, and NLH. The detailed scenario for the HELS-NES is presented in Appendix B, Table B-2.

Other model simulations for the HES-NES case were carried out and these models were run considering annual period, winter season (December-February) and summer season (June-August). The outputs seasonal model were highlighted only for the concentration during the winter and summer seasons which showed significant differences between those results. Those results were evaluated with the H_2S measurement data located in Reykjavík areas (Appendix B, Table B-2).

Considering the unavailability data of the background concentrations, which required in the AERMOD´s input model, therefore, the background concentration for the UBL and HELS-NES cases were not included in the model simulations.

3.3 Data collection of H_2S measurements

The study aimed to compare the results from software AERMOD with the observed H_2S monitoring that might affect the residential area and geothermal working area.

In Ulubelu geothermal fields, the obligation of monitoring requirement based on Environmental Impact Assessment (EIA). The company, PGE, follows the Indonesian odour standard; it measures for 1-hour averaging period for H_2S concentration (Ministry for Environment, Indonesia 1996). For the Ulubelu case, the ambient air concentration levels are monitored on three months' basis; therefore, these observation data could not use it in the study. In this study, H_2S observation points measured during the dry season in August 2017; 1 (one) sample near the power plant Units 3 and 4 for an 8-hour averaging period, and 3 (three) samples at Mekar Sari village, Ngarip village and Karang Rejo village (Figure 9a). The samples of the gas were analysed in accordance with the APHA 701 standard and the measurements were conducted by an external laboratory (PDAM Tirtawening, 2017).

The observation data of H_2S for the Hellisheidi and Nesjavellir cases were taken from the Icelandic Environmental Agency (Umhverfisstofnun - Environmental Agency of Iceland) and Icelandic Sudurland Health Agency. To compare the predicted values and the observed, the averaged hourly H_2S measurement data were obtained from Grensásvegur station (GRE), Hvaleyrarholt station (HEH), Kópavogur station (KOP), and Nordlingaholt station (NLH). These measurement points were considered as representative receptors in great area Reykjavík city (Figure 9b).

4. MODELLING RESULTS

This chapter describes the results for evaluating the model simulation based on various meteorological data input and terrain model setup options (i.e., elevated and flat). This study was done to check the applicability of AERMOD to predict H_2S concentration corresponding to odour nuisance (1-hour period), occupational health impact (8-hour period), and public health impact (24-hour, seasonal, and annual periods).

Two different cases were modelled in the simulations. First, the emission source from the Ulubelu Power Plant in Indonesia (UBL case) represented the short-range dispersion model (i.e., less than 3 km). Second, the Hellisheidi-Nesjavellir Power Plant (HELS-NES case) examined model simulations for long-range dispersion (i.e., up to 25 km from the sources). The Taylor diagram was then used to summarize the relationship between the model and the observation data, the diagram applying the parameters; correlation coefficient (*r*), standard deviations (SD), and the root mean square error (RMSE) (see Section 4.1).

The model of the UBL case and the HELS-NES case was simulated by AERMOD to evaluate the effect of seasonal and annual weather condition at measurement points as well as receptors where located at residential area and workplaces (Section 4.2). The model simulations used the input of meteorological data (offsite and onsite) and terrain set up options based on model results from Section 4.1. Subsequently, the results of the model were compared to the observed data (especially for the HELS-NES case). The highest predicted concentrations for the UBL-HELS-NES cases were also compared to the WHO air quality guidelines for H_2S, the Indonesia occupational health standard, and the Icelandic H_2S legislations at the residential area in the Reykjavík area and Hveragerdi (HELS-NES case) and Ulubelu village (UBL case) as well as geothermal workplaces at the two cases.

4.1 Model performance

The model simulation is used to estimate air pollution on air quality, and it helps to design appropriate emission control strategies by applying pollutant abatement and setting monitoring controls (i.e., continuous or passive monitoring). The accuracy of model simulations should be able to be used as baseline information for making air quality policy decisions and assist the policymakers to plan for mitigating measures against the consequences of the air pollution.

In order to simulate the accuracy of model applicability. The models run were evaluated to compare the highest predicted concentrations at some specific receptors to observation values. The observation data for UBL case was collected on 28-31 August 2017. Meanwhile, the HELS-NES case collected on 9 November 2015, 1 March 2017, 23 June 2016 and annual from 2012 to 2016. The model scenarios for both cases are presented in Section 3.2.8

4.1.1 Model performance for Ulubelu case

A. The highest 8-hour and 24-hour values

The models run on evaluating the model of 24 hour period, mixed models of 8-hour and 24-hour periods, and terrain set up options (i.e. flat-elevated and elevated).

The results of the model considering time scales showed that the test case model of the 24-hour period worked better the test case mixed models of 8-hour and 24-hour periods (Figure 12). The Taylor diagram illustrates that the distance of the mixed model was far off to the observed value. On the other hand, the test case model of the 24-hour was closer to the observation point. The results of the model are useful when the values of correlation are high, and the RMSE value is a low error (i.e., low error) (Harrison, 2014), and the SD is low. In other words, the model fits the observed data if the distance of the model is closer to the observation data point.

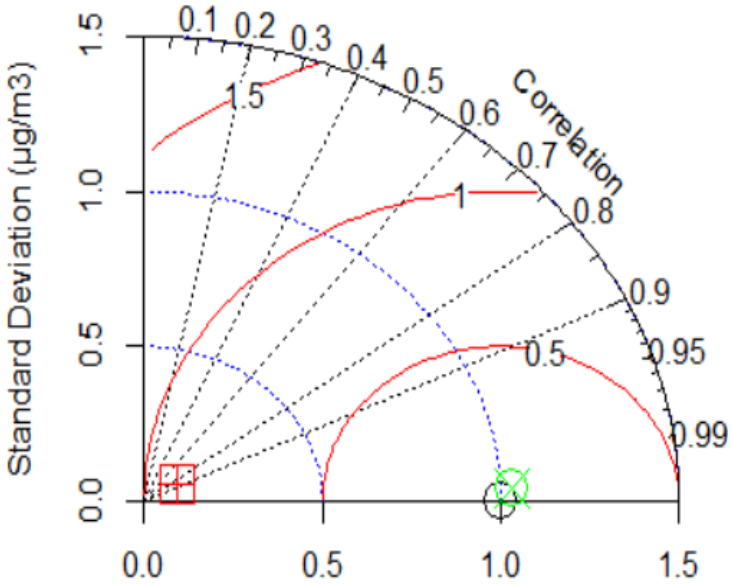

FIGURE 12: Taylor diagram of the UBL case showing results using the same model set up and different time scales compared to observation data. The mixed models of 8-hour and 24-hour periods, model of the 24-hour period and observation point are indicated by the square plus (red), circle cross (green), and white circle, respectively

For the terrain effect, flat-elevated terrain options performed better than the elevated option, because the flat-elevated terrain set up considered different terrain height of receptors (i.e. higher or lower) to the terrain height of emission source (Table C-1, Appendix C). For instance, both receptors at Mekar Sari (842 m a.s.l.) and Ngarip (869 m a.s.l.) which are located higher than the elevation of the emission source of Unit 3 and 4 (802 m a.s.l). Those values were obtained from the model simulated with the elevated terrain option. Meanwhile, the model set up of flat terrain option was considered with the terrain condition of the receptor (Karang Rejo, 796 m a.s.l) lower than the base elevation of the emission source of Units 3 and 4 (802 m a.s.l). The detailed results of model simulations and model performance are presented in Appendix C (Tables C-1 and C-2).

Overall, the UBL case indicated that the results of the modeled 24-hour period had a better performance than the results of mixed models at 8-hour and 24-hour averages period. Besides the model performance worked better when the model simulations accommodated the terrain correction model (i.e flat-elevated) based on terrain conditions of the receptors and the emission source.

4.1.2 Model performance for Hellisheidi and Nesjavellir case

B-1 Model performances for various meteorological data stations

The highest 1-hour and 24-hour values

Eight models were run at two different time scales, 1-hour and 24-hour periods, which using four sets of weather data (i.e., STRM, REYK, HELS, and OLKE). The 1-hour and 24-hour models run using meteorological data from STRM and REYK (offsite weather data) had a positive and similar correlation (*r* 1 hour = *0.3*, r 24-hour = 0.5). The model measured using OLKE and HELS (onsite weather data) had a negative correlation, *r* 1-hour = -0.3 and *r* 1-hour = -0.2, respectively (Table 7). The correlations of onsite data on the 24-hour were r 24 = - 0.5 (OLKE), and r = 0.7 (HELS). The negative correlation indicated the models did not work for the receptors GRE, HEH and NLH that located up to 25 km from the sources at the receptor.

To conclude, in terms of weather station locations, the model was run for STRM and REYK weather data performed better than OLKE and HELS for model simulations either 1-hour and 24-hour. Comparing the model results on time scales, the modeled 24-hour performed better than the 1-hour model to examine H_2S concentration at receptor in Reykjavík area (i.e. GRE, HEH, and NLH); the model indicated that close distance from weather stations to the measurement sites is better than a close distance to the emission source.

TABLE 7: Model performances at the time scales of 1-hour and 24-hour periods simulated by four meteorological stations in the Hellisheidi-Nesjavellir area (test case B-1)

Model periods	**Weather stations***	**Correlation (r)**	**Standard deviation (SD) model (µg/m^3)**	**Standard deviation observed data (SD) (µg/m^3)**	**Root mean square error (RMSE) (µg/m^3)**
B** Nesjavellir (NES) and Hellisheidi (HEH) – Iceland					
1-hour	STRM	0.3	4.9	35	33
1-hour	OLKE	-0.3	1.5	35	35
1-hour	HELS	-0.2	5	35	36
1-hour	REYK	0.3	5	35	33
24-hour	STRM	0.5	1.59	24	21
24-hour	OLKE	-0.5	0.4	24	22
24-hour	HELS	0.7	0.2	24	22
24-hour	REYK	0.5	1.6	24	21

*REYK = Reykjavík meteorological station, STRM = Straumsvík meteorological station, HELS = Hellisheidi meteorological station, OLKE = Ölkelduháls meteorological station.
**The input values of the test case B-1 were obtained from the model simulation as presented in Tables C-3 and C-4, Appendix C.

B-2 The effect on terrain set up correction and various meteorological data from STRM, REYK, and HELS

The highest 1-hour values
The model represented the performance of the 1-hour period considering terrain corrections (flat vs. elevated options). The concentration ranges at the GRE receptor using elevated terrain option (0.78 – 15.78 µg/m^3) was lower than the concentration range using flat option (0.85 – 17 µg/m^3), whereas the observed values were 41 – 77 µg/m^3. It indicated a flat model performed better than an elevated model. The detail results of the model and observation data are presented in Appendix C (Tables C-5 and C-6).

First, the model runs on the 9 November 2015 and 1 March 2017 (Figure 13a and b) showed flat model performed better than an elevated model. STRM model had the highest correlation (*r* flat = 0.4, *r* elevated = 0.3) followed by REYK (*r* flat = 0.3, *r* elevated = 0.04) and HELS (*r* flat = -0.05, *r* elevated = - 0.14). HELS showed a negative correlation between the modeled and the observed data. It indicated that the predicted concentration of the emission sources to the receptors in the Reykjavík area were affected by the terrain condition. In terms of standard deviation (SD) and root mean square error (RMSE), the model showed a large spread of the SD (SD flat = 5 – 7 µg/m^3, SD elevated = 4.5 – 10 µg/m^3, observed data with SD = 30 µg/m^3 and had a large root mean square error (RMSE) different for all the models (27-30.75 µg/m^3).

Second, the model runs on 23 June 2016 (Figure 13c and d) showed the correlations of the models for REYK and STRM datasets have a correlation coefficient of *r* flat and elevated options = 0.2, and HELS of *r* flat and elevated options were 0.15. Those were classified as the weak correlation between the modelled and the observed values (Evans, 1996). The SD values between the modelled (range of SD flat and elevated options = 0.3-1 µg/m^3) and the observed values (0.4 µg/m^3). The RMSE of these models had lower values (range of RMSE = 0.47 - 1.3 µg/m^3) compared to another model on 9 November 2015 and 1 March 2017.

The wind speed variability affected the results of the model simulation, for instance, the average wind speeds of the STRM and REYK for the model on 23 June 2016 was lower (1.5 m/s) than the average wind speeds for the model on 9 November 2015 also 1 March 2017 (3 m/s).

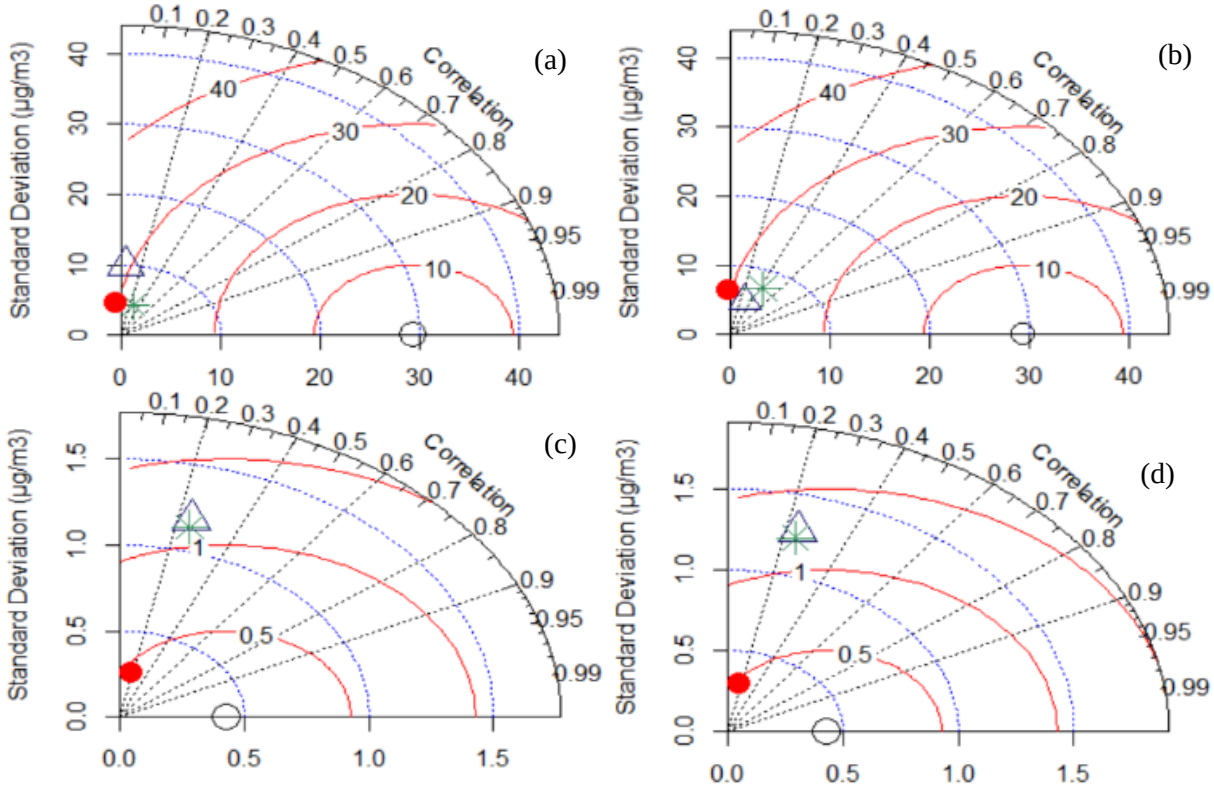

FIGURE 13: Taylor diagram presenting a comparison between the model results and the observation values for 1-hour averaging period considering different terrain conditions (elevated options, left side and flat option, right side). (a) Test case elevated model (b) test case flat model on 9 November 2015 and 1 March 2017 (c) test case, elevated (d) test case, the flat model on 23 June 2016. The green star, solid circle red, and triangle point up denote the symbol-meteorological stations of STRM, HELS, and REYK, respectively. The white circle indicates the observation value

Overall, in this test case, AERMOD did not work well for the modelling of the 1-hour period, and some of the model runs indicated that flat terrain estimated higher concentration than elevated terrain. The model performance indicated that STRM and REYK worked better compared to the observed data located in the greater Reykjavík area (GRE, HEH, and NLH) and the locations of those H_2S measurements are close to the weather stations.

The highest 24-hours values

The results of a model run considering terrain set up, different wind patterns on day samples, and a distance of weather stations to an observation point. The test case on 9 November 2015 and 1 March 2017 showed that the correlation of REYK (r = 0.6) on flat terrain option was at the highest compared to HELS (r = -0.1) and STRM (r = 0.5). The correlation of REYK and STRM is classified as moderate (0.4-0.6) (Evans, 1996), while the correlation of HELS for the elevated and flat terrain option was negative or no correlation (r elevated = -0.09 and, r flat = -1) (Table 8).

The comparison of a model result against the H_2S observed value was also presented, on 9 November 2015, the highest predicted concentrations on flat, and elevated terrain options (REYK, 4 µg/m^3 and HELS, 1 µg/m^3), while the observed value was 25.98 µg/m^3. Meanwhile, the model predictions on 1 March 2017 using flat terrain option (REYK, 6 µg/m^3, and HELS, 1.5 µg/m^3), on elevated (REYK, 4.95 µg/m^3, and HELS, 1.4 µg/m^3). The observed value on 1 March 2017 was 65.9 µg/m^3 (Appendix C, Table C-7).

The test case on 23 June 2016 showed that the correlation of REYK, STRM, and HELS for elevated and flat terrain option was significantly high (r = 0.9) (Table 8). This correlation was classified as a strong

relationship between the modeled and the observed values (Evans, 1996). The standard deviation of the observed data and the model values presented a small spread of the SD values from the modeled and the observed data. The test case on 23 June 2016 also showed that the observed value at receptor GRE (1.9 µg/m^3). The models using flat terrain option (REYK, 0.7 µg/m^3, and HELS, 0.09 µg/m^3) showed slightly higher than the models runs applied elevated terrain option (REYK, 0.6 µg/m^3, and HELS, 0.07 µg/m^3) (Appendix C, Table C-7).

TABLE 8: Model performances at the 24-hour average period for the different terrain options

Test case number	Periods	Weather stations*	Correlation (r)		Standard deviation (SD) model (µg/m^3)		Standard deviation observed data (SD) (µg/m^3)	Root mean square error (RMSE) (µg/m^3)	
			Elevated	Flat	Elevated	Flat		Elevated	Flat
B**. Nesjavellir (NES) and Hellisheidi (HEH) – Iceland 9 November 2015 and 1 March 2017									
	24-hour	REYK	0.5	0.6	1.6	1.8	24	21	21
	24-hour	STRM	0.5	0.5	1.6	1.7	24	21	21
	24-hour	HELS	-0.09	-0.1	0.5	0.6	24	22	22
23 June 2016									
	24-hour	REYK	0.9	0.9	0.09	0.09	0.5	0.3	0.3
	24-hour	STRM	0.9	0.9	0.09	0.09	0.5	0.3	0.3
	24-hour	HELS	0.9	0.9	0.008	0.008	0.5	0.4	0.4

*REYK = Reykjavík meteorological station, STRM = Straumsvík Meteorological station, HELS = Hellisheidi meteorological station;

**The input values of the test case were obtained from the model simulations presented in Appendix C, Table C-7.

All above, the condition of wind patterns and the distance weather stations to receptors explained the results. The test case on 9 November 2015 and 1 March 2017, the wind direction of HELS was northeast with the wind speed at 3 m/s to 4 m/s, this direction was not flowing to receptors in Reykjavík area, and the distance also affected it due to the receptor point was located at about 25 km away from the source (see Figure 11b). On the other hand, the wind direction REYK and STRM at the same days flew from the east toward to the receptors at the wind speed of 2 - 3 m/s. The test case n 23 June 2016, the wind speed of HELS was 3.8 m/s and it flew 96 % of the time to the north-west. Meanwhile, STRM and REYK had the same wind patterns, where the wind direction was south-west, and the wind speed flew 1.5 m/s at 93 % of the time. In addition, the percentage result values of the models were compared to the observation data.

For the test case on 9 November 2015, it was only 4% (model HELS) and 16 % (model REYK) highest concentrations matched to the measured data. The result comparisons on 23 June 2016 were 3.6 % for model HELS and 37 % model REYK. Whereas the sample data on 1 March 2017 was the lowest percentage among those samples, it was only 2 %, HELS, and 8 %, REYK highest concentrations matched to the observed values. Similar pattern on other data samples where model prediction values using REYK data was higher than model simulation values using HELS. It showed that models using REYK predicted higher concentrations than models HELS. The detail results of the models and observation data are presented in Appendix C, Table C-7.

The results demonstrated that the test case for the model on 23 June 2016 performed better than the model on 9 November 2015 and 1 March 2017. It indicated that models worked better with the weather conditions for the sample obtained on 23 June 2016 (low wind) than on 9 November 2015 and 1 March 2017. In terms of terrain effect, flat terrain option (9 November 2015 and 1 March 2017) showed higher concentration than the model set to elevated terrain option. Also, the results indicated that the model worked better when the measurement point is closer to the weather stations of STRM and REYK than far away from the HELS weather station.

Annual average

Figure 14 shows the model performances of REYK, HELS, and STRM using model set up of (a) elevated, and (b) flat, terrain options. Overall, the result of model points was far off to the observed data point, however, the annual model set up with flat terrain option performed slightly better than the model setting as elevated terrain option.

The model on flat terrain option showed the correlation between models STRM and REYK was the same (r = 0.5), while HELS was 0.6 (r). The diagram helped to visualize how closely the distance models to the observed data point, therefore, even though model HELS, presented a high correlation values, but the RMSE which indicated by the red solid line (1.5 = µg/m^3) was larger than other models (REYK and HELS, 1 = µg/m^3). The lower value of the RMSE meant model fit to the observation data. Another parameter, standard deviation (SD) model HELS was relatively smaller about 0.2 µg/m^3 than SD observation data 1.7 µg/m^3, on the other hand, the SD models REYK and STRM was the same as 0.5 µg/m^3.

The model on elevated option was less performed than the flat models. The correlation of the models STRM and HELS were 0.6 (r), and model REYK was 0.55 (r). As explained on flat model results, RMS error values of model STRM (1.6 µg/m^3) and model HELS (1.5 µg/m^3) were higher than model REYK (1 µg/m^3). On elevated option, a standard deviation of the models was relatively smaller about 0.1-0.4 µg/m^3, in other words, the SD model was further away to the SD observation data (1.7 µg/m^3). These detail result values and observation data are summarized in Appendix C, Tables C-8 and C-9.

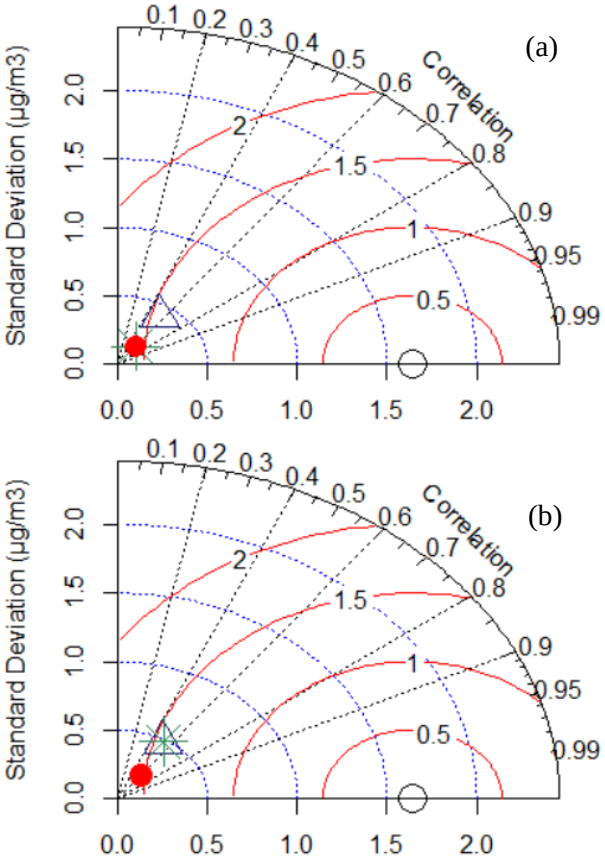

FIGURE 14: Taylor diagram presenting a comparison between the modeled and the observed values for the annual averaging period considering different terrain options a) elevated, and (b) flat, terrain options. The symbol models STRM, HELS, REYK are denoted by a green star, solid circle red, and triangle point up, respectively. The white circle indicates the observation value

The model of REYK and STRM illustrated a better performance than HELS. AERMOD recommends using site-specific meteorological data (US EPA, 2016). However, as described previously, the results acknowledged that HELS weather station, which is close to the emission source (3 km), was less accurate than the model of STRM and REYK data (25-30 km away from the Hellisheidi emission source).

4.2 Simulation of H_2S concentration

Four different time scales were modelled for the UBL and HELS-NES cases to evaluate the highest and the maximum concentrations during seasonal and annual periods. The highest H_2S concentration calculated values for a specific receptors at averages time scales whereas the maximum value obtained from the highest overall concentrations of all receptors. The model scenarios are presented in Section 3.2.8

4.2.1 Modelled for 1-hour average period

The maximum and highest values for 1-hour averaging period

The UBL case

The H_2S concentration spread more than 5 km to the east and northeast of the emission sources. The maximum level during the wet season for the model period of August 2016 to August 2017 was 1326

µg/m^3 on 6 November 2016 at 03:00 local time, and occurred at about 500 m northeast of the source units 3 and 4. During the dry season, the maximum H_2S concentration was 1629 µg/m^3 on 16 September 2016 at 02:00 (Figure 15).

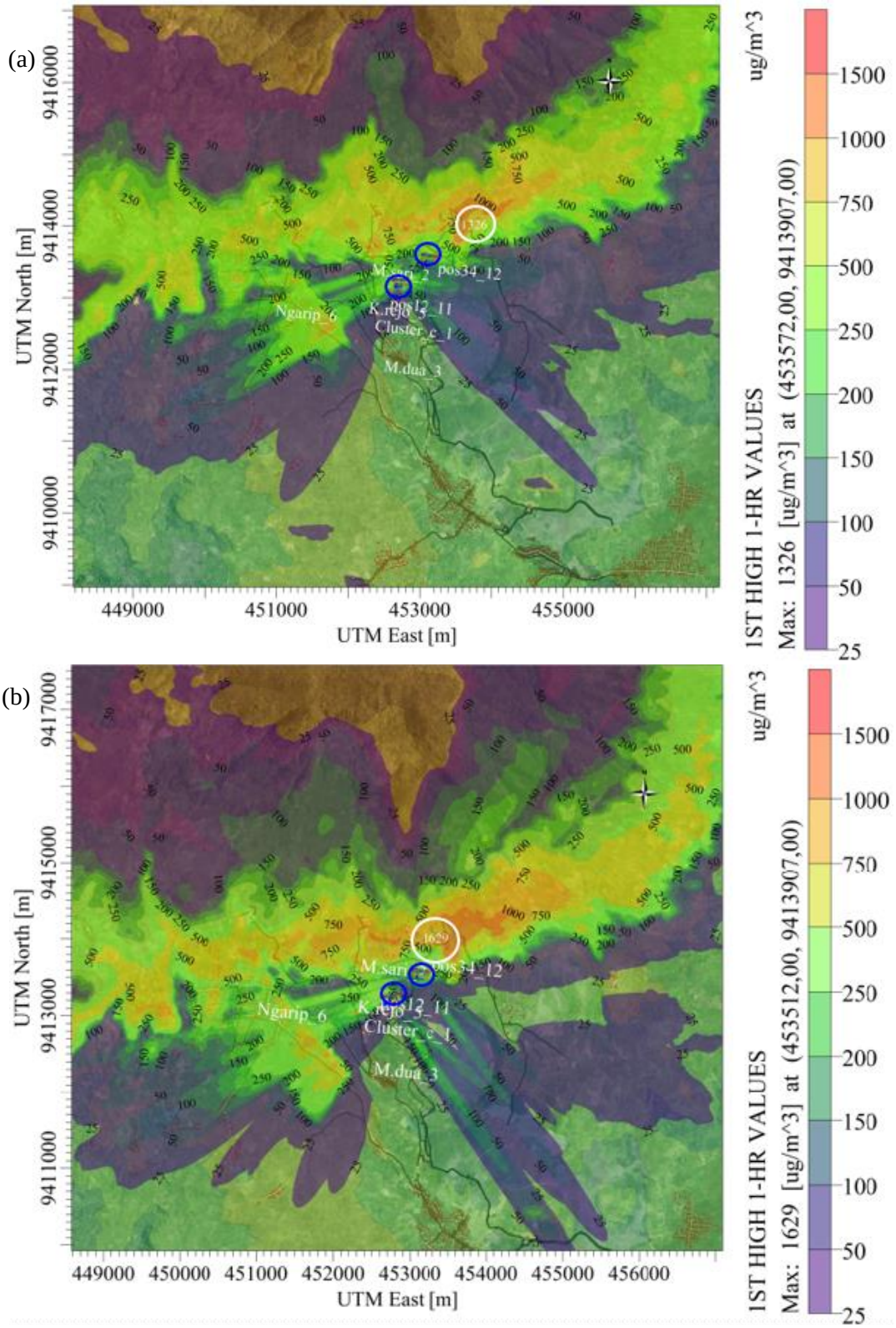

FIGURE 15: Predicted H_2S concentration for the model at 1-hour period using the model set up of elevated terrain option (a) wet season (b) dry season. The white and blue circles indicate the locations of maximum concentrations and the power plants, respectively

The model set up showed that the maximum concentration is located outside the Ulubelu residential area. The results of the models were in agreement with the most common wind direction, which was coming from the southwest (i.e., 230° for the wet season and 196° for the dry season), the wind pattern is presented in Figures 10a and b. Effects of H_2S concentration with various distances and terrain set up was evaluated between locations of the source to receptor area.

The results showed that the highest concentration range detected 10-25 µg/m^3 at receptor Muara Dua, which is located 1.5 km southwest of the source (Figure 15). A closer distance to the discharge emission, where the highest concentration range of receptor cluster C was 30-50 µg/m^3, which is located 1 km southwest of the source PP units 1 and 2. Other receptors were plotted at security office within power plants area units 1 and 2 and units 3 and 4. The concentration at receptor security office units 3 and 4 was 489 µg/m^3, this office is located 50 to 250 m from the cooling tower unit 3 and 4. Meanwhile, the predicted concentration at receptor the security office units 1 and 2 was 205 µg/m^3, the distance between security office and cooling tower unit 1 and 2 is 150-250 m (Figure 15).

For the terrain effect, flat terrain option performed better when terrain height of receptors is lower than the terrain height of emission source. Meanwhile, elevated terrain option simulated higher concentration when the terrain height of receptors is higher than the source. The detailed results of model simulations and model performance are presented in Table D-1, D-2 and D-3 in Appendix D.

The odour limit for the industry in Indonesia is set at 28 µg/m^3 (0.02 ppm) (Ministry for Environment, Indonesia 1996); however, the standard specifically for geothermal fields is not regulated yet.

The HELS-NES case

The H_2S maximum concentration for the 1-hour period indicated that the concentration during the summer season for the model period January 2012 to April 2017 was higher than that of the winter season. These occurred at receptors located in the greater Reykjavík areas and Hveragerdi.

Table 9 shows the concentration range using HELS (onsite meteorological data) had the lower predicted values (43 – 150 µg/m^3) during the winter season, while the model simulated using REYK (offsite meteorological data) estimated H_2S concentration range (58.68 – 167 µg/m^3). During the summer season, the model concentration range simulated by HELS and REYK was 64 – 181 µg/m^3 and 65 – 187.89 µg/m^3, respectively. The result of the model at receptor GRE and the measurement values during the summer season were 108 and 79 µg/m^3 (REYK), respectively. For the winter season, the model value versus the observed data was 69 and 173 µg/m^3. It showed that the results of the model underestimated the observation data. Appendix D, Figure D1 presents the distribution of H_2S concentration during the summer and winter seasons using REYK and HELS.

TABLE 9: Seasonal predicted H_2S concentration for the highest 1-hour averages period simulated by different meteorological data (HELS-NES case)

Receptor code / Receptors	**Winter (µg/m^3)**			**Summer (µg/m^3)**		
	REYK	**HELS**	**Observed values**	**REYK**	**HELS**	**Observed values**
1. Reykjavík point	58.68	43	-	65	64	-
2. Landpítali hospital	64	47	-	71	70	-
3. Mosfellsbaer point	89	66.5	-	94	86	-
4. Grensásvegur (GRE)	69	54	173	79	77	108
5. Kópavogur (KOP)	72.69	73	-	82	66	-
6. Hvaleyrarholt (HEH)	65.5	51.80	82*	72	67	54*
7. Nordlingaholt (NRH)	90	74	168*	97.99	96.92	99*
8. Waldorf	131.81	121	-	142.55	122	-
12. Hveragerdi	167	150	-	187.89	181	-

Reykjavík meteorological station = REYK, Hellisheidi meteorological station = HELS.
*The higher values of the observed data in 2015-2016.

Overall, the results showed a similar pattern of H_2S distribution for the winter and summer seasons. The model using HELS had a lower value than the model using REYK at the receptors in Reykjavík where located 25 km from the source. Also, the model presented a higher output concentration at receptors near the source when using HELS or on-site meteorological data (i.e., Hveragerdi and Waldorf receptors) (Table 9). In this case, Iceland has not regulated the odour standard for the geothermal industry.

4.2.2 Modelled for 8-hour period

The maximum values for 8-hour averaging period

The UBL case
The predicted concentration during the wet season had a maximum of 403 µg/m^3 on 8 November 2016 at 24:00 while the maximum concentration during the dry season was higher of 558 µg/m^3 on 12 August 2016 at 08:00. The results indicated that the highest concentration for all seasons occurred approximately 1-km northeast from the cooling tower area (Figure 16). The results of the models were in agreement with the most common wind direction, which was from the southwest (i.e., 230° for the wet season, and 196° for the dry season (see Figure 10a and b).

It is interesting to highlight that the peak concentration did not occur within the area of the power plants. However, it directed toward the Mount Tanggamus. The concentration of these power plants emission was distributed at a location with the elevation between 800 meters to 1000 meters above sea level (m a.s.l); the base elevations of the cooling tower of the Ulubelu power plant units 1 and 2 and units 3 and 4 is at 785 - 793 m a.s.l and 803 - 804 m a.s.l, respectively (Table D-2, Appendix D). The input of release height for the units 1 and 2 and units 3 and 4 were 15 and 14.5 m from the ground. Given this, the higher level of H_2S concentration existing outside the area of the emission sources may be explained by atmospheric stability where at midnight or early morning, it is likely there is a temperature inversion with buoyant above.

In this case, the predicted concentration from the model was compared with the Indonesian standard of occupational health, where the exposure limit set to 1400 µg/m^3 for 8-hour exposure time. The results of the model for all seasons did not exceed this limit at the receptors were located at cooling towers, powerhouse, and security office.

The HELS-NES case
The purpose of the 8-hour period is mainly for the occupational health for labors who exposed by the pollutant´s concentration in workplaces during winter and summer seasons. For the winter season, the maximum 8-hour concentration was 10595 µg/m^3 on 10 January 2012 at 24:00 local time and occurred at a radius 200 m from the CT of the Nesjavellir power plant. For the model using REYK meteorological data, on the same date and time predicted a lesser concentration at 7582 µg/m^3 with a radius about 100 m from the CT of Nesjavellir power plants (Figures 17 a and b).

For the summer season, the maximum concentration simulated by HELS was 6483 µg/m^3 on 1 June 2017 at 16:00 located 200 meters south-east of the CT of Nesjavellir power plants. The peak concentration using REYK was 1039 µg/m^3 on 4 June 2013 at 16:00 with a radius less than 20 meters from the CT of Nesjavellir power plants (Figures 17c and d).

The models showed higher H_2S concentration dispersed around the cooling tower (CT) where the pollutant is emitted from the power plants. The results showed that the model using HELS meteorological data (i.e., onsite) predicted higher concentration than the model using REYK weather data (i.e., offsite) for both seasons. The government of Iceland sets the standard of occupational health at 7000 µg/m^3 for 8-hour average. In this case, the concentration of H_2S near the cooling tower of the Nesjavellir power plant was predicted to exceed the limit during the winter time (Figures 17a and b).

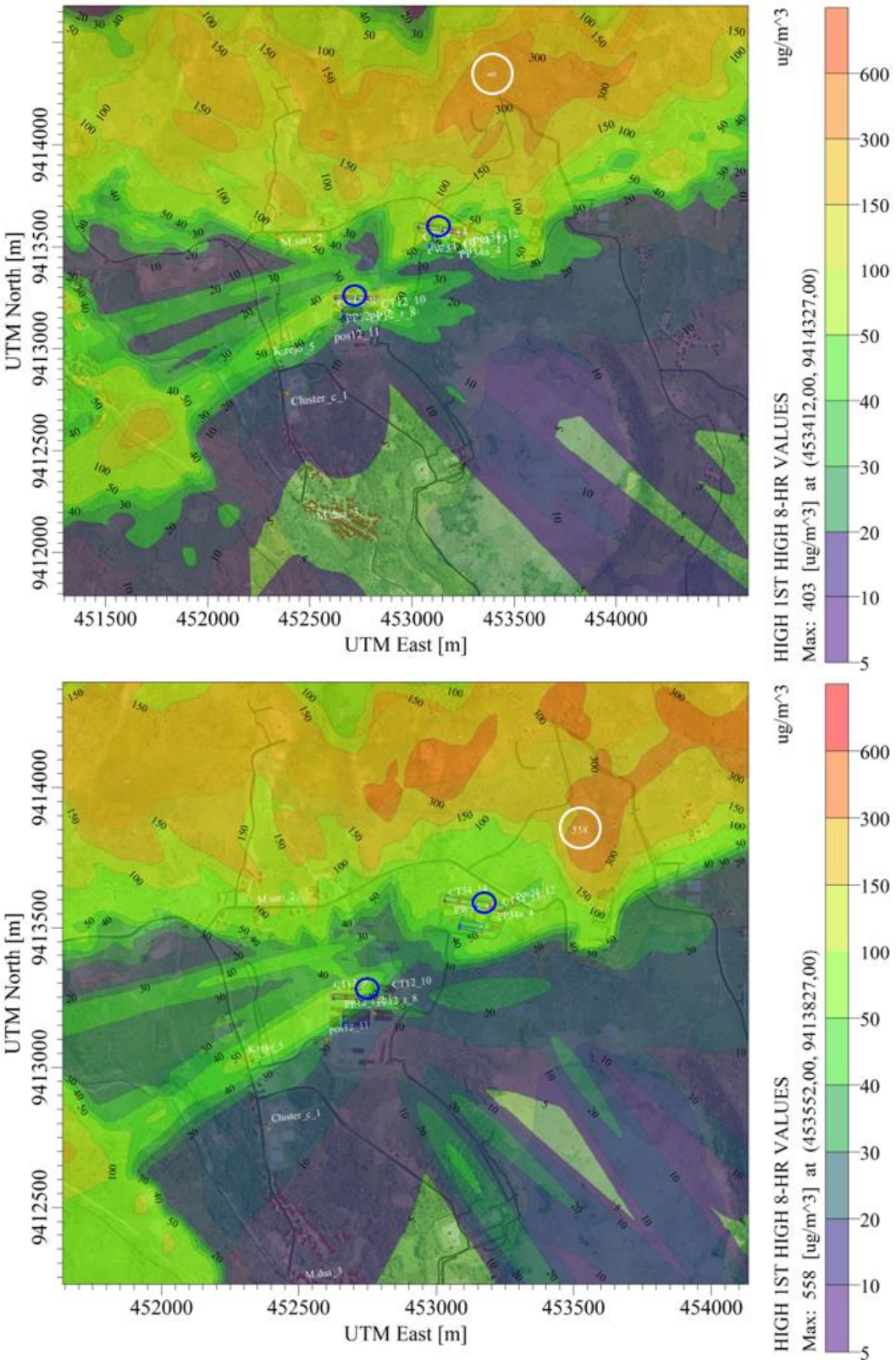

FIGURE 16: The predicted H_2S concentration of the model at 8-hour average with the model set up elevated terrain option for (a) wet season (b) dry season. The white circle and blue dots indicate the maximum concentration and location of the power plants, respectively

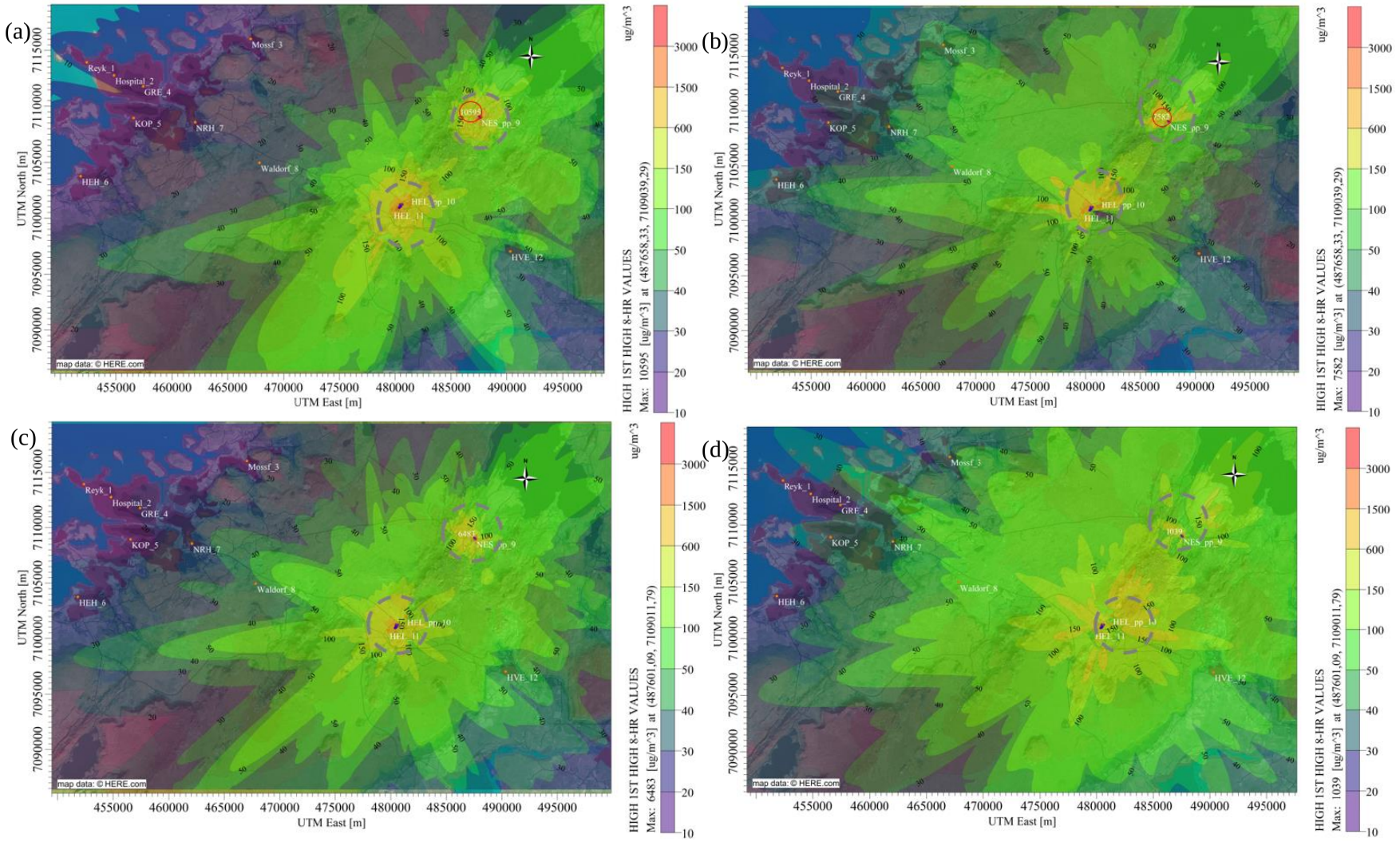

FIGURE 17: Predicted H_2S concentration for the 8-hour average simulated by the Hellisheidi and Reykjavík meteorological stations (a) HELS winter, (b) REYK winter, (c) HELS summer, (d) REYK summer. The gray dashed circle presents the location around Hellisheidi power plants, left side and Nesjavellir power plant, right side. The red circle illustrates where the H_2S concentration exceeded the Icelandic occupational health limit (7000 µg/m^3 for the 8-hour period)

4.2.3 Modelled for 24-hour period

The maximum and highest values for the 24-hour averaging period

The UBL case
The model indicated that the maximum 24-hour values for all models during the dry season were higher than during the wet season, this is because the wind direction and precipitation has an influence on the concentration.

The maximum concentration during the wet season was 168 µg/m^3 on 3 December 2016 at 24:00 located at 1.5 km northeast from the source's unit 1 and 2. It predicted the concentration was located outside the Ulubelu residential area (Figure 17a). This is explained by the wind rose diagram in Figure 10a that the dominant wind direction was southwest and the wind came from that direction approximately 32% of the time during the wet season.

The maximum concentration of the dry season was at 232 µg/m^3 on 24 April 2017 at 24:00 local time (Figure 18b). The predicted concentration was located in an unpopulated area, and it was approximately 500 meters north of the emission sources of unit 3 and 4 or 900 meters northeast of the emission sources unit 1 and 2. The wind direction was blowing from the southwest to the northeast, and it came approximately 28 % of the time during the dry season (Figure 10b).

The results also predicted that the receptor located approximately at 2.7 km west of the emission sources units 3 and 4 exceeded the Icelandic H_2S legislation and it highlighted that the concentration for the dry season extended over a wider area. It indicated lack of precipitation and lower wind speed that might have led to higher concentration during the dry season. In the study area, hourly averaged precipitation during the wet season was 0.4 mm, while the value for the dry seasons was 0.1 mm. Also, the average wind speed during the dry season (2 m/s) was lower than during the wet season (2.4 m/s).

Like the previous simulation of the 8-hour average period, the peak concentration was distributed at 800 - 1000 m a.s.l.

The model showed a higher concentration when terrain correction is considered; elevated terrain option was selected when the terrain height of the receptor is higher than the terrain height of the sources. Flat terrain option was intended for the receptors' base elevation lower than the base elevation of the sources. The H_2S highest concentration using terrain model set up (i.e. elevated and flat terrain options) for all seasons did not exceed the WHO air quality guideline (150 µg/m^3 averaged over 24-hour). However, when the model with elevated terrain option was set for the dry season period, some receptors had a much higher exposure (more than 50 µg/m^3) indicate the values on the much wider area when compared with the Icelandic H_2S legislation (50 µg/m^3 averaged over 24-hour).

The HELS-NES case
The highest concentration for the 24-hour period using REYK meteorological data predicted to be higher at receptors in the Reykjavík area and Hveragerdi. It is interesting to highlight that REYK categorized as off-site meteorological data. On the contrary, the model predictions using HELS (on site) meteorological data at the same receptors was predicted lower than the model results from REYK. Comparisons of the modeled values and the observed data were evaluated at receptor GRE using REYK and HELS meteorological data in 2016.

The predicted maximum concentration during the winter season was higher than the concentration for the summer season. Figure 19 presents the spatial distribution of H_2S concentration using HELS meteorological data for the winter season. The highest concentration ranges from receptors in the Reykjavík area, and Hveragerdi was 7 - 16.8 and 21 µg/m^3, respectively. The wind rose diagram of HELS meteorological data showed the dominant wind blew from the northeast to the south-west approximately 27% of the time (Figure 10g). In contrast, the dispersal concentration of H_2S using REYK was distributed wider toward Reykjavík. The wind rose diagram for the REYK model showed that the dominant wind direction was southeast and the wind came from that direction approximately 42% of

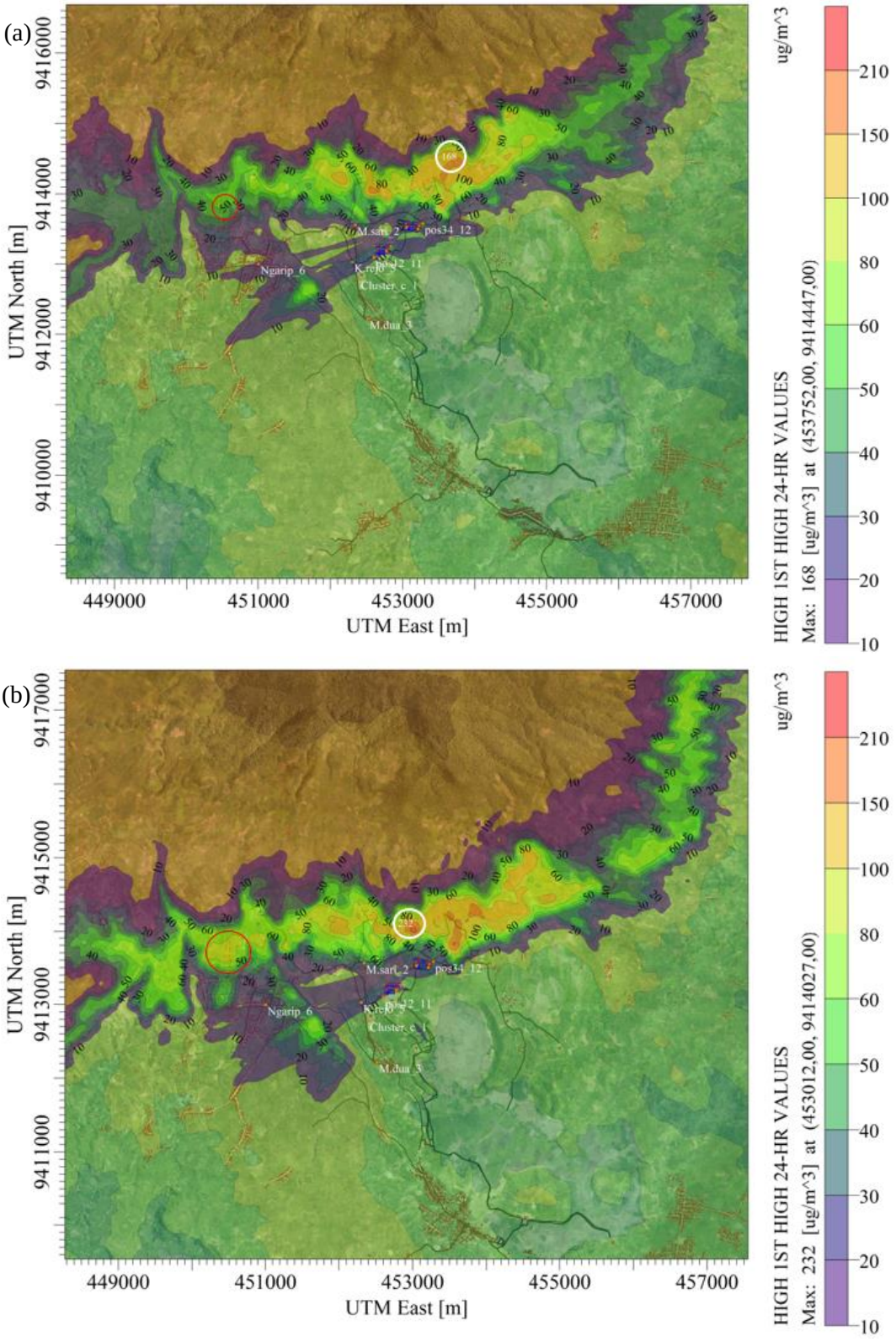

FIGURE 18: Predicted H_2S concentration for the highest 24-hour average with the model set up of elevated terrain option (a) wet season (b) dry season. The red circle indicates where the H_2S concentration exceeded the Icelandic public health limit (50 µg/m^3) and the while circle illustrates the maximum concentration

the time (Figure 10d). The highest concentration range was predicted from 16.79 - 28.94 µg/m^3. However, the concentration at receptor in Hveragerdi was slightly decreased as the level H_2S predicted by HELS (15.22 µg/m^3).

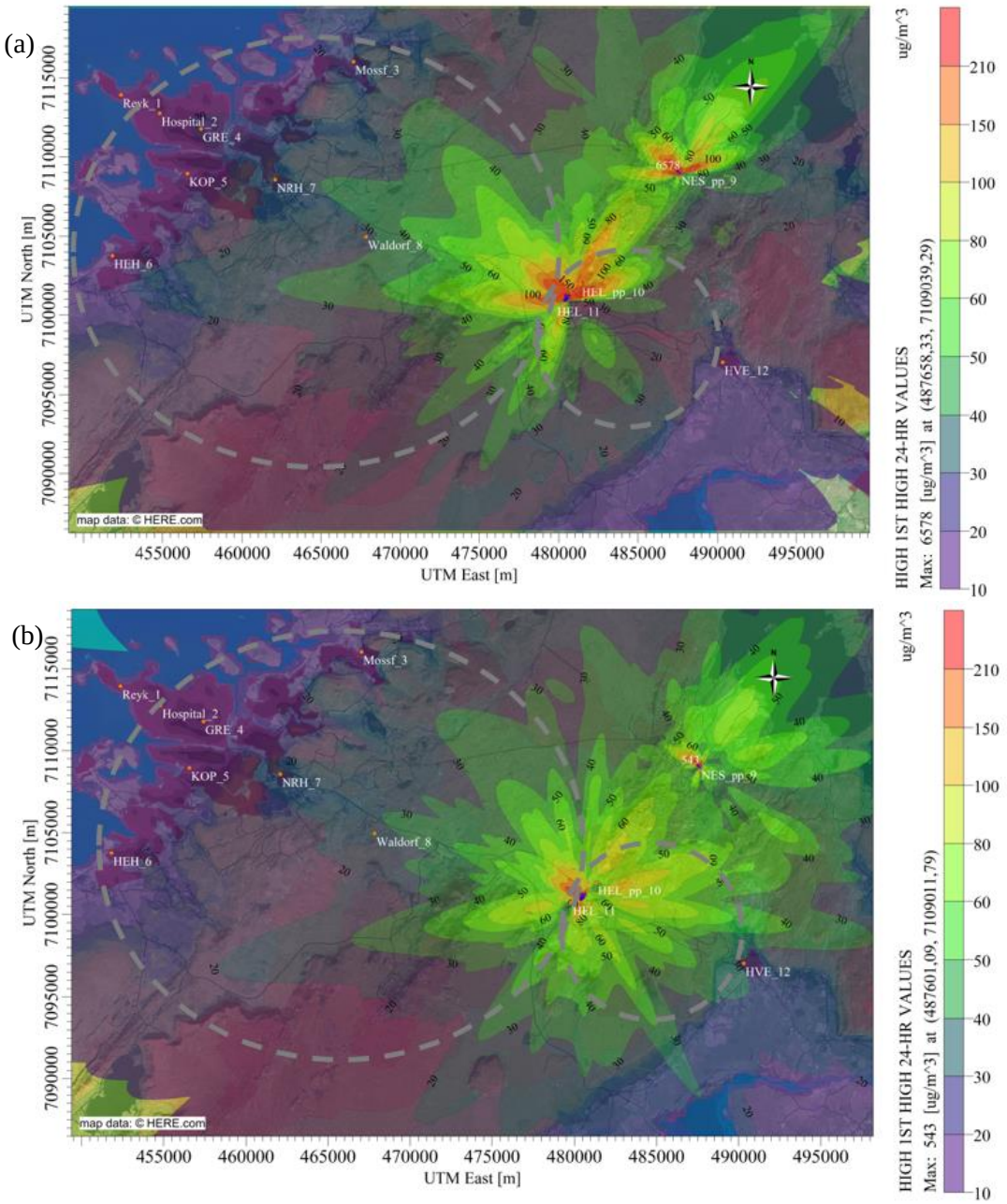

FIGURE 19: Predicted H_2S concentration for the 24-hour average simulated by the Reykjavík meteorological station (a) REYK winter, (b) REYK summer. The dashed grey circle (left side, the Reykjavík greater area, and right side, Hveragerdi area present the concentration distribution from the Hellisheidi and Nesjavellir power plants

During the summer season, the highest concentration range using HELS meteorological data was 7 – 16 µg/m^3 at the receptors in Reykjavík area, while highest concentration at receptor Hveragerdi was 19.76 µg/m^3. The windrose presented the most common wind direction for this season was northwest (Figure 10h). The concentration ranges of the model using REYK was 10.69 – 25 µg/ m^3, it is predicted to be higher than HELS at the receptors in Reykjavík area; at receptor Hveragerdi, the concentration increased to 28.88 µg/m^3. During the summer season, the winds of REYK were lighter than the winds during winter and they were much more spread directionally (Figure 10e). In the case discussed above, the results of the model for the 24-hour period for the summer and winter season indicated concentrations below the Icelandic public health limit (50 µg/m^3 for a 24-hour average).

Other model simulations were done to compare the results from the model to observed values at receptor GRE using REYK and HELS weather data in 2016. The models showed that the variance of wind

patterns had an impact on the predicted concentration at receptor GRE (Grensásvegur) located in Reykjavík. Figure 20 shows the predicted concentration for the 24-hour period using weather data 2016 indicated the majority of the predicted concentration underestimated the values of the H_2S measurement. The results of daily concentration that 80% of models underestimated values, where 14% of models were overestimated, and only 6% results were accurate to the observation data.

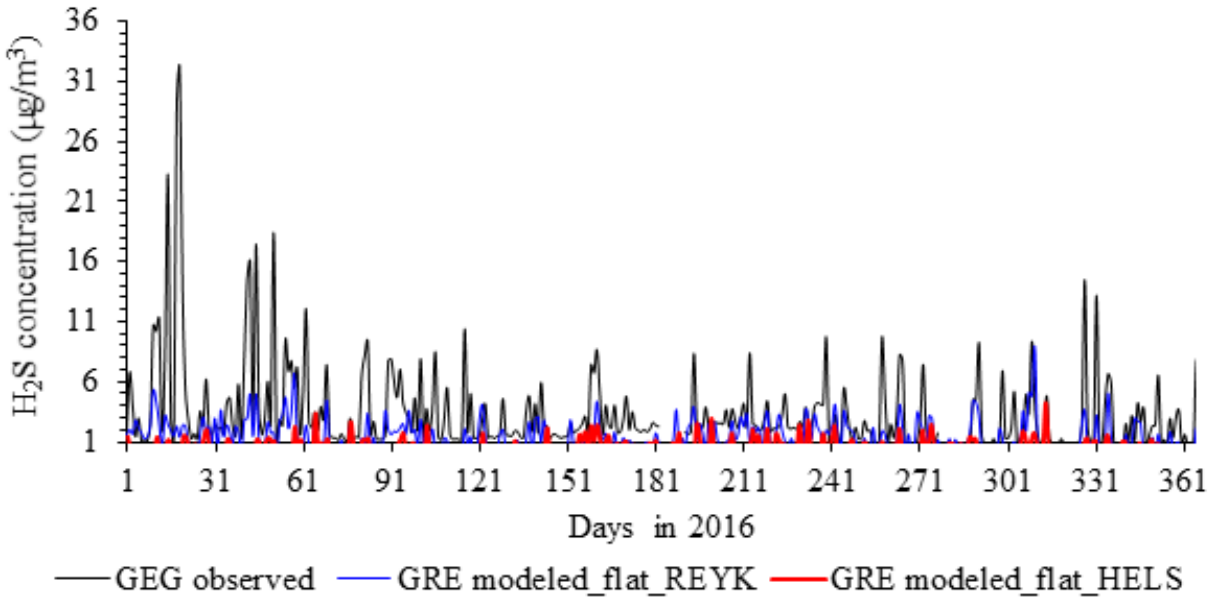

FIGURE 20: Comparison of the observed and the highest modelled values using flat terrain option at receptor GRE in 2016. The black, blue and red lines present H_2S maximum concentrations of the measured and the weather data input using REYK and HELS stations, respectively

For instance, a model on the day 19 (19 January, 2016), the highest concentration predicted 1 µg/m^3 (REYK) and 0.06 µg/m^3 (HELS). The observed value at this day was 32 µg/m^3, which was the highest among other values in 2016. The wind direction on this day from REYK meteorological data was east of the source (81°), and averaged wind speed was 3.5 m/s at 99% of the time. The wind pattern of HELS meteorological data was 54 degree (northeast of the source), and average wind speed was 4 m/s with 97% of the time. On 24 May 2016, the models showed the highest concentration of REYK (0.01 µg/m^3), and HELS (0.06 µg/m^3). The observed data was 1 µg/m^3. The wind direction of REYK meteorological data was southeast of the source (151°), and averaged wind speed was 8 m/s at 99% of the time. The wind direction of HELS was 138°, and average wind speed was 12 m/s, at 100% of the time.

Overestimation of the highest model value was observed using REYK meteorological data, for instance, on the day 31 (31 January 2016), the results of the model were 3 µg/m^3 (REYK) and 0.02 µg/m^3 (HELS), respectively, whereas the measured value was 2.5 µg/m^3. REYK modeled showed higher values than the observed. The wind direction of REYK was east of the source, the wind speed blew 4 m/s at 96% of the time. The wind direction of HELS was northeast, and the wind came at 9 m/s with 99 % of the time. The models on 7 April 2016 (day 98), the results showed REYK (3 µg/m^3) and HELS (1 µg/m^3), where the observed data was 1.7 µg/m^3. The wind direction of HELS and REYK was similar (south-east of the source), with the wind speed from both stations was 5 m/s (REYK) and 7 m/s (HELS).

The model predictions using REYK weather data showed similar values between the observed data against the results of the model. For example, the day 210 (28 July 2016) had similar values between the observed (3 µg/m^3), and REYK modeled, while HELS had lower value at 0.6 µg/m^3). The wind patterns of HELS were northeast of the source, with the wind speed blew 4 m/s, at 91 % of the time. The wind patterns of REYK (wind direction of REYK was east of the source with the wind being 2 m/s, approximately 44 % of the time. Another day on 9 August 2016 (day 222), where the observed value was 2 µg/m^3, the models of HELS and REYK predicted 2 and 1.6 µg/m^3, respectively. The wind

direction of the two meteorological was southeast of the source, the wind speed of REYK was 1 m/s, approximately 83% of the time, whereas HELS, the wind blew 2.7 at 49% of the time. The results indicated the model simulation was dependent on the wind speed and wind direction.

4.2.4 Modelled annual average concentrations

The UBL case
The maximum concentration simulated by the model set up of elevated terrain option (33 µg/m^3) was higher than the model set up with flat terrain option (6 µg/m^3 (Figure 21). The concentrations were spread from the northeast to the northwest of the emission sources and located at an elevation of 800 - 1000 m a.s.l. Most of those locations were unpopulated areas, except for the model terrain set up of elevated terrain option where the site was located 3 km west from the sources in Units 3 and 4. This exceeded the Icelandic public health limit sets at 5 µg/m^3 for annual average (Figure 21a). The model output underlined that the excessive concentration (more than 5 µg/m^3) might be located further away from the source. The wind direction for the period from August 2016 to August 2017 was southwest, and the average of the wind speeds was 2 m/s (Figure 9.c). This indicated that the results were affected by the different model set up of terrain options and the weather conditions that could have influenced the distribution at the annual average period.

The predicted concentration at all the plotted receptors was below the Icelandic public health limit (5 µg/m^3 for annual average), except for the model at the receptors located 2.7 km west of the sources in Units 3 and 4, whose result exceeded the limit.

The HELS-NES case
The results showed that the model using off-site meteorological data REYK (2 – 5 µg/m^3) was expected to be higher than the predicted values using onsite HELS meteorological data (0.94 – 2 µg/m^3) at the receptor in Reykjavík. A similar pattern was observed for the model prediction at the receptor in Hveragerdi, where the predicted concentration using the REYK and HELS was 2.97 and 2 µg/m^3, respectively (Figure 22). The distance of the HELS and REYK weather stations to the emission source are 4 and 25 km, respectively. This indicated that the locations of meteorological stations affected the results of the models plotted in the Reykjavík area. Also, since the receptors are located further away from the source, it is likely the topography of the HELS weather data station may inhibit a flow of air downstream, especially since the plant is upstream of Reykjavík in southerly winds.

The wind pattern also affected to the results of the model, the average wind direction of the five years HELS data was northeast of the source (Figure 10i), with an average wind speed at 7 m/s. Meanwhile, the wind direction of REYK blew from east and southeast with the wind speeds was 4 m/s (Figure 10f).

Furthermore, the model simulation using the Reykjavík weather station indicated that the receptor at Waldorf was expected to exceed the annual limit. It is also important to note that there is a school located 13 km northwest of the Hellisheidi power plant that would be affected by the emissions. The prediction from the model results indicated that the concentration would exceed the Icelandic public health limit sets at 5 µg/m3 (Figure 22a). However, when model predictions using Hellisheidi meteorological data, the results of the model at the same receptor Waldorf predicted that the concentration would not exceed the Icelandic public health limits (Figure 22b).

Looking at the comparison of the models (i.e., January 2012- December 2016) against the H_2S observed data at receptors GRE, KOP, HEH, and NLH that located in the Reykjavík area. The results also showed that the values of the models were lower than the predicted outcome (Table 10) and Figure 23 at GRE receptor. The model values showed REYK modeled predicted higher concentration than HELS modeled; the concentration ranges of REYK and HELS were predicted from 2.8 to 3.75 µg/m^3 and 0.9 to 1.5 µg/m^3, respectively. The concentration ranges of the observed values measured from 2.9 to 7 µg/m^3.

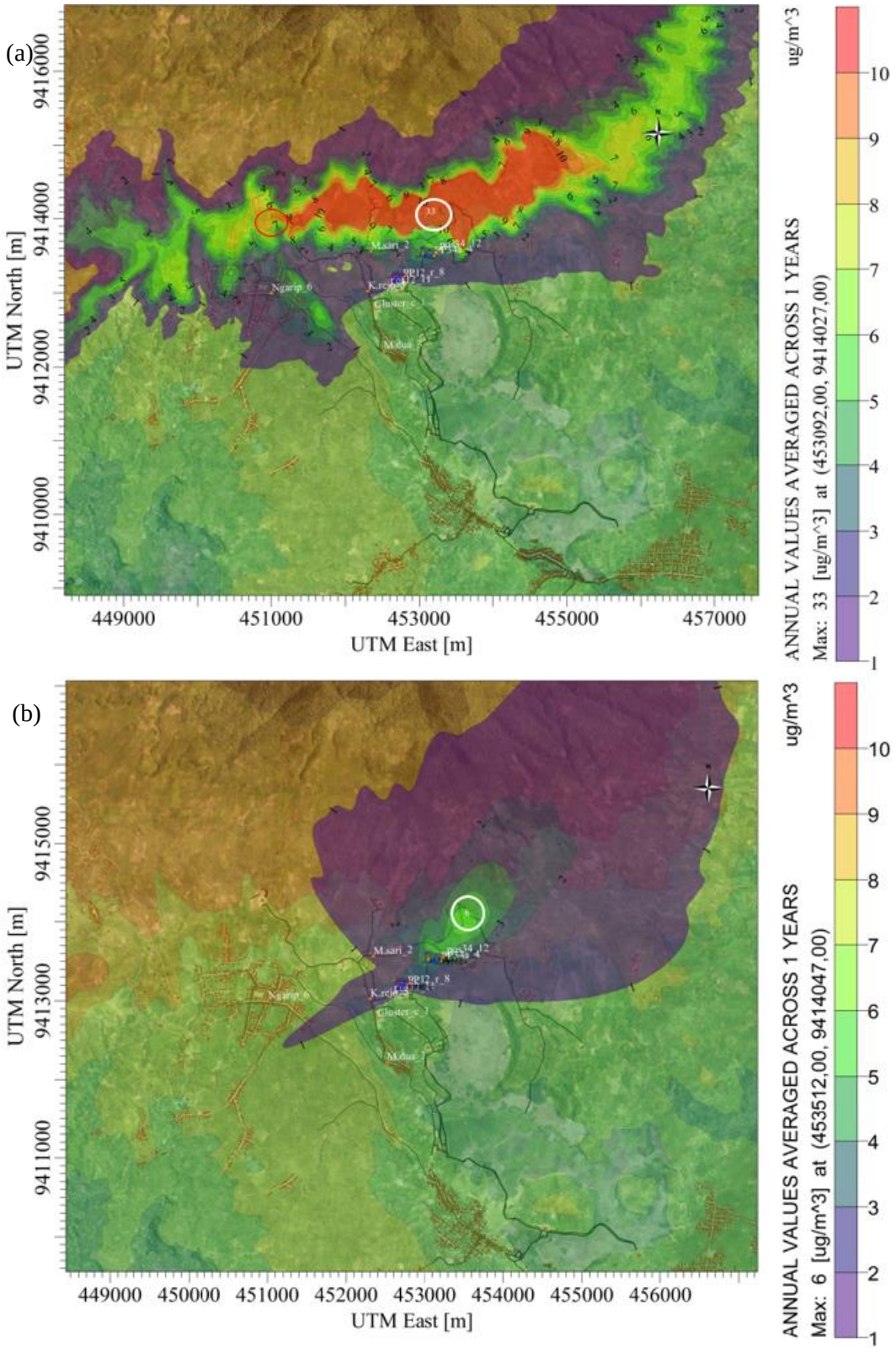

FIGURE 21: Predicted H_2S concentration at the annual average period, which considered different terrain options; (a) elevated terrain option and (b) flat terrain option (UBL case). The red circle shows the H_2S concentration at the annual period exceeded the Icelandic public health limit (5 µg/m^3 for annual average). The white circle illustrates the maximum concentrations for annual period

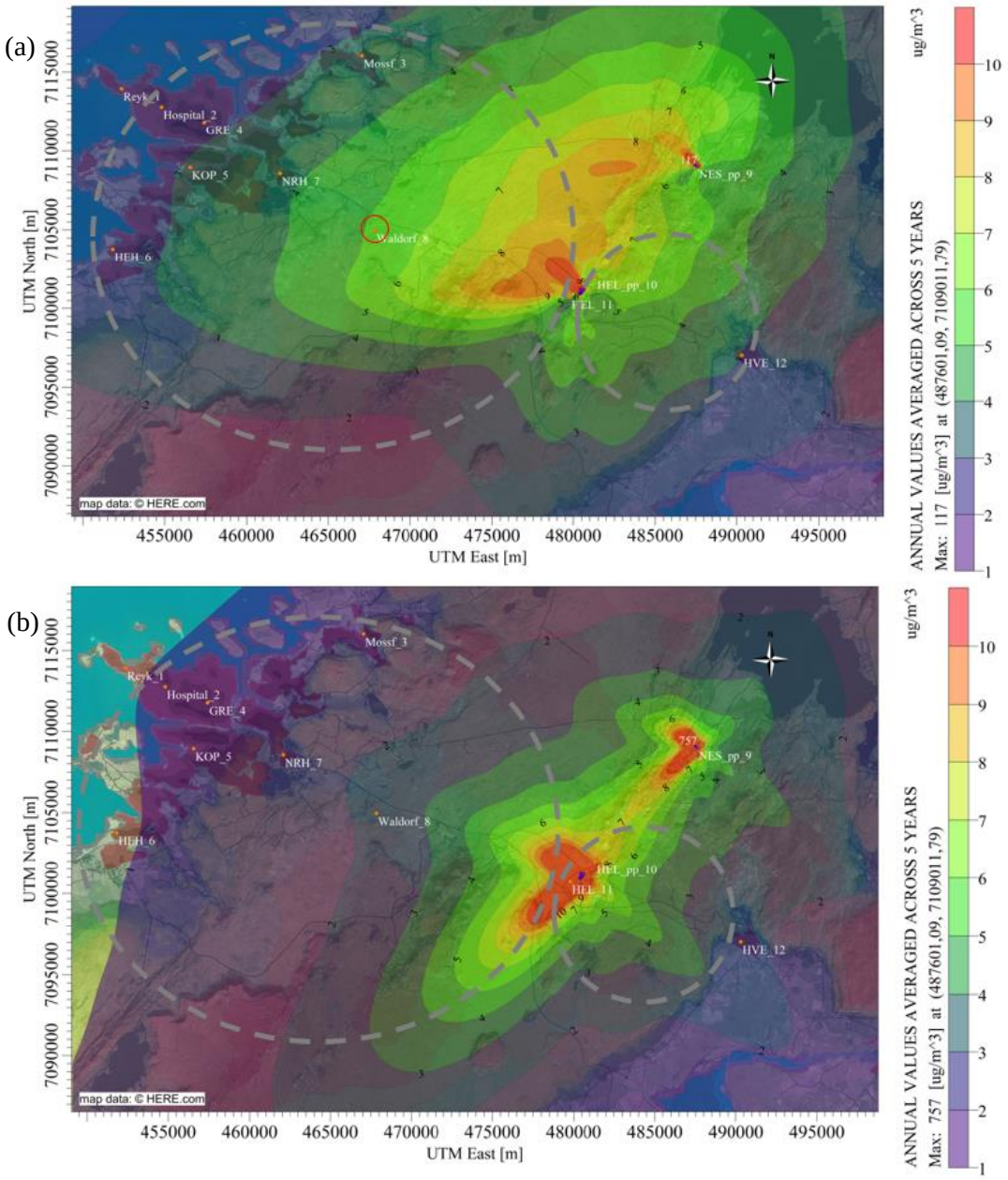

FIGURE 22: Predicted H_2S concentration for annual average simulated by various meteorological data (a) REYK (b) HELS. The dashed grey circle (left side, the Reykjavík greater area, and right side, Hveragerdi area present the concentration distribution from the Hellisheidi power plants

TABLE 10: Predicted H_2S concentration for annual average simulated by two different meteorological stations using HELS-NES case

a. The model using REYK meteorological data input

Receptor code/ Receptors	REYK (µg/m³)										
	5 years	2012		2013		2014		2015		2016	
	Modelled	Modelled	Observed	Modelled	Observed	Modelled	Observed	Modelled	Observed	Modelled	Observed
4. Grensasvegur (GRE)	2.8	2.6	4.8	2	5	2	7	1.4	4	1	3
5. Kópavogur (KOP)	3	2.98		2	-	2.59	2.9	1.45	2	1	-
6. Hvaleyrarholt (HEH)	2.7*	2.7		2	-	2	-	1	2	1	3
7. Nordlingaholt (NLH)	3.75	3.65		2.88	-	3	-	1.8	4	1.8	6

b. The model using HELS meteorological data input

Receptor code/ Receptors	HELS (µg/m³)										
	5 years	2012		2013		2014		2015		2016	
	Modelled	Modelled	Observed	Modelled	Observed	Modelled	Observed	Modelled	Observed	Modelled	Observed
4. Grensasvegur (GRE)	1	1	4.8	0.99	5	0.91	7	0.46	4	0.55	3
5. Kópavogur (KOP)	1	1	-	0.86	-	0.89	2.9	0.47	2	0.5	-
6. Hvaleyrarholt (HEH)	0.9	0.9		0.79	-	0.7	-	0.4	2	0.4	3
7. Nordlingaholt (NLH)	1.5	1	-	1	-	1	-	0.6	4	0.68	6

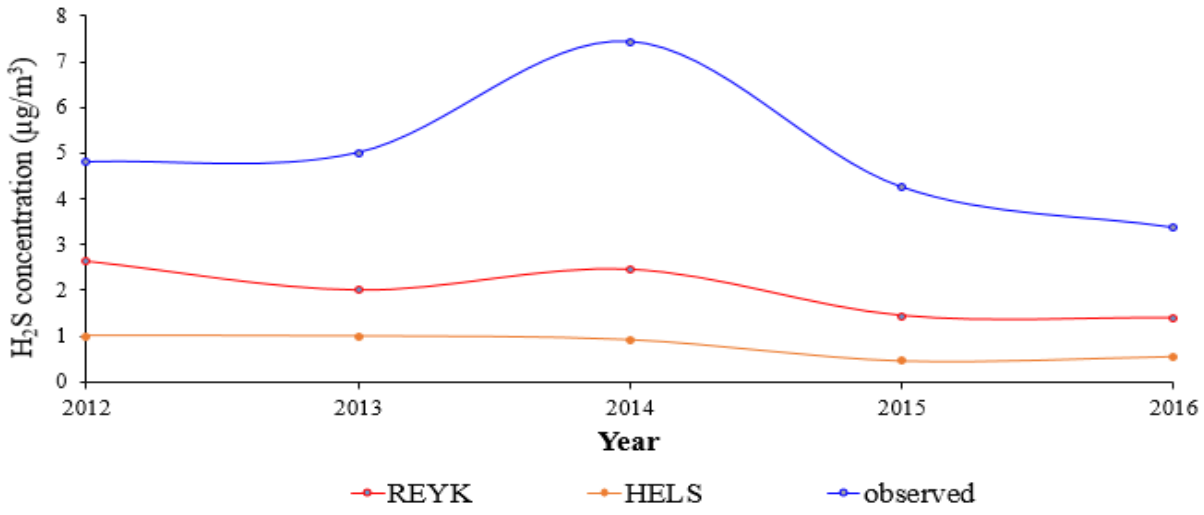

FIGURE 23: Comparison of the annual modelled and the observed values using on-site, and off-site meteorological data at GRE receptor. The blue, red and yellow lines present the concentration of the observed data, model REYK, and model HELS

5. POLICY RECOMMENDATIONS

This chapter discusses policy recommendations based on the results of the study of the UBL and HELS-NES cases, so as to mitigate the impact of an H_2S pollutant from geothermal exploitation and utilization. European Environment Agency (2017) suggests instrument policy can be used to address environmental and health as well as raise awareness of issues by using regulatory approach. An instrument of environmental policy needs to align with energy planning, as environmental and health concerns in current and future conditions may be expected as the impact of air pollutant emitted from power generations. The following are the key strategies based on the study.

1. Regulatory approach (i.e., legislation)
The geothermal power is expected to grow both in Iceland and Indonesia, alongside concern that would increase emission of the H_2S pollutant from emission sources. Therefore, to anticipate these issues, setting up an Environmental Impact Assessment (EIA) policy together with an H_2S ambient air policy are required to protect human health and the environment.

In accordance with Government of Indonesia regulation No 27 of 2012 regarding the environmental permit, geothermal exploration and exploitation are required to asses EIA. This issuance permit requires study of the EIA, known an *analisa mengenai dampak lingkungan* (*AMDAL*) or environmental impact statement (UKL UPL). The decree of the Ministry of Environment No. 5 of 2012 as derivative of environmental limit, a geothermal power plant, which generates more than 55 MW electricity shall undergo EIA.

Meanwhile, proposed 50 MW of thermal energy in Iceland is subject to EIA study in accordance to the *Act on Environmental Impact Assessment No. 106/2000* and by *Regulation on Environmental Impact Assessment 1123/2005.*

The EIA study of the proposed project should asses significant impacts of the project including air quality impact. The study found the models of the UBL and the HELS-NES case did not include H_2S background for the model simulations due to lack of the data of the H_2S concentration that applied in the model.

As one of the findings of the study, in the EIA study, it is recommended to observe H_2S background data prior geothermal activities and geothermal power plants. The measured H_2S background needs to be suited for the air model simulation; these include (Lakes Environmental Software, 2017),

- Specified background concentration based on period, which may be measured at an hourly, daily, monthly, seasonal or annual period.
- Specified H_2S background concentration based on area characteristics, which should be observed in affected residential areas, sensitive ecosystem (i.e., forest and moss) and public areas (i.e., school, hospital).

From the study, it indicated elevated concentration in some residential areas. Regarding the EIA study as well as a plan of monitoring and mitigation actions, the results of the model can be used to set H_2S observation points and duration of monitoring period located at residential areas and geothermal workplaces.

Setting up an integrated EIA, H_2S ambient air policy and appropriate model prediction software by the government is essential for curbing the problem. The collaboration of national and local policy is needed to support the integration network among those policies and model predictions of H_2S ambient air and emission

For the HELS-NES case, Iceland legislates H_2S ambient air on the government policy No. 514/2010 for the 24-hour averaging period (50 $\mu g/m^3$), with annual limit (5 $\mu g/m^3$), this limit attempts to protect public health concern from the emission of geothermal activities in the residential area.

In Indonesia, the government regulation has set ambient air quality No. 41 of 1999 concerning air pollution control. However, this regulation does not regulate H_2S limit. To date, the Indonesian State Ministry of Environment has set regulation regarding thermal emission standard decree No. 21 of 2008 concerning emission for stationary and thermal power generation activities. However, none of the H_2S public health legislation has been addressed to overcome the concern of H_2S pollutant in a standard for public health.

It is recommended to regulate the public health limit, by for example, following the WHO standard of air quality guidelines for H_2S (150 $\mu g/m^3$ for 24-hour average) for UBL case. Currently, based on the case of Indonesia in this study, the environmental policy related to H_2S limit could be improved.

Neither Iceland nor Indonesia has specific legislation for odour standard at geothermal fields. It is recommended to set the standard of H_2S for public health for a 24-hour period (Indonesia case), and odour standards at geothermal fields (Indonesia and Iceland cases) which reflect site conditions that affect the local community.

In terms of the H_2S modelling using AERMOD software, the results showed that for the HELS-NES case were underestimated to predict maximum H_2S concentrations at receptors in Reykjavík greater area, therefore it is suggested to estimate the concentration through the Gaussian plume calculations that can give a better indication of expected maximum values. (Finnbjörnsdóttir, et al., 2016).

2. Economic instrument

European Renewable Energy Council (EREC, 2010) studies policy instruments needed to support green technology, and Research and Development (R&D) should be established by a government to support the renewable energy more efficient. It is essential to set well-structured and coordinated programs of R&D in order to boost the innovation in construction and operation technology. This instrument will encourage the player of renewable energy, especially geothermal production, and to install the best technology for reducing the emissions (Sterner, 2003).

3. Educational instrument (e.g., education approach for good behaviour)

The education system is recommended to be embedded in environmental awareness on the proposed environmental information act provided to citizens and private enterprises. The educational instrument approach is used for creating good behavior for energy producers and consumers (Sterner, 2003). The information has to perceive the impact of the pollutant and how the impact of the pollutant can be minimized, as well as providing opinions in forming environmental policy.

In order to increase knowledge and awareness, it is recommended that all citizens have a right to receive H_2S information from both government authorities and geothermal companies. In the Iceland case, this has been implemented by disclosing in respect of the environmental matter, through act Act No. 21/1993 regarding the supply of and access to environmental information. The law ensures government, local government, and an institution to provide access to the public. In terms of H_2S monitoring due to geothermal activities, the public can access the data from H_2S station that are available on the wesite https://www.ust.is/einstaklingar/loftgaedi/maelingar/

In Indonesia, the government sets act no 32 of 2009 regarding environmental protection and management. The law states government, and local government is obliged to develop a system of information for environmental policy, and environmental management. It is recommended to set up a public health standard for H_2S and to improve the accessibility of H_2S impact, to monitor data and mitigation.

An evaluation of the methods for assessing H_2S emission levels from the power plant is also recommended, which considers the performance of the model in the proposed H_2S air pollution guidelines. To address the uncertainty of the model, developing a continuous study of the model simulation as well as building communication between the policy maker and multi-disciplinary teams become necessary. Such as:

- Geoscience to assist study on geothermal reservoir by analyzing NCG content (H_2S emission) from the geothermal field. Good understanding of reservoir in terms of NCG content of the geothermal field is important because the NCG content can vary from one geothermal field to the other. The content may also reduce, increase or remain stable during production. Therefore, monitoring of the NCG is essential to check whether the content of the NCG from the geothermal field is increasing, decreasing, or stable.
- Meteorology; to provide the database of meteorological data for model simulations near the emission source.
- Survey and mapping institution; to assist an updated terrain data with high resolution

Proper model simulation can help on making the rational strategies for air quality management, for instance installing the H_2S removal and sitting an adequate station for H_2S monitoring or passive monitoring at residential areas and geothermal workplaces.

The UBL weather station measures parameters of wind direction, wind speed, and temperature. However, additional parameters are needed to measure hourly cloud cover, ceiling height, and solar radiation, which are the variables required for air modelling. For the HELS-NES case, measuring hourly cloud cover is recommended for providing complete meteorological data in the model simulation. When it comes to the implementation, the policy should have a proper and good understanding of the context it is working within as well as other institutions and geothermal developers who might have a different view on the instrument.

6. DISCUSSION

The results of the model performances showed that the models run for Ulubelu (UBL case) performed better than the model simulations from Hellisheidi and Nesjavellir (HELS-NES case). In terms of seasonal model, it suggested that the model for the UBL case predicted a higher concentration during the dry season, while models of the HELS-NES case indicated that the predicted maximum concentration is expected to increase during the winter season rather than for the summer seasons, except the results of the 1-hour model which showed that the maximum H_2S concentration was higher during the summer season. The model predictions using different time scales (1-hour, 8-hour, 24-hour, annual, and seasonal periods), terrain model setup (i.e., flat vs. elevated options) and meteorological data (i.e., on site and off site weather data) affected the model results.

Overall, the models for the HELS-NES case, for the time scales at 1-hour and 24-hour average had difficulty in predicting H_2S concentration at the receptors located up to 35 km from the sources. A strong underestimation on model applicabilities occurred when predicting the highest concentration for the model at 1-hour averaging period. The results of the seasonal model for the HELS-NES case using meteorological data (Reykjavík-REYK and Hellisheidi-HELS) showed that the predicted maximum concentration of the 1-hour period at GRE receptor, during the winter (REYK, 69 $\mu g/m^3$, HELS, 54 $\mu g/m^3$) and the summer season (REYK, 79 $\mu g/m^3$, HELS 77 $\mu g/m^3$) underestimated the observed values (winter, 173 $\mu g/m^3$ and summer, 108 $\mu g/m^3$) (Table 9). It is shown that model simulation using off-site meteorological data (REYK), where the station is located in Reykjavík area (receptor GRE), and indicated higher prediction than using onsite meteorological data (HELS). The distances of the HELS and REYK meteorological stations to the emission source are 4 and 25 km, respectively. REYK weather station (52 m a.s.l) and GRE receptor (34 m a.s.l) are located in the same area in Reykjavík whereas the base terrain condition of the sources has a higher level at 270 m a.s.l. The wind patterns of REYK were flowing toward Reykjavík area. Meanwhile, the wind direction of HELS was not directed toward the GRE receptor (Figure 11g-i). The model was also affected by wind flows from the HELS (360 m a.s.l) carrying the plume downward GRE receptor (34 m a.s.l) was diverted by the hills. The model results indicate influence from wind patterns of those weather stations and topography conditions affecting receptor GRE in Reykjavík.

The results of the model, using onsite and offsite meteorological data, were compared to the H_2S occupational standard *(*7000 $\mu g/m^3$ for the 8-hour average) at the geothermal workplaces. None of the results have exceeded the limits except the model for the 8-hour average during the winter season at the distance of 20-100 m from the cooling tower of the Nesjavellir power plants (HELS-NES case).

The model for the 24-hour period for the HELS-NES case, as discussed previously, showed it did not perform well. For instance, when the model runs using meteorological data from 2016, the results of highest daily concentrations showed that 80% of the model runs underestimated values, followed by 14% overestimated and 6% accurate values to the Grensásvegur monitoring data (GRE) (Figure 20). The results with the accurate values occurred for the range of wind speeds from 1 to 3.7 m/s, and the wind direction from 86° to 124° (east, northeast, and southeast). The accuracy of model prediction is essential to estimate the concentration concerning health effects. The study found the offset daily highest predicted concentration to the observed values were less than 5% on that year, and it was due to the wind direction affecting the results. For instance, the wind directions in some particular days were flowing between 119 and -350°.

Thorsteinsson et al. (2013) showed that elevated H_2S concentration occurred at specific weather conditions, including when the wind speeds are low (1.5 and 4 m/s) and the wind direction from the east (54° - 124°). Another study done by Ólafsdóttir and Gardarsson (2013) showed a similar pattern, with higher H_2S concentration when the wind speeds and wind direction occurred at 1-3 m/s and 54° - 137°, respectively.

Based on season, the highest concentration for the 24-hour period at receptor GRE (using REYK weather data 2016) indicated the results of the model during the summer season (4 $\mu g/m^3$) was lower than the model (7 $\mu g/m^3$) during the winter season. The observed values during the summer and winter seasons

were 10 and 32 μg/m^3, respectively. As discussed above, the model did not work well to predict the concentration with the distance up to 25 km from the Hellisheidi power plants. The results of the model 24-hour period also showed that the value during the winter season had higher concentration compared to the concentration during the summer season. Study done by Finnbjörnsdóttir et al. (2015) concluded that the mean pollutant of H_2S for the 24-hour average was higher during the winter season (4 ± 8) μg/m^3 than the summer season (1.6 ± 2) μg/m^3 hence health impact on the human body might increase during the winter season than in the summer time.

The model run of annual average for the HELS-NES case showed that the concentration ranges of receptors using REYK and HELS weather data were predicted at 2.83 - 3.75 μg/m^3 (REYK data) and 0.94 - 1.54 μg/m^3 (HELS data), respectively. The concentration ranges of the observed values measured from 2.93 - 7.44 m^3 (Table 10). The models run of annual average also highlighted that at a school public facility at Waldorf it was expected to exceed the annual limit of 5 μg/m^3. The school is located about 13 km northwest of the Hellisheidi power plant.

Concerning timescales for the HELS-NES, the model applicabilities perform better for a long-term (i.e., annual) period set up compare to the short-term period (i.e., 24-hour) for Iceland case. Similar findings were studied by Zou et al. (2010) and Rszutek et al. (2017) that the model of 1-hour short-term period did not perform well compared to the model at an annual period. US EPA (2005) states the number of studies of the model accuracy for a short-term period estimates poorly at specific times and the highest concentration predicted, for instance, occurs at ±10-40% error.

The UBL case was modeled using Ulubelu meteorological data predicted the models for 8-hour, 24-hour (28-31 August 2017), and annual periods (August 2016-August 2017). The 8-hour model showed that the occupational limit was never exceeded for the 8-hour exposure time; 1400 μg/m^3 for the 8-hour period at the location of the power plant facility.

The models of 24-hour period suggested that the model simulation for the UBL case worked better for calculating the concentration of daily average at receptors in Karang Rejo, Ngarip, and Mekar Sari villages located up to 3 km away from the source.

The results of the seasonal model for the UBL case showed that the model for the maximum 24-hour value had higher concentration during the dry season compared to the maximum concentration during the wet season. The model simulation predicted that the concentration for the 24-hour average at some locations 2.7 km west of the source exceeded the Icelandic public health guideline. However, when compared to the WHO air quality guideline for H_2S (150 μg/m^3 for 24-hour average); it did not exceed the limit for the residential area. It also highlighted that the maximum concentration exceeded the WHO air quality guideline, though this predicted concentration is located in an unpopulated area, and it was approximately 500 m northeast of the sources, Units 3 and 4. Looking at the dominant wind direction of the UBL case, which for both the dry and wet season was southwest, the model agreed with the results of the maximum concentration located northeast of the source. In the study area, the hourly average of the precipitation during the wet season (0.4 mm) was higher than the value for dry season (0.1 mm). The results were also explained by the hourly average of the wind speed for the dry season (2 m/s), which was lower than wind speeds during the wet season (2.4 m/s), as well as due to the characteristic of H_2S being soluble in water. These results were in line with the study done by Thorsteinsson et al. (2013) and Ólafsdóttir et al. (2014) that high H_2S concentration correlated with low speed and little precipitation.

On the annual period, for the UBL case indicated that the results of the model using elevated terrain option exceeded the Icelandic public health limit (5 μg/m^3 for annual average) at the receptors with the distance 3 km west from the sources, Units 3 and 4 (Section 4.2.4). Regarding H_2S observation data, the elevated concentration at some receptor points is suggested to define the proposed locations of H_2S monitoring.

Comparison between the model set up of UBL case and HELS-NES cases are to evaluate weather conditions (onsite and offsite data) and terrain model setup in the model. For the HELS-NES case, the wind direction of the off-site meteorological data was toward the west of the source for most of the time,

while the wind direction of the on-site meteorological data was northeast, which was not toward the receptors located in Reykjavík (Figure 9). The wind direction from the source toward the receptor may lead error to the outputs of the model as well as topography condition between the onsite weather station and receptors in Reykjavík. These indicated that the variability of wind transportation and terrain affected the results of the model simulation. US EPA (2005) highlights the procedure for Long Range Travel (LRT) beyond 50 km where prognostic mesoscale meteorological models are encouraged for estimating concentration, which considers a statistical comparison with the observation of winds aloft and on the surface. Further study, therefore, it needs to consider using prognostic mesoscale meteorological models in the simulation for the 24-hour and annual periods. The meteorological data for the HELS-NES case indicated spread variability during the winter and summer seasons, while, the meteorological data for the UBL case were not much different during the dry and wet seasons. The various conditions of the two different conditions between tropical (UBL, Ulubelu) and cold weather (REYK, Reykjavík weather, and HELS, Hellisheidi meteorological stations) affected the results of the model simulation (Figures 10 and 11).

Regarding the model performance on terrain setup options in the model affected the results of the predicted values. In AERMOD, the flat option is selected when all the receptors being located lower than the source, on the other side, the elevated option is applied for receptors are located higher than the source. For the HELS-NES case, the model set up with the flat versus elevated options were employed. The results of flat terrain option showed higher prediction than using elevated option. Another factor explaining this performance may be that AERMOD tends to underestimate the results when the terrain base elevations of emission source are higher than terrain conditions at receptors (US EPA, 2005; South Coast AQMD, 2018).

For the HELS-NES, even though most of the result of model predictions were underestimated compared to the observed values, the models run showed that the flat terrain setup gave better results. Overall, the models run using AERMOD showed that concentrations were spread in Reykjavík city, which is located 25 km away from the source. AERMOD estimated poorly at a specific location (at GRE receptor). US EPA (2005) highlights, the model predictions present error at $\pm$10-40%.

For the UBL case, overall results of the model predicted high concentration when it was set to the elevated terrain option (Figure 21). However, for some specific receptors, the model set up of flat terrain option had a higher prediction. For instance, the model simulation at receptors of Mekarsari (842 m a.s.l.) and Ngarip (869 m a.s.l.) are located at higher elevation than the emission source, Units 3 and 4 (802 m a.s.l), and high values were estimated from the model set up of elevated terrain option. On the other hand, a high concentration obtained when the model set up receptor of Karang Rejo (796 m a.s.l) was set to flat terrain option considering the terrain condition of that receptor is lower than the base elevation of the emission source (802 m a.s.l).

The models run for those two cases demonstrate a possible tool to analyse the level of H_2S concentration that can be proposed for setting up or reviewing H_2S air pollution policy. For the HELS-NES case where most of the model application using AERMOD did not work well to predict the concentration at receptors. It is recommended to calculate the concentration with the Gaussian plume. Finnbjörnsdóttir, et al., (2016) studied model predictions of H_2S concentration from the Hellisheidi power plants using Gaussian calculations. The study showed that model predictions provide a better indication of predicted maximum values.

Therefore, understanding the input and model set-ups in an air pollution software is necessary to develop mitigative actions to prevent H_2S air pollutant impacts. Also, knowing the model performances for different time scales exposed in residential areas, and geothermal workplaces are essential for implementing or improving the H_2S air pollution policy, e.g., establishing a public health standard, particularly for the UBL case.

Geothermal power is expected to grow, as this energy emits much fewer air pollutants compared to the electricity produced by fossil fuels or coal resources. However, studies found that the H_2S air pollutant from geothermal utilization is expected to increase and might cause health problems. Therefore,

mitigative actions among stakeholders, such as the government, geothermal producers, and institutions are essential to minimize the possible impacts that air pollution on the human body and the environment.

Regulation of H_2S air pollutant is fundamental to control the emission from a geothermal power plant, and this includes setting the limits of odour, occupational health, and public health. Other options for mitigating the impact of H_2S pollutant are establishing monitoring plans and estimating the limit of H_2S concentration for geothermal future development (e.g., indicated locations, which could be affected by high H_2S concentration (Zannetti, 1990)). In Iceland, for example, SulFix plant is installed to reduce the emission of H_2S from the Hellisheidi power plants (SWECO, 2018). Therefore, the regulations should require appropriate model predictions to estimate H_2S concentration levels that might harm the community living in the geothermal field or further away from the emission sources.

7. CONCLUSIONS

The applicability of the models was assessed by considering different model set of terrain options and various meteorological data for the Ulubelu power plants (Indonesia), and Hellisheidi, and Nesjavellir power plants (Iceland). The study found that the model simulation tends to make a better prediction of H_2S concentration for a long-term period (i.e., annual period) than the model for the short-term periods (1-hour, 8-hour, and 24-hour average), except for the 24-hour average for UBL case. The limitation of the UBL case is due to the lack of H_2S observation data, which requires further assessment for estimating model performance for a short and long-term period.

When simulating models with different terrain setting (i.e., flat and elevated), the models run for the UBL case estimates better when terrain correction is taken into consideration in the software. The options of flat terrain option and elevated terrain option are chosen based on the condition where, for example, the flat option is better suited when the height of the receptor is lower than that of the source. Conversely, an elevated terrain option was selected when the height of the receptor is higher than the height of the source. For the HELS-NES case, flat terrain option was set to examine concentration at the receptors as the terrain height of all the receptors are lower than the terrain height of emission source. The model simulations of HELS-NES case does not perform well when using onsite meteorological data as input and had difficulty in calculating the concentration for travel distances up to 35 km from the sources. The performance result from the UBL case was better when estimating predicted concentration at receptors with a distance up to 3 km from the source. A possible reason is due to the case in which the model set up in the software is not able to capture rapidly changing weather conditions in Iceland along the distance from the source to receptors area. For a long-term dispersal, further studies are therefore necessary to forecast meteorological conditions as an input to the model simulation, covering the dominant wind direction and wind speed to receptor area.

Additionally, the model simulations were able to evaluate the effects that seasonal condition has on the H_2S concentration. The results from the HELS-NES case predicted that concentration during winter is higher than the concentration during the summer seasons, and for the UBL case, where the concentration is expected to be higher during the dry season.

In the research, the results of model simulations indicate an increasing level of H_2S concentration around the emission sources in both countries. In the UBL case, the closest residential area is located nearby the power plants (600 m).

Overall, the model simulations of the UBL cases did not exceed the Indonesian occupational health limit (1400 $\mu g/m^3$ for 8-hour average), nor the WHO air quality guidelines (150 $\mu g/m^3$ for 24-hour average). However, the predicted concentration at 2.7 km west of the emission sources, when compared with the Icelandic H_2S legislation, exceeded the limits (50 $\mu g/m^3$ for 24-hour average and 5 $\mu g/m^3$ for annual average) at some locations 3 km west of the emission sources.

For the HELS-NES case, the model simulation using offsite-meteorological data (the Reykjavík weather station) indicated that receptor Waldorf, located about 13 km northwest of the Hellisheidi power plant, was expected to exceed the annual limit of 5 $\mu g/m^3$. According to the model performance result for the 24-hour period, the model had difficulty in estimating the concentration. Therefore, the interpretation of predicted concentration for the model at the 24-hour period (public health limit) may not be appropriately explained. Further research it needs to investigate long-distance dispersal and the influence of atmospheric variability in the model simulation.

The results from AERMOD modelling for the UBL case provides valuable information for the strategy of a monitoring plan. Currently, the monitoring program for H_2S nuisance (1-hour period) is measured quarterly. Therefore the environmental strategy should be improved to accommodate hourly and annual average period monitoring, as well as compared to the H_2S air quality guideline. Also, the performance results of the model for the HELS-NES case at receptors in the Reykjavík area did not go well for the model at a short-term period. However, these results are useful for identifying indicative locations at

residential and public facilities, which could be affected, and a further study shall be needed to study long-term effect where H_2S concentration is indicated to elevate during the winter season.

Geothermal power generation is projected to grow significantly in the future, especially in Indonesia. Hence, the H_2S pollutant level is expected to increase as well, therefore to set up mitigation of the H_2S impact of public health becomes compulsory with great care of the software as well with parameter setting of the model. The approach can be made by setting H_2S air pollution guidelines, odour standards and integrating the policy of Environmental Impact Assessment (the required mandatory government project approval before the project commencement) together with H_2S air pollution guidelines, as well as with continued monitoring during operational activity.

REFERENCES

Aradóttir, Á.L., Thorgeirsson, H., McCaughey, J.H., Strachan, I.B., and Robertson, A., 1997: Establishment of a black cottonwood plantation on an exposed site in Iceland: plant growth and site energy balance. *Agricultural and Forest Meteorology, 1-81,* 1–9.

Aráuz Torres., M.A., 2014: *Modelling H_2S dispersion from San Jacinto - Tizate geothermal power plant, Nicaragua*. University of Iceland, MSc thesis, UNU-GTP, report 3, 54 pp.

Ármannsson, H., and Kristmannsdóttir, H., 1992: Geothermal environmental impact. *Geothermics, 21-5/*6, 869–880.

Atkinson, D., and Lee, R.F., 1992: *Procedures for substituting values for missing NWS meteorological data for use in regulatory air quality models*. U.S. Environmental Protection Agency, North Carolina, website: *www3.epa.gov/scram001/surface/missdata.txt*

ATSDR, 2014: *Public health statement: hydrogen sulfide*. Agency for Toxic Substances and Disease Registry, Atlanta, GA, USA.

Bates, M.N., Garrett, N., Shoemack, P., 2002: Investigation of health effects of hydrogen sulphide from a geothermal source. *Archives of Environmental Health: An International Journal, 57-5,* 405–414.

Bates, M., Crane, J., Balmes, J.R., and Garrett, N., 2015: Investigation of hydrogen sulphide exposure and lung function, asthma and chronic obstructive pulmonary disease in a geothermal area of New Zealand. *PloS one, 10-3,* website: *doi.org/10.1371/ journal.pone.0122062*

Björnsson, S., and Thorsteinsson, Th., 2013: Health protection limit of sulphur hydrogen and its concentration in the metropolitan area. *Naturalist, 83-3/4* (printed in 2014), 151–158.

Chou, C.H., 2003: *Hydrogen sulfide : human health aspects*. WHO, Geneva, 41 pp; website: *apps.who.int//iris/handle/10665/42638.*

Cimorelli, A.J., Perry, S., Venkatram, A., Weil, R.J., Paine, R.J., Wilson, R.B., Lee, R.F., Peters, W.D., Brode, R.W., Paumier, J.O., and Thurman, J., 2017: *AERMOD model formulation and evaluation*. U.S. Environmental Protection Agency, North Carolina, 177 pp.

Cimorelli, A.J., Perry, S.G., Venkatram, A., Weil, J.C., Paine, R.J., Wilson, R.B., Lee, R.F., Peters, W.D., Brode, R.W., Paumier, J.O., 2004: *AERMOD: Description of model formulation*. U.S. Environmental Protection Agency, North Carolina, 91 pp.

European Agency for Safety and Health at Work, 2009: *Directive 2009/161/EU - Indicative occupational exposure limit values*. EU-OSHA, Brussel, website: *osha.europa.eu/en/legislation/directives/commission-directive-2009-161-eu-indicative-occupational-exposure-limit-values*

Cooper, D.C., and Alley, F.C., 1994: *Air pollution control; a design approach* (2nd ed.). Waveland Press, Inc., Prospect Heights, Illinois.

Dickson, M.H., and Fanelli, M., 2004: *What is geothermal energy?* International Geothermal Association, website: *iga.igg.cnr.it/geo/geoenergy.php.*

European Environment Agency, 2017: *Policy instruments.* European Environment Agency, website: *www.eea.europa.eu/themes/policy/intro.*

EREC, 2010: *Renewable energy in European, markets, trends and technologies* (2nd ed.). European Renewable Energy Council, Gutenberg Press, London, 289 pp.

Evans, D.J., 1996: *Straightforward statistics for the behavioral sciences*. Brooks/Cole Publishing Company, 600+xxii pp.

Finnbjörnsdóttir, R.G., Carlsen, H.K., Thorsteinsson, Th., Oudin, A., Lund, S.H., and Gíslason, Th., Rafnsson, V., 2016: Association between daily hydrogen sulfide exposure and incidence of emergency hospital visits: a population-based study. *PloS One, 11*-5, 19,
website: *doi.org/10.1371/journal.pone.0154946.*

Finnbjörnsdóttir, R.G., Oudin, A., Elvarsson, B.T., Gíslason, T., and Rafnsson, V., 2015: Hydrogen sulfide and traffic-related air pollutants in association with increased mortality: a case-crossover study in Reykjavik, Iceland. *BMJ Open, 5-4*, website: *doi.org/10.1136/bmjopen-2014-007272.*

GEA, 2016: *2016 annual US. and global geothermal power production report.* Geothermal Energy Association, Davis CA.

Gunnarsson, I., Aradóttir, E.S., Sigfússon, B., Gunnlaugsson, E., and Júlíusson, B.M., 2013*:* Geothermal gas emission from Hellisheidi and Nesjavellir Power Plants, Iceland. *Geothermal Resource Council, Transactions, 37,* 785–789.

Gunnlaugsson, E., 2016: Environmental management and monitoring in Iceland: reinjection and gas sequestration at the Hellisheidi power plant. *Paper presented at "SDG Short Course I on Sustainability and Environmental Management of Geothermal Resource Utilization and the Role of Geothermal in Combating Climate Change", organized by UNU-GTP and LaGeo, in Santa Tecla, El Salvador*, 8 pp.

Harrison, R. M., 2014: *Pollution; causes, effects and control* (5th ed.). RSC Publishing, Birmingham, website: *www.rsc.org/books.*

Hosseinzadeh, A., 2014: Air quality impact assessment: H_2S dispersion modelling for the Sabalan geothermal plant, NW-Iran. Report 15 in: *Geothermal Training in Iceland 2014*. UNU-GTP, Iceland, 237-260.

IEA, 2018: *World energy outlook 2017.* International Energy Agency, website: *www.iea.org/weo2017/.*

Kristmannsdóttir, H., Sigurgeirsson, M., Ármannsson, H., Hjartarson, H., and Ólafsson, M., 2000: Sulfur gas emissions from geothermal power plants in Iceland. *Geothermics, 29*, 525–538.

Lakes Environmental Software, 2018: *AERMOD View, Gaussian plume air dispersion model.* Lakes Environmental Software.

Lakes Environmental Software, 2017: *AERMOD View knowledgebase*. Lakes Environmental Software, website: *www.weblakes.com/kb/AERMOD/index.php*

Langner, C., and Klemm, O., 2011: A comparison of model performance between AERMOD and AUSTAL2000. *J. Air and Waste Management Association, 61-6*, 640–646.

Lin, C.H., Mao, I.F., Tsai, P.H., Chuang, H.Y., Chen, Y.J., and Chen, M.L., 2010: Sulfur-rich geothermal emissions elevate acid aerosol levels in metropolitan Taipei. *Environmental Research, 6-110*, 536–543.

MEMR, 2015: *Indonesian strategic plan 2015-2019*. Ministry of Energy and Mineral Resources of Republic Indonesia, Jakarta.

Meteorological Resource Center, 2002: *Meteorological data processing: stability*. Meteorological Resource Center, website: *www.webmet.com*

Ministry for Environmental and Natural Resources in Iceland, 2010: *Regulation no. 514/2010 for hydrogen sulphide concentration in atmosphere*. MENR, Reykjavík.

Ministry for Environment, Indonesia, 1996: *Odour standard*. MfE, Jakarta.

Ministry of Manpower and Transmigration, Indonesia, 2011: *Value and threshold limits on physical and chemical, No. 13/MEN/X/2011*. MMT, Jakarta.

Ministry of Welfare, Iceland, 2012: *Regulation no. 1296/2012, amendment on regulation for pollution and the working environment, no. 390/2009 (in Icelandic)*. Ministry of Welfare, Reykjavík.

MITei: 2017a: *Electricity security of supply in Iceland*. MIT Energy Initiative, website: *energy.mit.edu.*

MITei, 2017b: *Electricity security of supply in Iceland; An assessment about how to achieve electricity security of supply by 2020 and 2030 in the most economical way*. MIT Energy Initiative, retrieved from website: *www.os.is.*

Moreira, D., and Marco, V., 2009: *Air pollution and turbulence: modelling and applications* (3rd ed.). CRS Press, Boka Raton, FL, USA.

Mutia, T.M., 2016: *The impacts of geothermal power plant emissions on terrestrial ecosystems in contrasting bio-climatic zones*. University of Iceland, Faculty of Life and Environmental Sciences, Reykjavík, PhD thesis, 147 pp.

OECD, 2014: *OECD Environmental performance reviews; Iceland*. OECD, Paris, website: *dx.doi.org/10.1787/9789264214200-en*

Ólafsdóttir, S., 2014: *Near field fate of atmospheric hydrogen sulfide from two geothermal power plants*. University of Iceland, Reykjavík, PhD thesis, 133 pp.

Ólafsdóttir, S., and Gardarsson, S.M., 2013: Impacts of meteorological factors on hydrogen sulfide concentration downwind of geothermal power plants. *Atmospheric Environment, 77*, 185–192.

Ólafsdóttir, S., Gardarsson, S.M., and Andradóttir, H.O., 2014: Spatial distribution of hydrogen sulfide from two geothermal power plants in complex terrain. *Atmospheric Environment, 82*, 60–70.

Orkustofnun., 2018: *Energy statistics in Iceland 2018*. Orkustofnun, Reykjavik, under publication,

PDAM Tirtawening, 2017: *Laboratory analysis of H_2S air ambient at Ulubelu geothermal field*. Bandung.

PGE, 2015: *Annual integrated report*. Pertamina Geothermal Energy, Jakarta.

Puja Dewi, M., 2018: *Women in PT Pertamina Geothermal Energy*. WING, website, *wing.wildapricot.org/resources/Documents.*

Putranto, A.D., 2016: *H_2S and NH_3 dispersion analysis from geothermal power plants emission and its influence to ambient air quality (case study: PT. Pertamina Geothermal Energy Area, Kamojang)*. Institute of Technology, Bandung (ITB).

Reykjavik Energy, 2016: *Environmental report OR 2016*. OR, Reykjavik, report 100 pp.

Richter, A., 2018: Top 10 geothermal countries based on installed capacity – year end 2017. *Think Geoenergy*, p. 1, website: *www.thinkgeoenergy.com/top-10-geothermal-countries-based-on-installed-capacity-year-end-2017/*

RStudio Team., 2016: *Integrated development for RStudio*. RStudio, Boston, website: *www.rstudio.com/.*

Rzeszutek, M., Szulecka, A., Oleniacz, R., and Bogacki, M., 2017: Assessment of the AERMOD dispersion model over complex terrain with different types of meteorological data: Tracy Power Plant experiment. *E3S Web of Conferences, 22*, website: *doi.org/10.1051/e3sconf/20172200149.*

South Coast AQMD, 2018: *SCAQMD modeling guidance for AERMOD*. South Coast Air Quality Management District, CA, website: *www.aqmd.gov/home/air-quality/air-quality-data-studies/meteorological-data/modeling-guidance.*

Statistics Iceland, 2018: *Population of Reykjavik*. Statistics Iceland, Reykjavík.

Sterner, T., 2003: *Policy instruments for environmental and natural resources management*. The World Bank, Washington, Resources for the Future.

SWECO, 2018: *Geothermal sustainability assessment protocol: Hellisheidi geothermal project*. Orka Náttúrunnar, report, 131 pp.

Taylor, K.E., 2001: Summarizing multiple aspects of model performance in a single diagram. *J. Geophys. Research, 106*, 7183-7192.

Taylor, K.E., 2005: *Taylor diagram primer*. K.E. Taylor.

Thorsteinsson, Th., Hackenbruch, J., Sveinbjörnsson, E., and Jóhannsson, T., 2013: Statistical assessment and modelling of the effects of weather conditions on H_2S plume dispersal from Icelandic geothermal power plants. *Geothermics, 45*, 31–40.

US EPA, 2004: *Users guide for the AERMOD terrain preprocessor (AERMAP)*. U.S. Environmental Protection Agency, North Carolina.

US EPA, 2005: *Environmental revision to the guideline on air quality models: adoption of a preferred general purpose (flat and complex terrain)*. U.S. Environmental Protection Agency, retrieved from *www.federalregister.gov/.*

US EPA, 2016: *AERMOD implementation guide*. U.S. Environmental Protection Agency, North Carolina.

Ulubelu District, 2017: *Population size of the Ulubelu villages (7 villages)*. Ulubelu District offices.

Weil, J.C., Venkatram, A., Wilson, R.B., Paine, R.J., Perry, S.G., Lee, R.F., and Peters, W.D., 2016: *User's guide for the AERMOD meteorological preprocessor (AERMET)*. UN EPA, North Car., 310 pp.

WHO, 2000: *Air quality guidelines for Europe* (2nd ed.). World Health Organisation, Copenh., 288 pp.

Wieringa, J., 1992: Updating the Davenport roughness classification. *J. Wind Engineering and Industrial Aerodynamics, 41–44*, 357–368.

Zannetti, P., 1990: *Air pollution modelling: theories, computational methods and available software*. Computational Mechanics Publications, Southampton, 425 pp.

Zou, B., Zhan, F.B., Wilson, J.G., and Zeng, Y., 2010: Performance of AERMOD at different time scales. *Simulation, Modelling, Practice and Theory, 5-18*, 612–623.

APPENDIX A: Class stability on calculating the plume for the model simulations based on Gaussian formulae (A-1) and building inputs (A-2)

A-1: Description of procedure for determining class stability based on Turner's method from the Section 2.2.5 (retrieved from the Meteorological Resource Center, 2002, Section 6.4.1).

1. If the total cloud cover or opaque cloud cover is 10/10 and the ceiling is less than 7,000 feet, then net radiation index is equal to 0 (whether day or night)
2. For night times: (from one hour before sunset to one hour after sunrise):
    a. If total cloud cover is 4/10, net radiation index was equal to -2.
    b. If total cloud cover is > 4/10, net radiation index was equal to -1.
3. For daytimes
    a. Determine the insolation class number as a function of solar altitude (referring to Table 4, the data of solar altitude was obtained fromwebsite:*aa.usno.navy.mil/data/docs/AltAz.php*)
    b. If total cloud cover is 5/10, use the net radiation index (for this study refer to Table 3) corresponding to the isolation class number.

If cloud cover is > 5/10, modify the insolation class number using the following six steps:

1. Ceiling < 7,000 ft, subtract 2
2. Ceiling 7,000 ft, but < 160,000 ft, subtract 1
3. Total cloud cover equal to 10/10, subtract 1 (only apply to ceiling 7,000 ft since cases with 10/10 coverage below 7,000 ft are considered in item 1 above).
4. If insolation class number has not been modified by steps 1-3 above, assume modified class number equal to insolation class number.
5. If the modified insolation class number is less than 1, it is equal to 1.
6. The net radiation index used is based on Table 3 corresponding to the modified insolation class number.

A-2: Building properties for the UBL and HELS-NES cases. The reference point (SW corner) was selected to define the size of the building as model inputs in the AERMOD

TABLE A-1: Modelled building properties of Ulubelu power plants

Source	X* (m)	Y* (m)	Base elevation (m a.s.l)	Height (m)	Width (m)	Length (m)
Tower Structure Unit 1	452626	9413244	797.96	12	89	18
Tower Structure Unit 2	452732	9413241	790.57	12	89	18
Power House Units 1 & 2	452662	9413182	792.77	15	92	24
	452661	9413158	790.39	27	92	24
	452661	9413147	790.98	6	92	10
Tower Structure Unit 3	453029	9413596	803.92	11	102	20
Tower Structure Unit 4	453144	9413576	803.76	11	102	20
Power House Units 3 & 4	453083	9413508	796.99	29	87	20
	453082	9413498	796.87	19	87	10

*Coordinates in UTM zone 48 South-Hemisphere

TABLE A-2: Modelled building properties of Hellisheidi and Nesjavellir power plants

Source	X* (m)	Y* (m)	Base elevation (m a.s.l)	Height (m)	Width (m)	Length (m)
Hellisheidi						
Tower Structure Unit A	480377.58	7100920.09	271.85	11	25	30
Tower Structure Unit B	480419.67	7100962.2	277.07	11	25	30
Tower Structure Unit C	480465.91	7101002.32	261.51	11	25	30
Tower Structure Unit D	480507.11	7101044.81	265.84	11	25	30
Tower Structure Unit E	480632.35	7101193.91	252.41	11	35.53	30.66
Power House	480380.81	7101108.57	270.71	18		
Nesjavellir						
Tower Structure	487596.16	7108979.50	207.26	9.7	71.83	15.74
Power House	487423.38	7109098.52	177.98	15.8		

*Coordinates in UTM zone 27 North-Hemisphere

APPENDIX B: Model scenarios for the Ulubelu case (UBL) and Hellisheidi and Nesjavellir case (HELS-NES)

TABLE B-1: Model scenarios for the Ulubelu power plants case study.

Test case / scenario	Averaging time options	Terrain set up options**	H_2S observation station/ receptor	Input value of emission rate*		
				PP Units 1 & 2 (g/s)	PP Unit-3 (g/s)	PP Unit-4 (g/s)
Model performance						
28 August, 2017	8-hour	Elevated, and flat and elevated	PP34	16.96	16	15
28-29 August, 2017	24-hour		Mekar Sari	17	16	15
29-30 August, 2017	24-hour		Ngarip	16.75	15.91	15
30-31 August, 2017	24-hour		Karang Rejo	16.64	15.76	15
Model simulation* **						
Wet season, dry season and annual period Aug. 2016 – Aug. 2017	1-hour, 8-hour, 24-hour	Elevated	Ulubelu villages, H_2S measurement points workplaces at UBL PP	21	16.75	21

* Input values based on dates of the H_2S measurement activities

** Model simulations considering different terrain options (flat & elevated) between receptors & source

*** Results of the models were not compared to observed data due to lack of H_2S measurement. They were, however, assessed with WHO air quality guidelines, and Icelandic and Indonesian H_2S limits.

TABLE B-2: Models scenario for the Hellisheidi and Nesjavellir power plants case study

Test case / scenario	Averaging time options	Terrain set up options	H_2S observation station/ receptor*	Weather input data**	Input value of emission rate*	
					Hellisheidi PP (g/s)	Nesjavellir PP (g/s)
Model performance						
B-1: Various meteorological data stations						
1 March 2017 & 9 Nov. 2015	1-hour 24-hour	Elevated	GRE, HEH, NLH	STRM, HELS, REYK, OLKE	129.6 212.6	268.9 212.6
B-2 The effect on terrain set up correction						
1 March, 2017 9 Nov., 2015, & 23 June, 2016	1-hour & 24 hour	Flat vs. elevated	GRE, HEH, NLH	HELS, REYK, STRM	129.6 212.6 129.6	268.9 212.6 268.9
2012 2013 2014 2015 2016	Annual Annual Annual Annual Annual	Flat vs. elevated	GRE, HEH, NLH	HELS, REYK, STRM	540 412 392 212.6 129.6	358 290 356.95 278 268.9
Model simulation						
Winter season, summer season & annual period January 2012- 30 April 2017	1-hour, 8-hour, 24-hour, seasons, annual	Flat	Reykjavík capital area, GRE, HEH, NLH, Work places at HEL & NES PP	HELS, REYK	540****	358****

*H_2S stations: GRE = Grensasvegur; H_2S Station, HEH = Hvaleyrarholt; H_2S Station, NLH = Nordlingaholt.

**Met. stations of Straumsvík = STRM; Ölkelduháls = OLKE; Hellisheidi = HELS; Reykjavík = REYK.

*** Based on the period of H_2S observation plus 5 % - Data was gathered from Reykjavík Energy, 2016 (page 84).

**** Gunnarsson et al., 2013 (page 787).

APPENDIX C: Comparison of modelled results with observed values for Ulubelu (UBL case) and Hellisheidi and Nesjavellir (HELS-NES case).

The model simulations evaluate various meteorological data, as well as model setup with different terrain options (e.g., flat and elevated)

TABLE C-1: Result of comparison of the observed and predicted concentration for the UBL case

Receptors	Base elevation (m a.s.l)	Averaging periods	Elevated (µg/m^3)	Flat (µg/m^3)	Obs. values (µg/m^3)**
Power plant units 3 & 4	802	8-hour (28 Aug., 2017)	1.9	2*	22
Mekarsari	842	24-hour (28-29 Aug., 2017)	1.5*	0.2	1
Ngarip	869	24-hour (29-30 Aug., 2017)	0.073*	0.0013	0.0014
Karang Rejo	796	24-hour (30-31 Aug., 2017)	0.025	0.0026*	0.0014

*Input values on Taylor Diagram based on the difference elevation of receptors and emission sources;
** Observed values were obtained at a point receptor with different time scales of 8-hour and 24-hour.

TABLE C-2: Model performances at 8-hour and 24-hour period for different terrain options for the Ulubelu case (test case A.)

Test case number	Periods	Weather stations	Correlation (r)		Standard deviation (SD) model (µg/m^3)		Standard dev., observed data (SD) (µg/m^3)	Root mean square error (RMSE) (µg/m^3)	
			Elevated	Flat	Elevated	Flat		Elevated	Flat
A	8-hour, 24-hour	UBL	0.75	0.85*	0.96	1*	10.9	8.8	8.6*
	24-hour		0.99	0.99*	0.8	0.8*	0.8	0.0025	0.0035*

*Input values on Taylor diagram based on difference in elevation of receptors and emission.
**Input values of test cases A-1 and A-2 were obtained from model simulations presented in Table C-1,
UBL = Ulubelu meteorological station

TABLE C-3: Results of comparison of observed and predicted concentration for a 1-hour averaging period using four different meteorological data for the HELS-NES case

Meteorological data	GRE receptor		HEH receptor		NLH receptor	
	Elevated (µg/m^3)	Obs. values (µg/m^3)	Elevated (µg/m^3)	Obs.values (µg/m^3)	Elevated (µg/m^3)	Obs. values (µg/m^3)
1st March 2017						
Straumsvík						
08.00 – 09.00	15	124	7	12	6.83	119.67
10.00 – 11.00	8.67	77.79	2	10	8	89.69
16.00 – 17.00	2.8	60	7	7	6	57.6
20.00 – 21.00	7.6	74.87	9	4	0.2	44
22.00 – 23.00	3.86	41	0.01	2.5	4.98	38.59
Ölkelduháls						
08.00 – 09.00	0.026	124	0.025	12	0.03	119.67
10.00 – 11.00	0.4	77.79	0.36	10	0.4	89.69
16.00 – 17.00	0.1	60	0.1	7	0.2	57.6
20.00 – 21.00	0.09	74.87	0.09	4	0.094	44
22.00 – 23.00	0.09	41	0.09	2.5	0.096	38.59
Hellisheidi						
08.00 – 09.00	0.4	124	6	12	0.5	119.67
10.00 – 11.00	0.2	77.79	2.69	10	0.84	89.69
16.00 – 17.00	0.05	60	0.05	7	0.05	57.6
20.00 – 21.00	0.01	74.87	0.01	4.48	0.02	44
22.00 – 23.00	0.01	41	0.01	2.5	0.01	38.59
Reykjavík						
08.00 – 09.00	15	124	7	12	6.83	119.67

Meteorological data	GRE receptor		HEH receptor		NLH receptor	
	Elevated (µg/m^3)	Obs. values (µg/m^3)	Elevated (µg/m^3)	Obs.values (µg/m^3)	Elevated (µg/m^3)	Obs. values (µg/m^3)
10.00 – 11.00	8.67	77.79	2.3	10	8	89.69
16.00 – 17.00	4	60	2.9	7	5.7	57.6
20.00 – 21.00	7.6	74.87	9	5	0.2	44
22.00 – 23.00	3.8	41	0.01	2.52	4.95	38.59
9th November, 2015						
Straumsvík						
08.00 – 09.00	6	19	5.4	4.4	16.59	31
10.00 – 11.00	10.87	24.79	6.55	7	22.87	41
16.00 – 17.00	8.48	76.66	7	5.84	13.68	57
20.00 – 21.00	2.8	2	3	53.5	9	29
22.00 – 23.00	2.9	1.53	4	14.5	5	13.7
Ölkelduháls						
08.00 – 09.00	3.68	19	3	4.44	4	31
08.00 – 09.00	0.04	24.79	0.04	7	0.04	41
10.00 – 11.00	0.085	76.66	0.08	5.8	0.09	57
16.00 – 17.00	0.03	2	0.03	53.5	0.03	29
22.00 – 23.00	2	1.53	5.32	14.5	2.79	13.7
Hellisheidi						
08.00 – 09.00	0.7	19	0.66	4.4	0.78	31
10.00 – 11.00	10.8	24.79	9.5	7	22.79	41
16.00 – 17.00	0.02	76.66	5.55	5.84	0.6	57.5
20.00 – 21.00	0.03	2	0.03	53.5	0.04	29
22.00 – 23.00	2.67	1	0.75	14.5	3.6	13.7
Reykjavík						
08.00 – 09.00	6.28	19	5	4	16.59	31
10.00 – 11.00	10.87	24.79	9.55	7	22.87	41
16.00 – 17.00	4.64	76.66	3.6	5.84	14	57.5
20.00 – 21.00	2.8	2	3	53.5	9	29
22.00 – 23.00	2.9	1	4	14.5	5	13.7

TABLE C-4: Model evaluation results for the 24-hour averaging period simulated by four different meteorological stations for the HELS-NES case

Weather stations	GRE receptor		HEH receptor		NLH receptor	
	Elevated (µg/m^3)	Observed values (µg/m^3)	Elevated (µg/m^3)	Observed values (µg/m^3)	Elevated (µg/m^3)	Observed values (µg/m^3)
1st March 2017						
Straumsvík	5	65.94	3	9.56	5	58.61
Ölkelduháls	0.1	65.94	0.1	9.56	0.1	58.
Hellisheidi	1	65.94	0.9	9.56	1	58.6
Reykjavík	5	65.94	3	9.56	5	58.6
9th November 2015						
Straumsvík	3.67	25.98	3	11	7	31.5
Ölkelduháls	0.7	25.98	0.79	11	0.89	31.5
Hellisheidi	1	25.98	1	11	0.99	31.5
Reykjavík	3.67	25.98	3	11	7	31.5

TABLE C-5: Results of comparison of the model for 1-hour and observed values using various meteorological data which considered terrain conditions for the HELS-NES case

Periods	GRE Receptor (μg/m^3)			HEH Receptor (μg/m^3)			NLH Receptor (μg/m^3)		
	Elevated	Flat	Obs. values	Elevated	(Flat)	Obs. values	(Elevated)	(Flat)	Obs. values
Straumvík meteorological data									
1st March 2017									
02.00 - 03.00	15.7	17	48	7	8.67	23.55	1	1.37	37.6
04.00 - 05.00	9	10.86	69	3.98	4.7	16.98	5.5	6	47.7
06.00 - 07.00	1	1	57.97	10	11.6	4	13	14	70.77
08.00 – 09.00	15	23	124	7	27.99	12	6.8	25.6	119.67
10.00 – 11.00	8.67	31	77.79	2	8	10	8	34	89.69
12.00 – 13.00	2	2.68	76.8	5.46	6	7.99	8.7	9.46	60.99
14.00 – 15.00	0.78	0.85	51	7	7.79	10.47	6	6.6	44.67
16.00 – 17.00	2.8	6	60.47	7	11.56	7	6	9	57.6
18.00 – 19.00	10.9	12	52	5	6	5.65	5.37	6	61
20.00 – 21.00	7.62	8.48	74.87	9	10	4	0.2	0.2	44
22.00 – 23.00	3.86	4.59	41	0.01	0.01	2.5	4.98	5.89	38.59
24.00 – 01.00	0	0	56	0	0	9	0	0	30.5
9th November 2015									
02.00 - 03.00	0.06	0.07	2	10	11.56	1	5.60	6	6
04.00 - 05.00	4	4.92	8	4	4.9	0.3	11	12	12.99
06.00 - 07.00	8.9	10.75	20	0.02	0.02	2.67	5	6	38.5
08.00 – 09.00	6	6.99	19	5	6.4	4	16.59	17.98	31
10.00 – 11.00	10.8	11.99	24.79	6.55	11	7	22.87	24.57	41
12.00 – 13.00	3.8	4	53.62	1.87	2	13	15.84	18	41.83
14.00 – 15.00	8	9.68	73.62	7	8.49	4.64	11.72	13	47.67
16.00 – 17.00	8	9	76.66	7	8.49	5.84	13.68	16	57
18.00 – 19.00	3.9	4	26	3.64	4	24.68	8	9.3	54.65
20.00 – 21.00	2.8	3	2	3	3.6	53	9	10	29
22.00 – 23.00	2.9	3	1.5	4	4.89	14	5	6	13.7
24.00 – 01.00	0	0	3	0	0	1.82	0	0	5.35
23rd June 2016									
02.00 - 03.00	0.1	0.2	1.78	0.1	0.2	1	0.1	0.2	2
04.00 - 05.00	0.5	0.6	1.85	0.5	0.6	1	0.6	0.65	2
06.00 - 07.00	2.79	3	1.77	2.46	2.69	1.62	3	3.57	2
08.00 – 09.00	3	3.8	1.97	3	3	1	4	4.59	2
10.00 – 11.00	0.5	0.58	2	0.46	0.5	1	0.58	0.65	2
12.00 – 13.00	1.2	1	1.99	1	1.2	0.94	1	1.56	2
14.00 – 15.00	0.5	0.54	1.98	0.4	0.49	1	0.56	0.6	1.98
16.00 – 17.00	0.1	0.2	2	0.2	0.2	1	0.2	0.2	2
18.00 – 19.00	0.66	0.7	2	0.59	0.6	1	0.76	0.8	2
20.00 – 21.00	0.1	0.2	1.83	0.2	0.2	1	0.2	0.2	1.75
22.00 – 23.00	0.1	0.12	1.76	0.1	0.1	0.93	0.12	0.1	1.87
24.00 – 01.00	0	0	1.6	0	0	1.67	0	0	1.58
Hellisheidi meteorological data									
1st March 2017									
02.00 - 03.00	11	13	48	0.34	0.38	23.55	8	9.44	37.61
04.00 - 05.00	2.99	3	69	2.66	2.89	16.98	3.5	3.73	47.71
06.00 - 07.00	11.55	12.72	57.97	2.66	2.89	4	12.96	14	70.77
08.00 – 09.00	0.4	0.4	124	6	6.96	12	0.47	0.5	119.67
10.00 – 11.00	0.15	0.2	77.79	2.69	3	10	0.8	0.91	89.69
12.00 – 13.00	0.005	0.006	76.8	0.004	0.005	7.99	0.005	0.006	60.99
14.00 – 15.00	0.005	0.006	51	0.005	0.005	10	0.006	0.006	44.67
16.00 – 17.00	0.05	0.05	60	0.05	0.05	7	0.05	0.05	57.62
18.00 – 19.00	0.01	0.02	52	0.01	0.03	5.65	0.02	0.02	61
20.00 – 21.00	0.01	0.1	74.87	0.01	0.09	4.48	0.02	0.1	44
22.00 – 23.00	0.01	0.01	41	0.01	0.01	2.5	0.01	0.01	38.59
24.00 – 01.00	0	0	56	0	0	9	0	0	30.5
9th November 2015									
02.00 - 03.00	0.3	0.3	2	14.99	16.59	1	10.8	11.60	6
04.00 - 05.00	6	6.99	8	4.55	5	0.3	0.95	1.07	12.99
06.00 - 07.00	0.5	0.55	20	0.47	0.52	2.67	0.55	0.6	38.5
08.00 – 09.00	0.7	0.78	19	0.66	0.73	4.44	0.78	0.85	31
10.00 – 11.00	10.83	11.95	24.79	9.51	11	7	22.79	24	41
12.00 – 13.00	0.1	11.95	53.62	10	11	13.5	0.38	24	41.8
14.00 – 15.00	0.03	11.95	73.62	0.03	11	4.64	0.03	24	47.67

Periods	GRE Receptor (μg/m^3)			HEH Receptor (μg/m^3)			NLH Receptor (μg/m^3)		
	Elevated	**Flat**	**Obs. values**	**Elevated**	**(Flat)**	**Obs. values**	**(Elevated)**	**(Flat)**	**Obs. values**
16.00 – 17.00	0.02	0.03	76.66	5.55	6.19	5.84	0.62	0.68	57.5
18.00 – 19.00	0.01	0.02	26	0.01	0.02	24.68	0.02	0.05	54.65
20.00 – 21.00	0.02	0.03	2	0.03	0.04	53.5	0.036	0.04	29
22.00 – 23.00	2.67	2.97	1.5	0.75	0.84	14.5	3.6	4	13.7
24.00 – 01.00	0	0	3	0	0	1.8	0	0	5.35
23rd June 2016									
02.00 - 03.00	0.04	0.05	1.78	0.04	0.05	1.49	0.04	0.05	2
04.00 - 05.00	0.01	0.02	1.85	0.01	0.02	1	0.02	0.03	2
06.00 - 07.00	0.03	0.04	1.77	0.03	0.04	1.62	0.03	0.04	2
08.00 – 09.00	0.94	1	1.97	0.86	0.98	1	1	1	2
10.00 – 11.00	0.1	0.1	2	0.1	0.1	1	0.12	0.1	2
12.00 – 13.00	0.07	0.08	1.99	0.07	0.08	0.94	0.08	0.09	2
14.00 – 15.00	0.1	0.1	1.98	0.1	0.1	1	0.1	0.1	1.98
16.00 – 17.00	0.05	0.06	2	0.05	0.06	1	0.06	0.07	2
18.00 – 19.00	0.005	0.006	2	0.005	0.005	1	0.006	0.006	2
20.00 – 21.00	0.004	0.005	1.83	0.004	0.005	1	0.005	0.005	1.75
22.00 – 23.00	0.02	0.03	1.76	0.02	0.03	0.9	0.03	0.03	1.87
24.00 – 01.00	0	0	1.6	0	0	1.67	0	0	1.58
Reykjavík station meteorological data									
1st March 2017									
02.00 - 03.00	15.73	17	48	7	8.67	23.55	1	1	37.6
04.00 - 05.00	9	10.86	69	3.98	4.7	16.98	5.5	6	47.7
06.00 - 07.00	1	1.3	57.97	10.48	11.6	4	13	14	70.77
08.00 – 09.00	15	16.67	124	7	8	12	6.83	8	119.67
10.00 – 11.00	8.67	10	77.79	2	2.71	10	8	9.88	89.69
12.00 – 13.00	2	2.72	76.8	6	6.83	7.99	11.89	12.88	60.99
14.00 – 15.00	0.7	0.78	51	6.32	6.9	10.47	5.56	5.89	44.67
16.00 – 17.00	4	4.30	60	2.91	3	7	5.70	5.97	57.62
18.00 – 19.00	11	12.49	52	5.46	6	5.65	5.38	6	61
20.00 – 21.00	7.6	8.49	74.87	9	10	4.48	0.1	0.2	44
22.00 – 23.00	3.8	4.59	41	0.01	0.01	2.52	4.95	5.9	38.59
24.00 – 01.00	0	0	56	0	0	9	0	0	30.5
9th November 2015									
02.00 - 03.00	0.06	0.07	2	10.38	11.57	1	5.61	6	6
04.00 - 05.00	4	4.93	8	4	4.94	0.33	79.78	12	12.99
06.00 - 07.00	8.93	10.76	20	0.02	0.02	2.6	5	6	38.5
08.00 – 09.00	6	6.99	19	5	6.4	4	16.59	17.98	31
10.00 – 11.00	10.87	11.99	24.79	9.55	11	7	22.87	24.57	41
12.00 – 13.00	3.8	4.46	53.62	1.86	2	13.53	15.83	18.19	41.8
14.00 – 15.00	8.39	9.69	73.62	7	8	4.64	11.83	13.56	47.67
16.00 – 17.00	4.64	5.5	76.66	3.59	4	5.84	14	16.75	57.52
18.00 – 19.00	3.92	4.44	26.29	3.64	4	24.68	8.49	9	54.65
20.00 – 21.00	2.83	3	2	3	3.6	53.52	9	10	29
22.00 – 23.00	2.92	3.48	1.5	4	4.89	14.53	5	6	13.73
24.00 – 01.00	0	0	3	0	0	1.82	0	0	5
23rd June 2016									
02.00 - 03.00	0.1	0.2	1.78	0.1	0.2	1.49	0.1	0.2	2.3
04.00 - 05.00	0.54	0.59	1.85	0.5	0.56	1	0.6	0.65	2.3
06.00 - 07.00	3	3	1.77	2.63	2.88	1.62	3.6	3.86	2.29
08.00 – 09.00	3.5	3.83	1.97	3	3	1	4	4.62	2
10.00 – 11.00	0.5	0.59	2	0.46	0.5	1	0.58	0.65	2
12.00 – 13.00	1	1	1.99	1	1	0.94	1.4	1.56	2
14.00 – 15.00	0.5	0.5	1.98	0.4	0.49	1	0.56	0.6	1.98
16.00 – 17.00	0.1	0.2	2	0.2	0.2	1	0.2	0.2	2
18.00 – 19.00	0.65	0.69	2	0.59	0.63	1	0.75	0.79	2
20.00 – 21.00	0.1	0.2	1.83	0.2	0.2	1	0.2	0.2	1.75
22.00 – 23.00	0.1	0.2	1.76	0.1	0.1	0.93	0.1	0.1	1.87
24.00 – 01.00	0	0	1.6		0	1.67	0	0	1.58

TABLE C-6: Model performances at the 1-hour average period for the different terrain options

Test Case Number	Periods	Weather stations*	Correlation (r)		Standard deviation (SD) model (µg/m³)		Standard dev. Obs. data (SD) (µg/m³)	Root mean square error (RMSE) (µg/m³)	
			Elevated	Flat	Elevated	Flat		Elevated	Flat
B. Nesjavellir (NES) and Hellisheidi (HEH) Iceland**									
9th November 2015 and 1st March 2017									
B.2	1-hour	REYK	0.04	0.3	10	5	30	30.58	28
	1-hour	STRM	0.3	0.4	4	7	30	28.5	27
	1-hour	HELS	-0.14	-0.05	4.65	6	30	30.75	30.52
23rd June 2016									
B.2	1-hour	REYK	0.2	0.2	1	1	0.4	1	1
	1-hour	STRM	0.2	0.2	1	1	0.4	1	1
	1-hour	HELS	0.1	0.1	0.3	0.3	0.4	0.47	0.48

*REYK = Reykjavík meteorological station; STRM = Straumsvík meteorological station, HELS = Hellisheidi meteorol. station.
**The input values of the test case B-2, 1- hour model runs were obtained from the model simulation presented in Table C-5.

TABLE C-7: Results comparison of model for the 24-hour and the observation values using four meteorological data and considered model setup (elevated and flat options) for the HELS-NES case

Periods	GRE receptor (µg/m³)			HEH receptor (µg/m³)			NLH receptor (µg/m³)		
	Elevated	Flat	Obs. values	Elevated	Flat	Obs. values	Elevated	Flat	Obs. values
The 24 hour models using Straumsvík weather station data									
9th November 2015	3.67	4	25.98	3	3.54	11	7	8	31.5
1st March 2017	5	5.6	65.9	3	3.77	9.5	5	5.97	58.6
23rd June 2016	0.6	0.7	1.9	0.5	0.6	1	0.7	0.78	2
The 24 hour models using Hellisheidi weather station data									
9th November 2015	1	1	25.98	2	2.5	11	1.9	2	31.5
1st March 2017	1	1.5	65.9	0.9	1	9.5	1	1.5	58.6
23rd June 2016	0.07	0.09	1.9	0.07	0.083	1	0.08	0.1	2.12
The 24 hour models using Reykjavík weather station data									
9th November 2015	3.67	4	25.98	3	3.5	11	7	8	31.5
1st March 2017	4.95	5.59	65.9	3	3.75	9.5	5	6	58.6
23rd June 2016	0.6	0.7	1.9	0.55	0.6	1	0.7	0.8	2

GRE = Grensasvegur H_2S station; HEH = Hvaleyrarholt H_2S station; NLH = Nordlingaholt H_2S station.

TABLE C-8: Results of comparison of modelled annual average and observed values using two meteorological data and model setup (elevated and flat options for HELS-NES case

	GRE Receptor (µg/m³)			HEH Receptor (µg/m³)			NLH Receptor (µg/m³)			KOP Receptor (µg/m³)		
	Elevated	Flat	Obs. values	Elevated	Flat	Obs. values	Elevated	Flat	Obs. values	Elevated	Flat	Obs. values
The model set up using Hellisheidi weather station data												
2016	0.5	0.55	3	0.4	0.4	3	0.7	0.7	6	0.5	0.5	-
2015	0.4	0.4	4	0.4	0.4	2	0.6	0.6	4	0.5	0.4	2
2014	0.79	0.9	7	0.6	0.7	-	1	1	-	0.76	0.89	3
2013	0.86	0.99	5	0.7	0.79	-	1	1	-	0.8		-
The model set up using *Reykjavík* weather station data												
2016	1	1	3	0.96	1	3	1.6	1.8	6	1	1	-
2015	1	1	4	1	1	2	1.6	1.8	4	1	1	2
2014	2	2.5	7	2	2	-	2.86	3	-	2	2.59	3
2013	1.8	2	5	1.76	2	-	2.55	2.88	-	2	2	-

TABLE C-9: Model performances at the annual average period for the different terrain options

Test case number	Periods	Weather stations*	Correlation (r)		Standard deviation (SD) model (µg/m³)		Standard deviation observed data (SD) (µg/m³)	Root mean square error (RMSE) (µg/m³)	
			Elevated	Flat	Elevated	Flat		Elevated	Flat
B Nesjavellir (NES) and Hellisheidi (HEH) – Iceland**									
B-2 annual	Annual	REYK	0.55	0.5	0.4	0.5	1.7	1	1
	Annual	STRM	0.59	0.5	0.1	0.5	1.7	1.55	1
	Annual	HELS	0.6	0.6	0.1	0.2	1.7	1.5	1.5

*REYK = Reykjavík meteorological station, STRM = Straumsvík meteorological station, HELS = Hellisheidi meteor. station;
**The input values of the test case B-2 annual models were obtained from model simulation presented in Table C-8.

APPENDIX D: Model simulations of H_2S concentration using model terrain options for various time scales during dry and wet seasons (*UBL case*), and during winter and summer seasons *(HELS-NES*)

TABLE D-1: Model simulation for the 1-hour period (UBL case)

Receptor code	Receptor	X* (m)	Y* (m)	Base elevation (m a.s.l)	Wet season (µg/m^3)		Dry Season (µg/m^3)	
					Elevated	Flat	Elevated	Flat
3	Muara dua	452516	9412220	733	19.64	24*	18.48	24.59*
1	Cluster C	452392	9412781	769	50.44	60*	39	46.54*
5	Karangrejo	452304	9413027	796	219	251.64*	257.62	292.84*
2	Mekarsari	452343	9413562	842	513*	205	372*	190.8
6	Ngarip	451006	9412997	869	242.62*	128.54	314*	188

*Highest concentration between the two seasons

TABLE D-2: Model simulation for the 8-hour period (UBL case)

Receptor code	Receptor	X* (m)	Y* (m)	Base elevation (m a.s.l)	Wet season (µg/m^3)		Dry Season (µg/m^3)	
					Elevated	Flat	Elevated	Flat
8	PP units 1 & 2_R	452774	9413193	785	45.75	59.5*	14	18*
11	Securi. post units 1 & 2	452602	9413098	787	26.6	33*	21.8	27*
10	Cool. tower units 1 & 2	452831	9413257	788	105	136*	17	22.59*
7	PP units 1 & 2_L	452658	9413187	793	49.83	59.87*	46	55*
15	PP units 3 & 4_left side	453055	9413525	799	42*	40.63	43.98*	42
9	Cool. tower units 1 & 2	452618	9413256	801	60	64*	59	62.52*
12	Securi. post units 3 & 4	453279	9413582	802	97	114.90*	47	55.46*
4	PP units 3 & 4_right side	453212	9413503	802	28.73	29*	73.97	69*
13	Cool. tower units 3 & 4	453230	9413556	803	108.9	123.62*	49	45*
14	Cool. tower units 3 & 4	453036	9413589	804	93.5*	85.74	54*	48

TABLE D-3: Model simulation for the 24-hour period (UBL case)

Receptor code	Receptor	X* (m)	Y* (m)	Base elevation (m.a.s.l)	Wet season (µg/m^3)		Dry Season (µg/m^3)	
					Elevated	Flat	Elevated	Flat
3	Muara dua	452516	9412220	733	1	1.7*	2	2*
1	Cluster C	452392	9412781	769	5	6.13*	5.74	6.7*
5	Karangrejo	452304	9413027	796	23	25.94*	21.66	24*
2	Mekarsari	452343	9413562	842	23*	9	29*	14
6	Ngarip	451006	9412997	869	12*	7.56	17.65*	9.

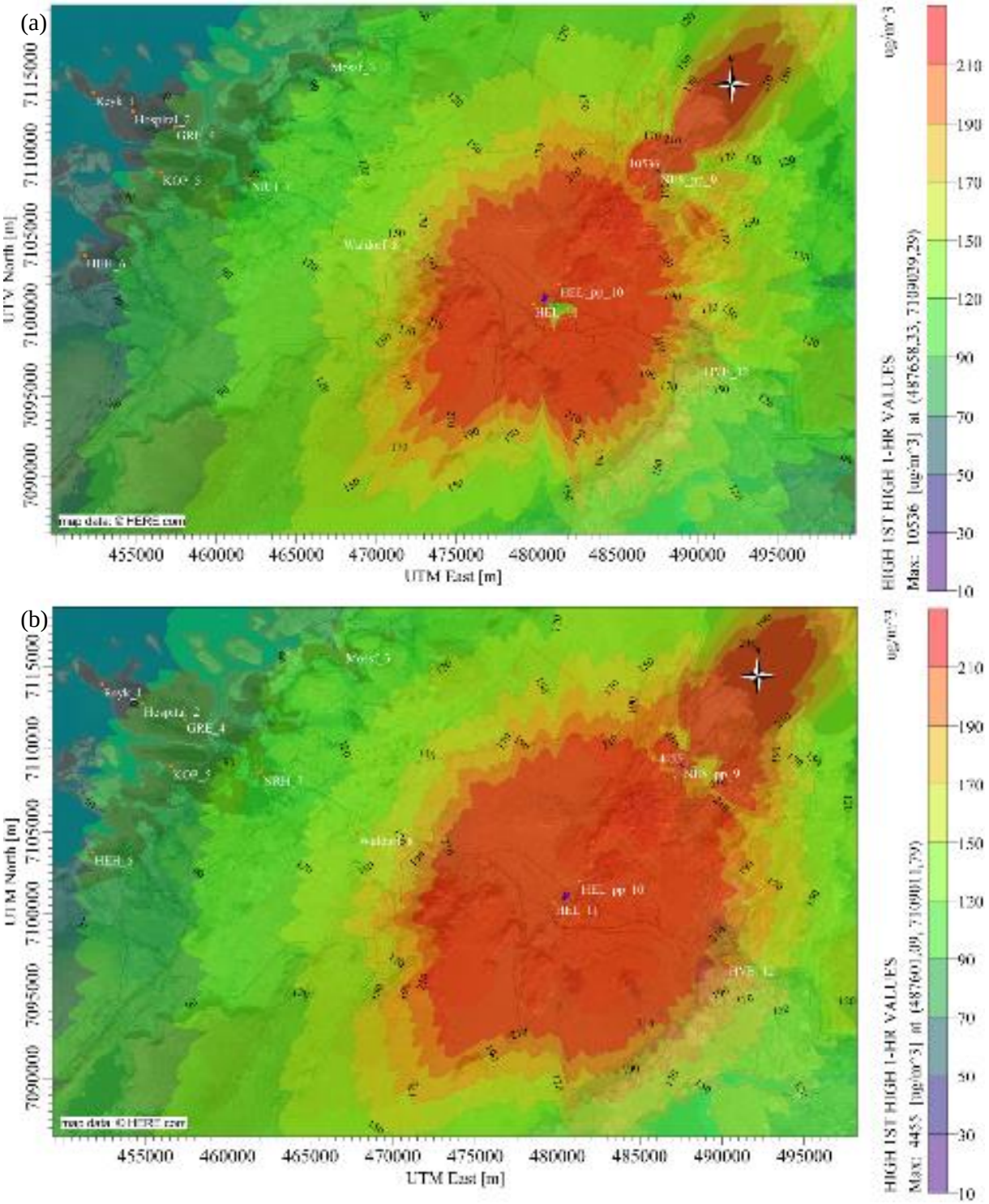

FIGURE D1: Model simulation of H_2S concentration for 1-hour average from the Reykjavík and Hellisheidi meteorological station data (HELS-NES): (a) REYK winter season; (b) REYK summer season

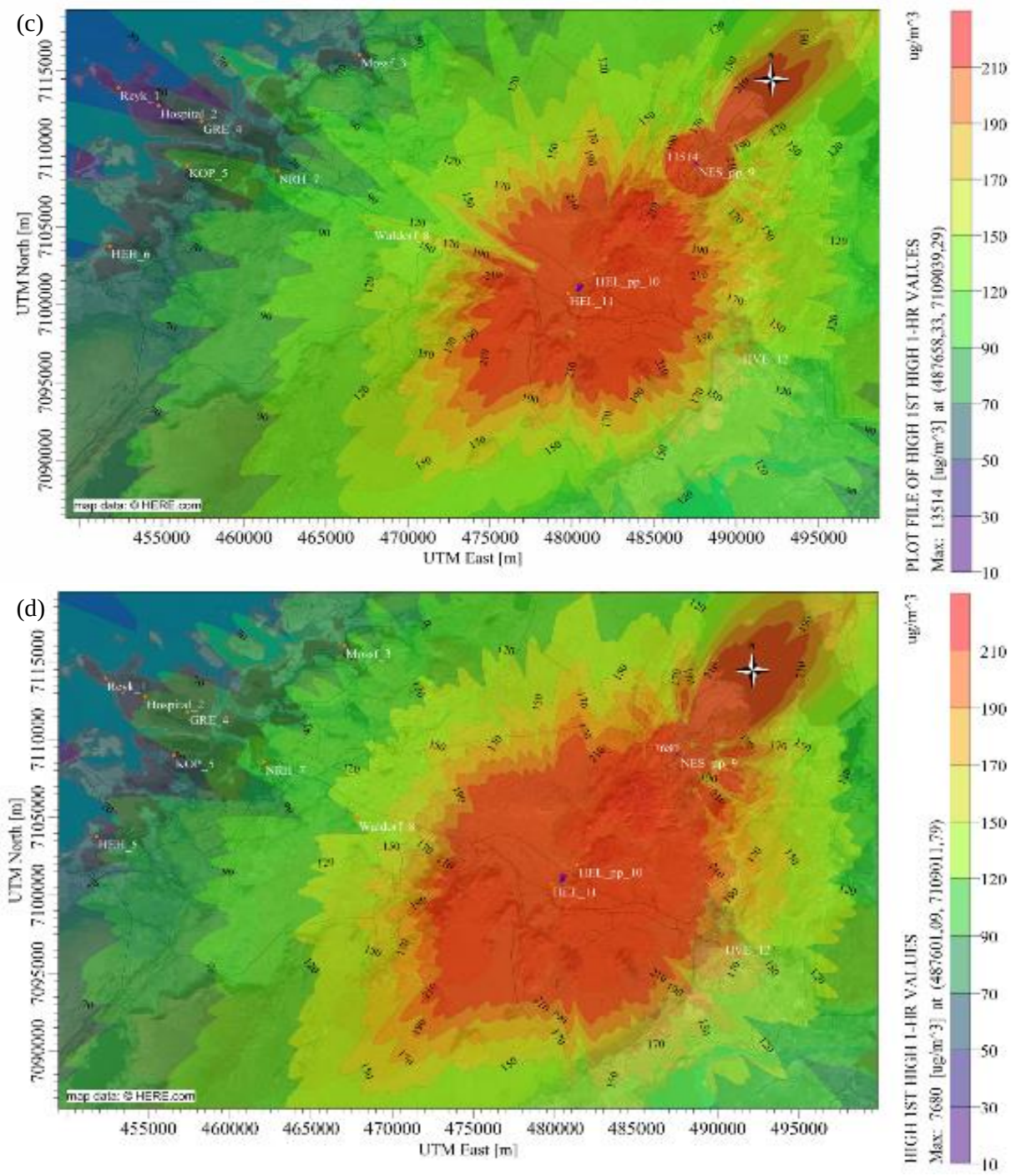

FIGURE D1 cont.: Model simulation of H_2S concentration for 1-hour average from Reykjavík, and Hellisheidi meteorological station data (HELS-NES): (c) HELS winter season; (d) HELS summer season